2009

Data acquisition for modeling and visualization of vascular tree

William Lafayette Mondy
University of South Florida

Data Acquisition for Modeling and Visualization of Vascular Tree

by

William Lafayette Mondy

A dissertation submitted in partial fulfillment
of the requirements for the degree of
Doctor of Philosophy
Department of Chemical and Biomedical Engineering
University of South Florida
College of Engineering

Co-Major Professor: Les A. Piegl, Ph.D.
Co-Major Professor: Don Cameron, Ph.D.
William E. Lee III, Ph.D.
Jing Wang, Ph.D.
Nathan Crane, Ph.D.

Date of Approval:
May 29, 2009

Keywords: Bio-mimicking, Bio-CAD, Micro-CT, Vascular scaffold, Capillary bed.

Table of Contents

List of Tables

List of Figures

Data Acquisition for Modeling and Visualization of Vascular Tree

William Lafayette Mondy

ABSTRACT

Data can be acquired from tissue's vascular structure and used for modeling and visualization. To acquire data from a vascular tree, we make its structure available for the gathering of data by separating it from the structures of surrounding tissues, which includes the capillary structure. The capillary structure contains important information, but, because of its size, is the most difficult to acquire data from. In this work, we look at methods for contrasting the vascular structure from surrounding tissues, and focus on the use of corrosion casting for this procedure. We collected image data using micro-computer tomography (micro-CT) and converted data into stereolithography models. Models were imported into computer aided design (CAD) software, which was used to further process the models in order to ensure that the necessary structures were in place for the recreation of the capillary structures' relationship to targeted cell systems. Recreating the cell system-capillary system relationship is the reason building this model is so important. It is this relationship that we seek to model so that, in the future, we can create designs that guide the fabrication of three-dimensional (3D) scaffolding, which mimic capillary patterns with supportive structure that serve as an extracellular matrix for 3D tissue engineering. This method had been designed to enhance a variety of therapeutic protocols including, but not limited to, organ and tissue repair, systemic disease mediation and cell/tissue transplantation therapy.

Preface

We would like to acknowledge Dr. Pieter Cornillie and Professor Paul Simoens from the Department of Morphology at the Faculty of Veterinary Medicine, Ghent University, Ghent, Belgium, for their assistance with the modified Batson's #17 corrosion casting method used in this report. Also many thanks to John Sled PhD at the Mouse Imaging Centre of Toronto Canada for his help with mouse kidney samples; Tim Sledz at Micro photonics USA for his assistance with micro-CT data; Professor Jean Pierre Timmermans and his technical staff at the Laboratory of Cell Biology & Histology and the Micro-CT Scan Research Group of the university of Antwerp for their help and guidance with histological and micro-CT specimen preparations; Dr. Phil Salmon at the Skyscan Company, Kontich Belgium, for his help with Micro-CT scanning and Drs. Bert Masschaele and Manuel Dierick of Ghent University Department of Subatomic and Radiation Physics for their technical advice with Micro-CT image processing. In addition I would like to thank Jeremy Woodward and Professor John Maina from the University of Witwatersrand, Johannesburg South Africa for their assistance with 3D reconstruction of histological sections of capillary structures from avian lung tissues; Betty Loraamm of USF's Biological Electron Microscope Facility - Sandra Livingston and Candy and Adriana at the core histology labs of USF's college of medicine, for the use of their facilities. Finally, I would like to thank my advisors, Professor Don Cameron who stuck with me through some hard times; and Professor Les Piegl, who believed in

my project and had enough faith in me to let go of the reins and allow me to find my way through to this project's end.

This research has been supported by the NSF grant awards IGERT DGE #0221681 and S-STEM DUE #0807023, and the Alfred P. Sloan Foundation Minority Ph.D. program at EDUCATIONAL AND RESEARCH INTERESTS, USF.

Chapter One

Introduction

Motivation for Research

Tissue engineering is a promising field in biomedical research. Presently, the clinical applications for engineered tissues are limited. Biotech companies founded in the 1990's to profit on engineering tissues for clinical use have struggled to stay in business due to limited success in engineering 3D tissues for transplant therapies. Partial layers of skin tissues grown in culture are the only organs to date that have been successfully engineered and sold for use in a clinical setting. These tissues are avascular and limited in their dermal thickness, which makes engineering these tissues from skin possible. Dermal layers contain limited vasculature structures. The sub-dermal layer of the skin contains most of the vasculature found in skin and is the site for glands, nerves and hair follicles, none of which are produced in these *in vitro* skin tissue structure manufactured for clinical use.

With the onset of new discoveries in stem cell development, clues are being discovered that will allow in the near future the large-scale production of not only stem cells, but all types of cells in a non-differentiating proliferative state. Techniques are needed that will open pathways to the *in vitro* engineering of unlimited types of tissues for transplantation and large womb healing. Even the engineering of organs may not be far away. The successful completion of such a project will involve utilizing the

interdisciplinary transfer of information from molecular biology, cellular biology, biochemistry, chemical engineering and even electrical engineering.

Recent studies show that the cells that compose the blood vessel wall are extremely predisposed to respond cytochemically, genetically, morphological and behaviorally when they experience a specific type stress produced by particular changes in blood flow (Kyriakis and Avruch 2001; Opitz, Schenke-Layland et al. 2004; Opitz, Schenke-Layland et al. 2007). The development of sensors that allow us to accurately measure the stress levels that cause cells to behave in a different but well-understood manner will lead to non-chemical ways of inducing changes in blood vascular diseases, such as arteriolosclerosis, as well as ways of increasing vascular genesis in hard-to-heal tissue, such as the lung, and divergently decreasing angiogenesis in tumors. It is conceivable that once a specific wave frequency's tolerance is observed, mechanical wave-induced forces will be used not only for disease treatment but also for the engineering of vascular tissues, and, subsequently, organ systems for transplantation.

An intact functional vascular network, which includes the capillary structures, is needed in order for researchers to have the necessary capability to grow true 3D tissue structures. These capillary structures are necessary in order to make available elements and compounds for the maintenance, function and growth of 3D engineered tissue structures. Without a capillary bed, tissues grown in a culture are limited to diffusion dynamics for the movement of materials to and from cellular structure as a means to supplying them with the factors necessary for their maintenance and growth. Relying on diffusion forces limits the growth and survival of cells to approximately 200-microns

beyond the tissues boundary with cell culture media. Without a 3D capillary bed, structures supplying the necessary nutrients and metabolic factors only two dimensional (2D) growths are achievable (Simms, Bowman et al. 2008). This is unacceptable if tissue engineering is to reach its anticipated potential. Three-dimensional tissue structures must be realized before true tissue engineering can be claimed.

In order to successfully support the engineering of 3D tissue structures, we seek to design vascular tree models from which 3D scaffolds that duplicate the structural patterns of specific vascular trees, which are characteristic of specialized tissue structures (Mertsching, Walles et al. 2005; Schreiner, Karch et al. 2006; Linke, Schanz et al. 2007; Wischgoll, Meyer et al. 2007). Duplication of structural patterns is necessary because the functional morphology of tissues relies greatly on the capillary flow pattern existing in a particular tissue type. Examples of specialized capillary flow patterns that have structural designs that are essential to the functional morphology of a tissue structure are: The air exchange capillary beds found in the perialveolar spaces of the lung; the capillary tufts found in the glomerulus of the kidney; the dermal papillary loop; the deep horizontal plexus; and the perforating arterioles and venules of the cutaneous vasculature.

The therapeutic needs for 3D tissue structures, along with the failures demonstrated in literature to stimulated capillary bed formation *in vitro*, prompted us to research the possibility of mimicking vascular tree designs using computer-aided design (CAD) models. It is our aim to show that CAD models can be created using stereolithographically (STL)-constructed 3D models that use data acquired directly from vascular structures. Creating models using this method, we plan to be capable of

mimicking the design of the tissue-specific capillary bed that contains vascular tree systems. Designs could be readily used to create 3D vascular scaffold by rapid prototyping techniques.

Previous studies of the vascular networks found in organs, which undergo gas or fluid exchange with the external environment, has provided a unique view of the 3D range covered by capillaries, arteries and veins. The visualization of the circulatory system's role in sustaining large areas of cellular growth has long been realized through various histological techniques. Using our knowledge of these studies, we derived an approach that uses existing techniques in ways that enable us to design methods for constructing vasculature tree replicas that include capillary beds.

New developmental clues are being discovered, and fundamental pathways in stem cell development are being better understood. This will allow scientists in the near future to benefit from the large-scale production of not only stem cells, but all types of cells in a non-differentiated proliferative state. Scientists need techniques that will open corridors into using these cells in the *in vitro* engineering of unlimited types of tissues for transplantation, large womb healing and the engineering of complete organs. The successful completion of such projects will involve utilizing the transfer of interdisciplinary information and technologies from molecular biology, cellular biology, medicine, biochemistry, chemical engineering, material engineering, computer engineering and electrical engineering.

The diffusion of nutrients' metabolic waste and other factors occurs through the extracellular matrix at a rate too slow for cells to survive in groups much larger than a few cell layers without some type of specialization occurring in the cells' metabolism or organization. This is the basis for the formation of the body cavity and the circulatory system in early metazoans more than 600 million years ago. Even today, researchers are exploring how chemotactic behavior is initiated through the release and diffusion of certain cellular factors (Solari, Kessler et al. 2006). An example of such behavior has been studied in the single-cell slime mold *Dictyostelium discoideum*. When nutrients are used up, these organisms form colonies to survive. Individual organisms are attracted to the cells, releasing the highest levels of cAMP. The single-cell *Dictyostelium discoideum* respond metabolically to cAMP (Bolourani, Spiegelman et al. 2006) by using the same signal transduction pathways common to those that signal endothelial and smooth muscle cells to migrate and differentiate during vasculogenesis and angiogenesis (Takahashi, Kawahara et al. 1996; Roztocil, Nicholl et al. 2007).

The cellular specializations that occur during the development of tissue structures is environmentally regulated and maintained (Howlett and Bissell 1993; Nelson and Bissell 2006). In order to obtain the desired result from cell-culturing techniques for the development of 3D tissue constructs and to bioengineer the large tissue structures into a true intercellular circulatory system, it is necessary to use one that mimics the system found in the tissue sought to be created.. The key question that we sought to answer in this thesis is: How do you recreate such an intrinsic design?

Prior Work

Previous studies of the vascular network found in organs, which undergo gas or fluid exchange with the external environment, has provided a unique view of the 3D range covered by capillaries, arteries and veins. This provides the visualization of the circulatory system's role in sustaining large areas of cellular growth, so, from these studies; we derived techniques that enable us to design a method for the construction of replicas of vasculatures for specific tissue regions.

It has been shown that scaffolds that support vessel wall development can be created for blood vessels, but these scaffolds have been used to make large, mostly straight tubes of a constant diameter, without much branching or a complex of small vessels or capillaries of any sort (Sodian, Fu et al. 2005). New methods are needed for developing designs for bimolecular scaffolding that support a wide array of cellular functions and are not rejected by the host (Choi, Choung et al. 2005; Berry, Yazdani et al. 2006; Williamson, Black et al. 2006). For nearly twenty years, studies of the 3D structure of blood vessels (Schraufnagel 1987) and other luminal systems found in the body (Hojo 1993) have produced techniques that use a blend of vinyl chloride latexes that consist of a plasticized vinyl chloride copolymer with a vinyl chloride copolymer, to create a latex replica of the microvasculature system, which demonstrates the luminal surfaces of these structures. Extensive literature exists that demonstrates techniques for creating a vascular cast that replicates the capillary systems for most tissue types (Hurley and Stein 1957; Lametschwandtner, Lametschwandtner et al. 1984; Schraufnagel 1987; Lametschwandtner, Lametschwandtner et al. 1990; Aharinejad and Lametschwandtner

1992; Gross, Joneja et al. 1993). These studies, beginning in the 1950's, were performed to better understand the microvascular design for specialized tissue structures. Prior to vascular casting, scientists had to rely on 2D images obtained from histological sections of the tissue being studied, cut using rotary microtomes from which to they could visually reconstruct some idea of how the 3D microvascular system for a given tissue structure appeared. In the early days, this took a lot of imagination and drawing skills to produce reasonable 2D drawing of these 3D structures. In the late 1970's through the early 80's, with the onset of computer imaging, micrographs taken of series of tissue sections were aligned and the preserved structure reconstructed in the third dimension. But prior to this morphological reconstruction, 3D vascular replicas were already being cast with various latex, epoxy and methacrylate resins, which after the tissue was corroded, gave investigators the ability to visualize, using scanning electron microscopy, the dynamic complexity of the 3D microvascular structural arrangements occurring in specialized tissue structures. In the early 1990's, computer-based 3D visualization of complex microvascular systems began to improve with the algorithmic use of segmentation techniques. This led to improvements in the resolution captured in the digital images being created and the spatial representation of complex microscopic structures. Automatic extractions of microvascular contour and their volumetric representation were algorithmically achieved (Ro, Handels et al. 1995). In order to reduce the amount of visual image information from which we constructed 2D data sets, these studies used vascular corrosion casts. Vascular corrosion casts were embedded in plastic resins and sectioned with rotary microtomes, similar to the tissues sectioned and prepared for earlier reconstruction techniques. Recent studies have included the use of fluorescence additive

during the preparation of casting resins for the fluorescent imaging of surfaces created using cryomicrotomy (Lagerveld, ter Wee et al. 2007). The 3D computer reconstructions created with this technique are limited to 50 microns, so the resolution at this level is inefficient for the reconstruction of capillaries that have diameters ranging from 6 to 12 microns.

Subsequent advances in imaging technique for 3D visualization of vascular tree systems relied on the imaging of the physical behavior of atomic particles under the influence of X-rays, magnetic waves, sound waves or high-frequency light. Instruments utilizing the characteristics of such atomic interactions were developed to produce data for acquiring and constructing images in 3D. One such technique is computer tomography (CT). Image data obtained using this technique has been used to construct models of various bony tissue structures using 3D prototype fabrication techniques that create tissue scaffolding (Schipper, Ridder et al. 2004) NMR data has been similarly used to fabricate models of various tissue for scaffold prototypes (Cheah, Chua et al. 2003). These imaging techniques fail to provide the resolution necessary to demonstrate fine tissue structures that exist at the microscopic level. With development in micro computer tomography (Micro-CT) in the 1990's, and through the use of blood-pooled contrasting agents, images that demonstrated much finer anatomical features became obtainable.

The inability to provide nutrients and oxygen to cells far from the tissue/culture media interface has made 3D tissue structures resist production. The diffusion of nutrients' metabolic waste and other factors through the extracellular matrix occurs at a rate too slow for cells to survive if they are much further than a few cell layers, unless

there is some type of specialization occurring in the cells' metabolism or organization. This is the basis for the formation of body cavities and circulatory systems in early metazoans over 600 million years ago. Even today, researchers are exploring how chemotactic behavior is initiated through the release and diffusion of certain cellular factors (Solari, Ganguly et al. 2006). When the nutrients of the single-cell organism *Dictyostelium discoideum* are used up, they form colonies to survive. Individual organisms are attracted to the cells, releasing the highest levels of cAMP. Free-living *Dictyostelium discoideum* respond metabolically to cAMP (Bolourani, Spiegelman et al. 2006) and use the same signal transduction pathways common to those that signal endothelial and smooth muscle cells to migrate during vasculogenesis (Takahashi, Kawahara et al. 1996; Nicholl, Tanski et al. 2004). Specializations make it imperative that the proper environment is supplied to the developing tissues in order to obtain the desired result from cell culturing techniques. In order to bioengineer large 3D tissue structure, a true intercellular circulatory system is necessary. The question then is, how do you recreate such an intrinsic design?

Much work is being done in the area of angiogenesis (Kilian, Alt et al.). Although some success have been obtained in the area of *in vitro* blood vessel formation, (Weber, Rossi et al. 2002; Bergers and Song 2005) these successes have resulted in limited diameters, and the lengths have been small. Also, limited success has been achieved using scaffold constructed as flat sheets of collagen type I (Boccafoschi, Habermehl et al. 2005), but the growth both of smooth muscle and endothelial cells show no improvement over cell cultures without such scaffolding. In another instance, non-woven polytetrafluoroethylene (PTFE), polyethylene terephthalate (van Meeteren, Ruurs et al.)

and poly nanofiber mats (Grigoriy A. Mun) (Horiuchi, Suzuki et al.) were constructed for used as scaffolds to substitute for basement membrane collagen and elastin fibers (Ma, Kotaki et al. 2005). Modifications were made in its surface in an attempt to mimic the fibrous proteins found in extracellular matrix, constructing a biocompatible surface for endothelial cells. This was a noble attempt to create a substrate compatible with endothelial cell growth, even stimulating endothelial cells to express surface adhesion proteins PECAM, VCAM-1 (or CD106) and ICAM-1 (or CD54) (Ma, Kotaki et al. 2005). But this attempt was also done on a flat surface and did not come close to providing the necessary environment for blood vessel formation. A more recent study used electro-spun Type I Collagen, elastin and poly (Stitzel, Liu et al. 2006) woven into micron to nano-scale fibers and constructed into a tube shaped-scaffold (Stitzel, Liu et al. 2006) improved the compliance and strength of scaffolds by adding the biodegradable poly-lactide-co-glycolide (PLCG). The resulting scaffold did not educe severely limited or systemic tissue reaction when grafted *in vivo*. These tubes demonstrated cells infiltration and differentiation, and they microscopically showed some similarities to actual blood vessels (Stitzel, Liu et al. 2006). But these are straight tubes of a constant diameter, and there was no branching into a fine complex of small vessels to large capillaries. Even micro-CT that has resolution around 8 microns has not, in the past, produced volumetric images of areas large enough to resolve entire vascular tree structures, nor were the capillary systems completely demonstrated (Muller 2006). The 3D reconstruction of serial montages demonstrating capillary and pre-capillary anastomosis and other such microscopic tissue structures has successfully created models used to understand their structural dynamics (Zhai, Birn et al. 2003). Not only is this a

labor-intensive process, the file size that would result during the modeling of such high-resolution reconstructions has prevented the recreation of entire vascular tree structures.

The application of computer science and engineering technology into medical science has led to the bio-CAD structural refinement of many medical devices such as artificial joints, bone implants, vascular stents and prostheses (Sun 2005). These devices are mechanical in their application and have made vast improvements over their predecessors that were designed before the advent of computer technology products that aided in the design and manufacturing processes (Sun 2005; Witkowski, Komine et al. 2006; van Lenthe, Hagenmuller et al. 2007; Wang and Tang 2007). In contrast, the use of bio-CAD to engineer tissue structures has not yielded products with comparable success in physiological applications (Sun, Darling et al. 2004; Sun, Starly et al. 2004; Sun, Starly et al. 2005).

Resolving a Complete Vasculature Tree

There has not been a significant demand for the complete reconstruction of capillary bed structures using micro-CT. As a result, there has been very limited success with complete reconstructions of these structures (Ikura, Shimizu et al. 2001; Badea, Hedlund et al. 2006; Badea, Hedlund et al. 2007). The success of computer-aided design to reverse engineer vascular tree tissue scaffoldings weighs heavily on the ability to reconstruct, in 3D, complete capillary bed systems. The use of micro-CT to visualize a complete vasculature tree system, which includes a corresponding capillary bed, has been a priority for researchers utilizing the current high-end micro-CT imaging techniques (Ritman 2004; Bentley, Jorgensen et al. 2007; Jorgensen, Eaker et al. 2008). While the

present instrumentation, technically, has the resolving capabilities (Sasov and Van Dyck 1998; Parkinson and Sasov 2008), the limitation of the contrast agents used in this technique have prevented the complete resolution of capillary systems (Badea, Hedlund et al. 2006). In this thesis, we examine the possibility of obtaining 3D images of a complete microvascular tree structure using micro-CT as part of a novel method to reverse engineer the bio-CAD for vascular scaffolding production.

Using a cast made from the lumen of the appropriate vascular tree, a scaffold can be designed to replicate the vascular tree's framework. Our novel method for engineering tissue structures is built around reverse engineering CAD for vascular scaffolding, which mimic the actual vascular tissue structures designed around models created using vascular cast. The micro-CT of vascular casts is explored for its effectiveness as a tool for acquiring the necessary images at a resolution capable of resolving complete capillary structures. The current successes obtained in the 3D reconstruction of tubular microstructures with diameters ranging in size from 5 – 12 microns have been accomplished by serial section reconstruction using microscopical techniques, including confocal optical sectioning along with subsequent 3D image reconstruction. These techniques are limited in scope and are labor intensive, but they provide detailed 3D image representation for small areas (Jirkovska, Kubinova et al. 1998; Karen, Jirkovska et al. 2003; Woodward and Maina 2005; Woodward and Maina 2008). The resulting images are limited by the area of tissues sectionable face or the microscope's field of view (Karen, Jirkovska et al. 2003; Woodward and Maina 2005).

Limitations of Contrasting Agents

There are a few obstacles to the complete visualization of vascular tree systems using the currently applied micro-CT techniques. The challenge is centered on imaging the capillary bed structure. The problem is the lack of a contrast agent that allows the demonstration of large vessels, while at the same time demonstrates capillary beds (Elleaume, Charvet et al. 2002; Hainfeld, Slatkin et al. 2006; Litzlbauer, Neuhaeuser et al. 2006). One of the causes is the endocytosis of heavy metal based contrasting agent by the endothelial cells comprising the blood vessel walls (Langheinrich, Leithauser et al. 2004). The endocytotic formation of large contrasting-agent filled vacuoles by endothelial cells lining the vasculature leads to its deformations. These large vacuoles can obstruct the narrow lumen of small vessels, blocking complete perfusion and preventing the accurate micro-CT imaging of the capillary bed system.

Less viscous contrasting agents, or those without radio-opaque additives, have an intensity issue, in which not enough contrast exists between the agent in the capillary lumen and the surrounding tissues to distinguish one from the other (Hainfeld, Slatkin et al. 2006; Mukundan, Ghaghada et al. 2006; Kong, Lee et al. 2007; Habibi, Krishnam et al. 2008). The less viscous, iodine-based *in vivo* contrast agents are metabolized and create unstable images that fade rapidly from capillary structures (Priebe, Aukrust et al. 1999; Kim, Kim et al. 2005; Ford, Graham et al. 2006).

Our goal is to demonstrate our ability to acquire 2D micro-CT image slices that can be reconstructed into models that clearly demonstrate capillary beds. In order to overcome the difficulties with micro-CT contrast agents hampering complete

visualization of capillary bed systems, we decided to go back to our original idea of using corrosion casts to obtain image data of the microvasculature. Viscosity issues have long ago been worked out with this technique, as complete perfusions of capillary bed structures have been demonstrated (Lametschwandtner, Lametschwandtner et al. 1984; Lametschwandtner, Lametschwandtner et al. 1990; Simoens, De Schaepdrijver et al. 1992). Batson's methylmethacrylate (Polysciences) was chosen because of its proven success in creating durable vascular casts (Gross, Joneja et al. 1993; Krohn and Bertelsen 1997).

A specimen's size and thickness is an issue addressed with the eroding away of tissues, characteristic of the corrosion casting technique. Given the significant reduction in background noise, thanks to the removal of the surrounding soft tissue, this technique provides clean structures of which 3D images can then be created and stored as mesh structures in a stereolithography file format, compatible with computer-guided 3D fabrication. We processed data sets into stereo lithographic models from various tissue samples in an attempt to mimic vascular tree systems.

Bio-CAD /CATE

Structural data must be acquired with the specifications necessary to provide a structural environment that would meet the vascular and physiological needs for the growth and homeostasis of 3D tissue genesis. The structural environment must be designed to support the necessary cell behaviors of specific cell types. In the late 1990's, as the identification of molecules that controlled branching during tissue development increased, the architectural branching patterns created during tissue morphogenesis

became well understood (al-Awqati and Goldberg 1998). Computer-aided technologies have been utilized to enhance the obtainable result in imaging technology, CAD-based anatomical modeling and rapid prototyping. These fields of research have been utilized separately and together in the effort to develop artificial replacement constructs for damaged tissues. (Karen, Jirkovska et al. 2003; J. Nam 2004) Computer Aided Tissue Engineering (CATE) has been used for the modeling, design and manufacturing of numerous types of tissue scaffolds (J. Nam 2004). From the design of internal and external architectures, through bio-mimicking techniques to creating non-mimicked structures such as chambers for drug delivery, these bio- mimicked design are based on 3D reconstruction of real anatomical data acquired through computer tomography, magnetic resonance imaging and the reconstruction serial microtome/ laser sections(Weihe, Wehmoller et al. 2000; Sun and Lal 2002). These scaffolds have been modular, multi-layered and vascular-tree based (J. Nam 2004). Porous artifacts have been created in CAD of scaffold for tissues like bone, in which this type of structure is suitable.(Schroeder, Regli et al. 2005)Using stochastic geometry, uniform and binomial-point process and Poisson process are combined to create Boolean models to represent the porous artifacts(Fang, Starly et al. 2005).

Modeling

The resolution of a CT scanner is not the same as the voxel size of the scan, so it is quite likely that the resolution of the scanner is preventing investigators from resolving complete capillaries in some cases. Vessels that have diameters smaller than the point spread function will be reduced in intensity and difficult to detect. The extent to which the contrast agents fill the capillaries can be verified on histological sections so as to rule

this out as an explanation. Histological studies at the electron microscopy level have shown that endothelial cells, through endocytosis, attempt to remove heavy metal-containing contrasting medias from the vascular lumen (Kim, Park et al. 2007; Mondy and N. De Clerck 2009, In Press). This endocytosis causes the formation of large cytoplasmic vesicles demonstrated in Figure 1, which protrude into the vascular lumen. This cellular behavior is capable of blocking the efficient perfusion on contrasting agents in to the microvasculature for micro-CT imaging.

We have approached the challenges micro-CT presents with regards to accurately resolving complete capillary structures by 3D scanning non-metal containing corrosion casts of vascular structures with micro-CT (Mondy and N. De Clerck 2009 In Press).

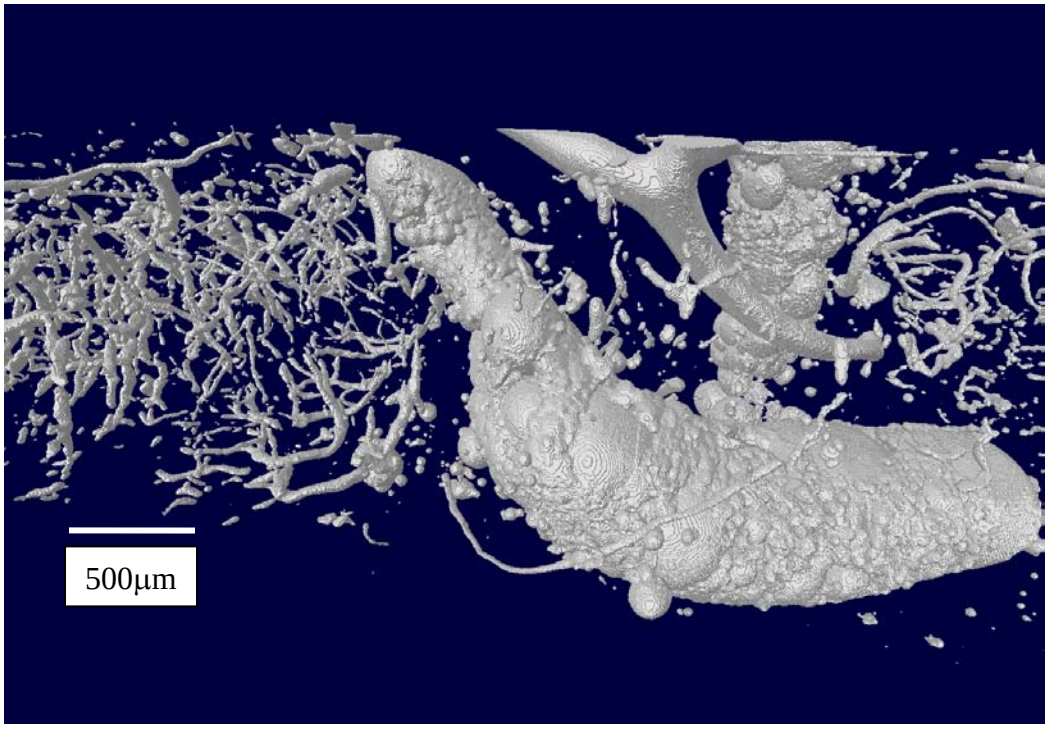

Figure 1: Globular spheres of Microfil. Region of Interest (ROI) constructed from rabbit kidney vascular network perfused with Microfil contrasting agent. Globular spheres of Microfil are present in the luminal walls as evidence of flow obstruction.

Reconstruction in stereolithography format allows the compatibility of subsequent 3D models with most CAD software.

Biomaterials and Vascular Scaffolding

The biomaterials used can be designed to direct cell differentiation polymerization and migration, and they can be a tool for the manipulation of stem cell behavior during the implementation of tissue engineering designs (Prasad and Krishnan ; Welsh and Tirrell 2000; Hunt and Shoichet 2002; Wang, Kim et al. 2006; Couet, Rajan et al. 2007). Recent methods of tissue scaffold construction for regenerative tissue structures begin with a viscous liquid that polymerizes into a porous, fibrous, biocompatible network (Chen and Ma 2004; Liu, Won et al. 2006; Wei, Jin et al. 2007). The biodegradable polymers used to construct these scaffolds attempt to mimic the fibrous structure of type I collagen architectures seen in the fibrous capsules found throughout the targeted tissue's extracellular matrix. The nano-scale of these fibrous matrixes was created using phase-separation of poly L-lactic acid (PLLA) (Chen and Ma 2004). This fibrous scaffold could be made porous through the use of paraffin beads by a dispersion method(Chen and Ma 2004). With these techniques, the size of both the nano-fibers and the spherical pores can both be controlled by variation in the scaffold's fabrication process. Varying the mechanical properties, the inter-fiber distances and the inter-pore connectivity are all possible by variation in the fabrication procedures, making these types of scaffolds adaptable for various tissue structural types. Another recent approach combines direct polymer melt and electrospining of nanofibers to create scaffolds that mimic the nano-fibrous nature of the extra cellular matrix (Park, Kim et al. 2008). In this process, CAD operations were used to create such features as pore size and interconnectivity.

Using CAD software to interface hydrogel technology with 3D prototyping, the manipulation of 3D laser microfabrication techniques can be used to create a scaffold for vasculogenesis. This same process, with modifications in the image selection, can be used to create scaffold designs that model any extra cellular matrix tissue structure.

Vascular scaffolds must allow for varying degrees of layering, permit cell migration, contain the necessary growth factors found in the extra cellular matrix of developing blood vessels (van Meeteren, Ruurs et al. 2006) and be suitable for the engineering of an *in vitro* cellular replica of the vascular tree. The type of biomaterial used in constructing a tissue scaffold and its bioactive characteristics, can be tailored to play key roles in the seeded stem cell's developmental behaviors. (Elisseeff, Ferran et al. 2006) For vascular tissue engineering, the most promising biomaterial and fabrication method being used in scaffold production comes through the use of hydrogels.

Hydrogel

Hydrogels come in various formulations and can be fabricated into scaffold structure in a few ways (Anseth, Bowman et al. 1996; Elisseeff, Anseth et al. 1999; Elisseeff 2008). Their ability to be formulated for the controlled release of growth factors, like TGF-beta and FGF, is only one of the promising characteristics that can be produced with hydrogels (Elisseeff, McIntosh et al. 2001). Even more promising is the ability to use light to not only pattern its polymer structure (Gattas-Asfura, Weisman et al. 2005; Zourob, Gough et al. 2006; Khalil and Sun 2007), but also, through photo cross-linking, (Bryant, Nuttelman et al. 1999) the encapsulation and 3D patterning of bio-molecules for the guided control of cell behavior (Burdick and Anseth 2002; Bryant, Bender et al. 2004;

Hahn, Miller et al. 2006) and tissue developmental (Cao and Shoichet 2002). Hydrogels can be fashioned from many types of materials, including simple carbon molecules such as ethylene oxide (Elisseeff, Anseth et al. 1999); carbohydrate monomers, including those in dextran (Levesque and Shoichet 2006) and agarose (Luo and Shoichet 2004); protein monomers, like the self-assembling sub-units of elastin (Mithieux, Rasko et al. 2004), a key material in the structure of blood vessels; and even DNA (Um, Lee et al. 2006). The photosensitivity of hydrogels has allowed investigators to pattern in the gel sites for the attachment of bioactive peptides to regulate cell behavior in specific patterns (Weber, Hayda et al. 2007).

Using a vascular scaffold that is combined with scaffolds produced to mimic extracellular matrix tissue structures capsules, we will have the framework to reverse engineer any of the tissue structures produced in nature. With the completion of this work, we are one step closer to reverse bioengineered complete vascular tree systems. We will begin designing large arteries and arterioles, replicating the *in vivo* branching patterns demonstrated in image data. The microscopic capillary bed-containing central channels are essential to tissue engineering goals being sought in the scientific community, and so is connecting them to the corresponding venules and veins systems specific to the targeted tissue structure. The resulting vascular tree will serve as a support structure for further tissue genesis in bioreactor chambers that regulate vascular flow and media content that is generated using sensors that gather and feedback data to a computer that is capable of regulating the dispensing of molecular and environmental factors that control cell behaviors, such as migration proliferation differentiation and the production of bioactive chemicals.

Cell Culture

Embryonic stem cells, as their name suggests, come from embryos. In our case, these embryonic stem cells will come from mice and will be cultured in a lab. These embryonic stem cells are isolated by transferring the inner cell mass, which consists of the cells inside the blastocyst, into a tissue culture plastic filled with culture medium. (Draper, Moore et al. 2004) The choice of medium will also vary depending on the cell type of interest because different cell types require different medium in order to differentiate into the desired cell type. (Imreh, Wolbank et al. 2004) Since these embryonic stem cells have the ability to differentiate into any cell type, they will require addition help when growing *in vitro*. In the mice's case, the inner surface of the tissue culture plastic dish will be coated with specific cell types that have been treated to not divide. These coating cells are known as feeder cells. Feeder cells are used in culturing to maintain pluripotent stem cells, such as embryonic stem cells, and in most cases the feeder cells are fibroblast cells. (Draper, Moore et al. 2004) The main purpose for having these feeder cells coating the bottom of the culture dish is to provide a sticker surface for the embryonic stem cells attachment, as well as providing additional nutrients into the media. Currently, researchers are trying new ways of growing embryonic stem cells without the use of feeder cells in order to prevent contamination. (Draper, Moore et al. 2004)

Stimulatory Bioreactor

Research is now beginning to show that hydrostatic forces play an important role in the regulation of structural formation during vasculogenesis and angiogenesis. The supplemental objective of this proposed project is to reproduce the actuations of the heart, delivering, in addition to needed nutrients and developmental factors, the stress forces

experienced by the cells comprising the vessel walls. Successes in the field of *in vitro* vasculogenesis have been limited to relatively small leaky capillary networks and short scaffold-supported vascular-like tubes, which, in some cases, when grafted, stimulated limited in-vivo angiogenesis (Sreerekha and Krishnan 2006). These experiments used scaffolding for structural support and/or chemical factors for the extracellular support of inter- and intracellular communications needed to support migration, proliferation and differentiation stimulating vasculogenesis. A novel design has been developed that breaks through the present barriers to the bioengineering of blood vessels. A stimulatory design of interdisciplinary conception recreates the fluid dynamics found in blood vessels and supports neutralizing the gravitational forces experienced by antigenic cells during *in vitro* development.

Dissertation Outline

This dissertation describes a method for the acquisition of data for use in the modeling and visualization of the microvascular structures occurring in lung, kidney, brain and skin tissues. The purpose of this method is to obtain the ability to mimic the specific patterns of capillary bed systems uniquely occurring in specific tissues.

After our introduction on this topic we will describe the fundamentals of vascular tree systems beginning with their biological foundation. After this introduction we will discuss the anatomy of capillary bed systems, the microcirculation of blood through these systems, and the microscopic structural anatomy of the vascular wall as its changes throughout the circulatory system.

We will continue with a discussion on the need for new techniques in scaffolding designs and in tissue culturing methods in order to produce the 3-D tissue structures sought for in tissue engineering. This will follow with an introduction the state-of-the-art in virtual, *in vitro* and *in vivo* vascular tree construction and the sustained release systems designed association with scaffolding production to assist in vasculogenesis. Afterwards will follow an in detailed discussion on the current approach being taken to reverse engineer vascular tree systems, the problems that exist in this approach and solutions proposed to date.

Next we will discuss our approach to modeling vascular tree systems that include a complete and accurate representation of tissue specific capillary bed. We will lay out our research design which includes data acquisition, issues with resolution and accuracy, resolution at different levels with different devices, merging of the data and model creation, and issues with the size of data.

Finally we will present a case study where we will create a complete and accurate capillary bed representation from the dermal layers of rabbit skin. In this case study will show the creation of a complete and accurate Bio-CAD model for the skin vasculature. This will began with a 3-D model acquisition using micro CT of a Batson's corrosion casting. This will be followed by our 3-D creation of STL models in the initial processing required in order to attain these models. We will and by using computer aided design software to convert STL models into a design for vascular scaffolding that can support the construction of vascular structures from skin.

When these unique patterns are modeled and then fabricated into tissue scaffolding, we will overcome the barrier against 3-D tissue engineering that prevents the science of tissue engineering from being fully effective for use clinical settings.

Chapter Two

Vascular Tree Fundamentals

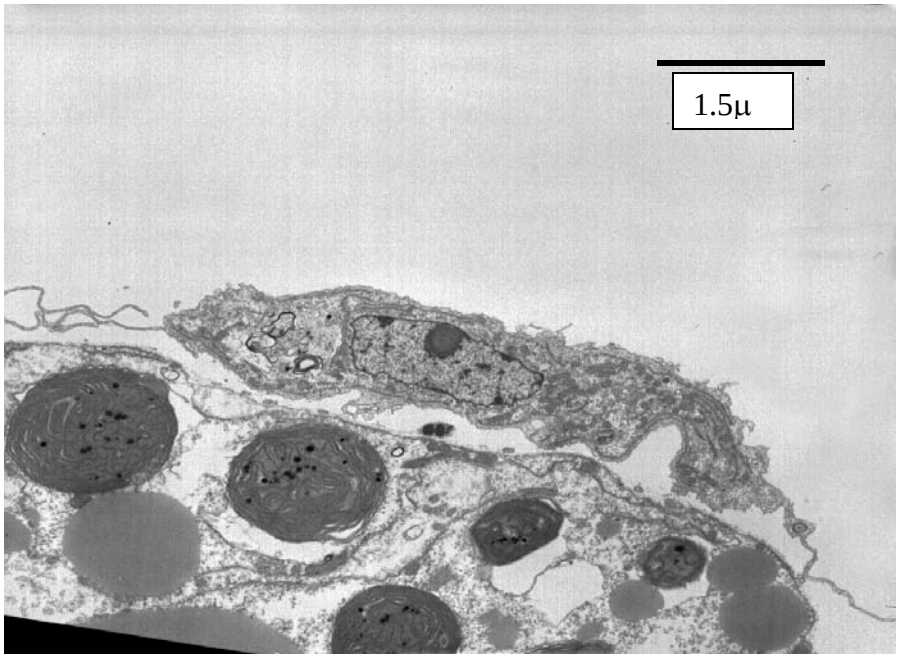

Figure 2: Free moving pluripotential Molluscan stem cell. A free moving pluripotential Molluscan stem cell that gains its nutrients from - and exchanges oxygen and carbon dioxide with - interstitial fluid that flows in the loose interstitium between organs by way of a rudimentary cardiovascular system.

Biological Foundation of Blood Vessels

The vascular tree system is the result of billions of years of multicellular environmental evolution. Beginning with cell colonies forming reproductive structure, single, free living cells began to form cooperatives where some cells became specialized with specific phenotypes that allowed the colony to form specialized structures that

enhanced the group's survival. The formation of supportive structures, reproductive structure, and feeding structures by traditional solitary cells began the movement towards the need for a vascular system. These multicellular structures formed based on metabolic needs and the restricted availability of fundamental resources such as oxygen, nitrogen and carbon. For survival in environments where these resources became low in concentration, these multicellular communities evolved to meet this challenge. We can see examples of this behavior in the colony forming, polyphyletic, slime molds (Maeda and Takeuchi 1969; Maeda 1970; MacWilliams and Bonner 1979; Bonner and Lamont 2005).

Figure 3: Free living single cellular animals. Ciliates, free living single cellular animals gain nutrients from - and exchange oxygen and carbon dioxide directly with its aqueous environment.

More advanced examples can be seen in the invertebrate phylums Porifera and Cnidaria (Wenner, Knott et al. 1983; Zrzavý, Mihulka et al. 1998). These form much larger body plans and adapt to the loss of surface area by the formation of canal like structure that make up a rudimentary circulatory system with no heart. The ciliary motion of specialized cells, along with water currents, keeps the flow of metabolites to and from the individual cell comprising these organisms. The formation of the heart along with a discreetly walled vasculature begins to form in the phylas Mollusca and Annelida (Wenner, Knott et al. 1983; Zrzavý, Mihulka et al. 1998) (Figures 3-5).

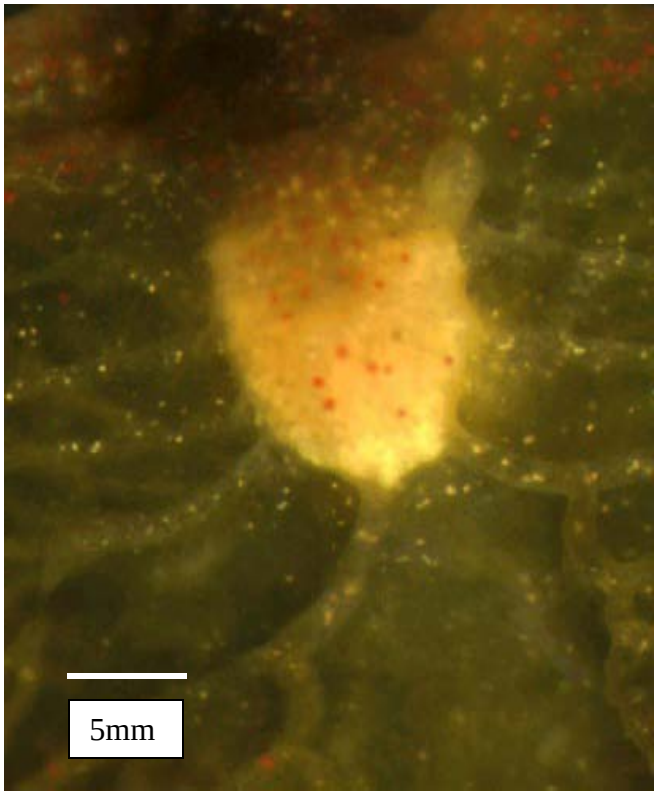

Figure 4: Open circulatory system. The two chamber heart of the sea slug *Elysia chlorotica* and its main vascular branches which lead to an open circulatory system between organs.

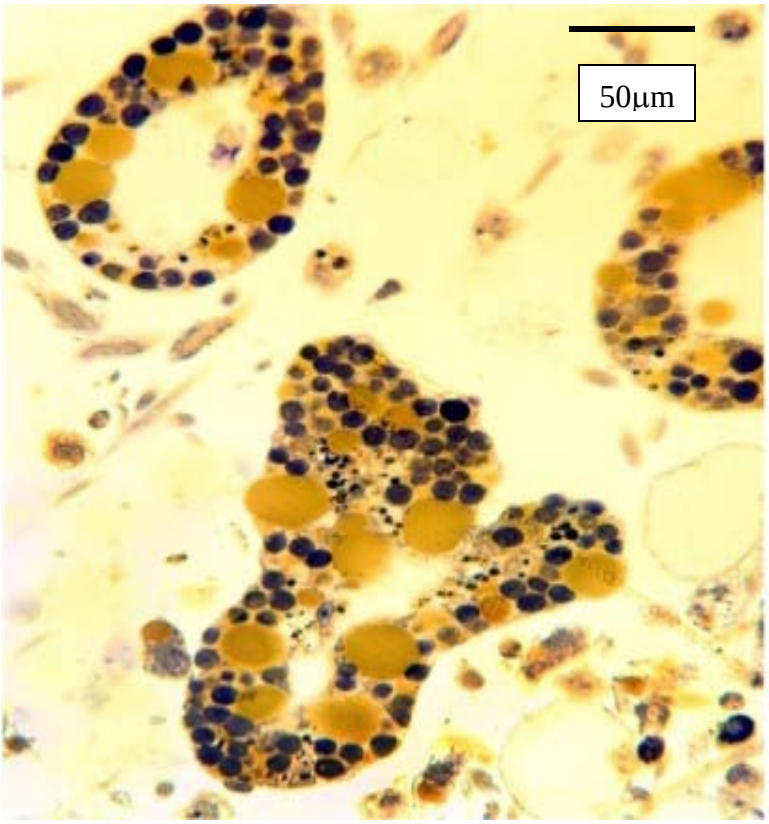

Figure 5: No capillary system. The open circulatory system of *Elysia chlorotica* has no capillary system just large sinusoidal spaces where cells and in this tissue fluid move freely to and from changing concentration gradients.

Vascular tree is a term used to describe a tubular likes system which carries blood to and from the heart. Together they termed the cardiovascular system. The cardiovascular system is one of two vascular systems found in vertebrates. The second is the lymphatic system which begins as blind capillaries that absorb and carries excess interstitial fluid called lymph back to the cardiovascular system via progressively larger lymphatic vessels that into veins near the heart.

Vascular tree systems make up two circuits in the cardiovascular system, the pulmonary circuit, which carries blood to and from the lungs for oxygenation and the

systemic circuit which carries blood to and from the tissues of the body providing oxygen and removing carbon dioxide.

The vasculature as it moves away from the heart is termed arteries. Arteries originate from the left ventricle as the aorta and branch smaller and smaller in diameter and empty into large arterioles. Most arteries empty into capillary beds via arterioles but the exceptions are the arteriovenous anastomoses. These structures are where the arteriole system bypasses capillary beds and empty directly into the venous system. In the structure of arteriovenous anastomoses the sub endothelial layers vary from that of normal arteriole and venules. You find in these layers plump polygonal longitudinally arranged smooth muscle cells and a thick tunica media. When the smooth muscle cells contract blood flow is cut off from going directly into the venous system and is forced into the nearby capillary beds. The vasculature that drains the capillary beds is called venules and as they get progressively larger in diameter they are called veins and finally terminate in the right atrium of the heart.

The Anatomy of Capillary Bed Systems

While, there are some common characteristics in the capillary bed system between organs, each organ has its own unique features. The capillary bed system of each organ has a unique design and in order to understand an organ you must be able to truly understand and visualize the structure of its capillary bed system and how it relates to the organ's complete vasculature (Figure 6).

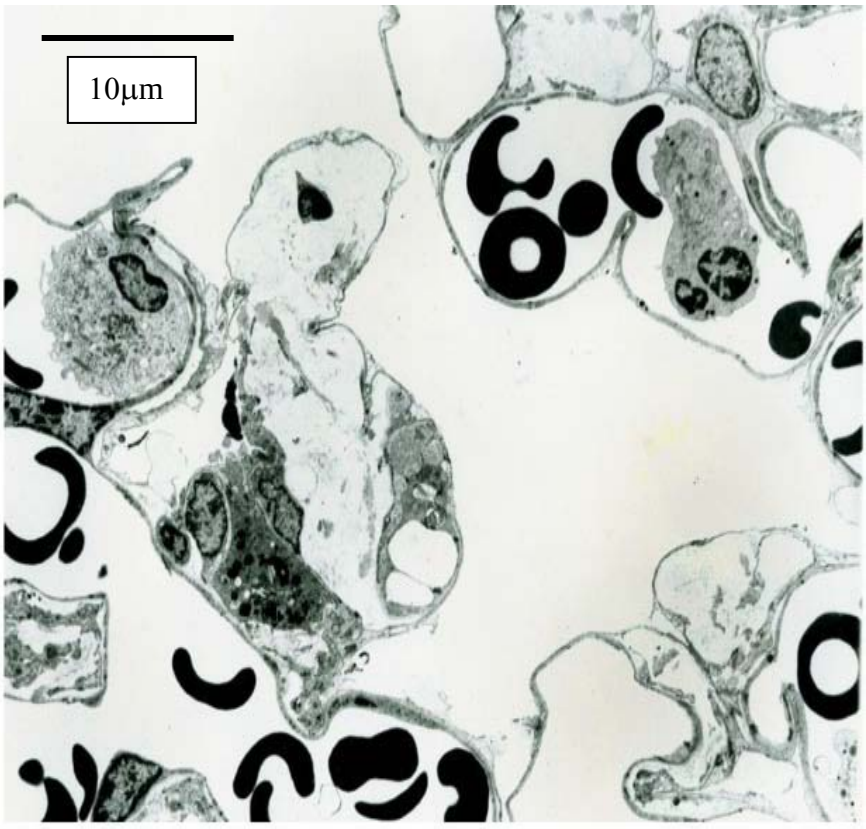

Figure 6: Perialveolar capillary spaces. Electron micrograph of lung tissue showing the perialveolar capillary spaces fill with leukocytes that protect the from invading organisms and red blood cells which exchange carbon dioxide for oxygen from the external environment.

Capillary beds are thin walled vessels responsible for the transport of gases, nutrition, metabolic waste, hormones and signaling molecules into and out of the intercellular spaces (Figures 7&8). The driving force for the movement of these materials is a combination of osmotic pressure and hydrostatic pressure. Crystalloids or molecules in true solution, and Colloids, molecules suspended in solution create the osmotic gradients that exist between the fluid and blood vessels and the interstitial or tissue fluid.

The concentration gradient of crystalloids alone does not create high enough of osmotic force to cause any diffusion across the walls of the capillaries, but the high

colloid concentration in the blood stream wants to pull tissue fluid into the capillaries. The hydrostatic pressure created by blood being pumped through the vasculature is a high at the arterial end of the capillary beds. This hydrostatic pressure over comes the osmotic pressure and drives blood plasma through semi permeable membranes between or within fenestrations endothelial cells at the arterial and of the capillary bed. As blood reaches the venous end of the capillary bed and hydrostatic forces drop considerably and are overcome by the colloid osmotic force within the capillary, which causes interstitial fluid to diffuse back into the capillary lumen.

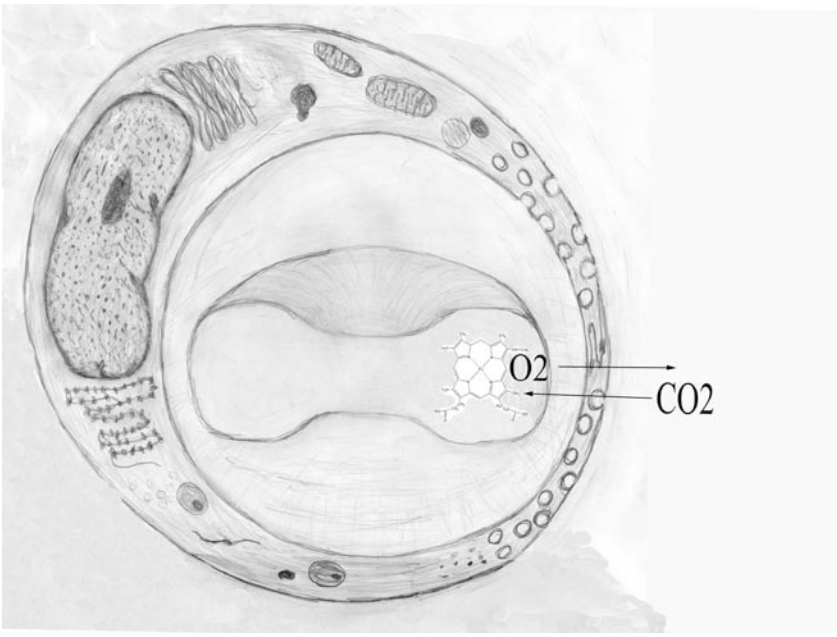

Figure 7: Typical capillary wall. A cross sectional drawing of a endothelial cell comprising the typical capillary wall and a red blood cell containing hemoglobin which participates in the gaseous exchange between the interstitial fluids between a cell's which make up the body's tissues and the body's external environment. (Illustration done by William Mondy)

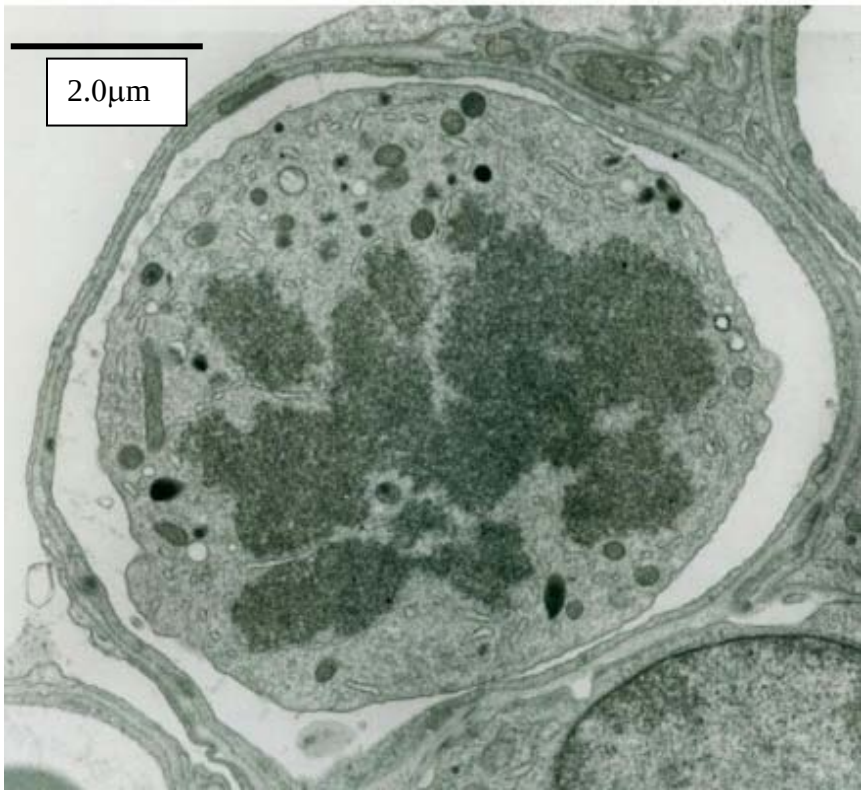

Figure 8: An alveolar capillary. While moving through an alveolar capillary in the lung a lymphocyte undergoes mitosis in response to an exposure to a bacteria toxin.

Microcirculation

The volume flow of blood being pumped from a heart at any given time creates variable forces on the blood vessel's walls. The structural properties of blood vessels are regulated by the internal blood forces and external structural forces exerted on them by the surrounding tissues. From a physiological point of view capillary blood flow and sometimes the neighboring arteriole and venules blood flow are considered to be the microcirculation of the cardiovascular system. The distance extending to and from the capillary bed the arteriole and venules blood vessels are to be considered as part of the

characteristics of a microcirculatory system are: a lower concentration of blood cells than you will find and larger vessels, decrease and apparent viscosity, the movement of fluid out of and back into the capillary lumen, a greater chance for activated leukocytes to attach to the vascular wall because of the narrowing of the lumen, increased in the proportion of smooth muscle cells composing the vessel wall. Smooth muscle cells are important factor because their contractile properties regulate the vessel's diameter, flow resistance and pressure gradient.

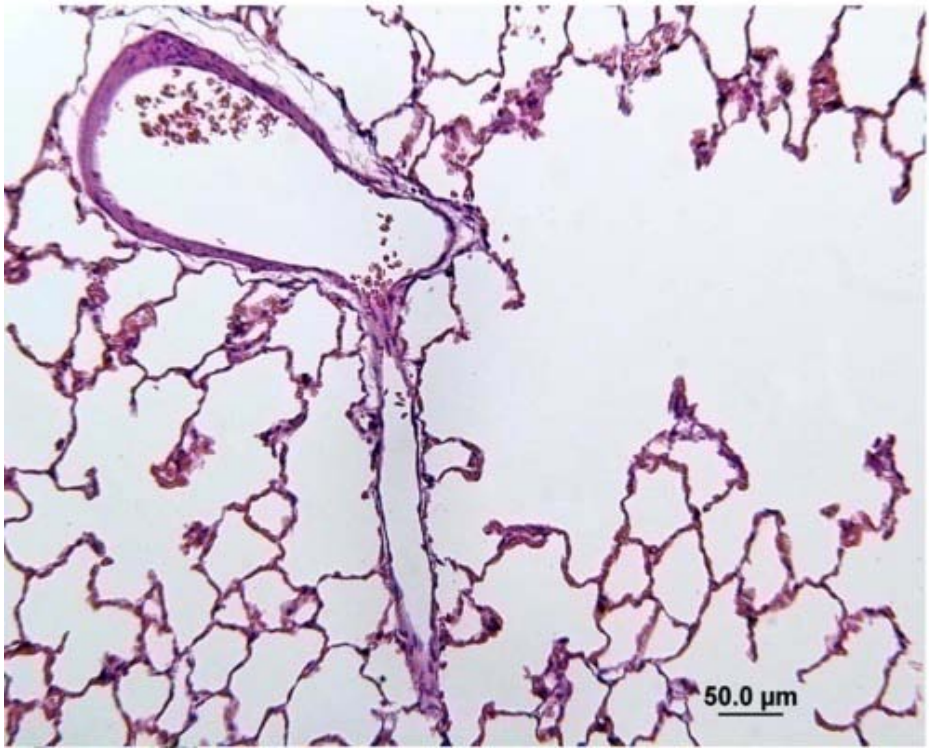

Figure 9: Perialveolar capillaries. Photomicrograph of a large artery and one of its medium-size arteriole branches shown contributing blood to the perialveolar capillaries in this histological section of mouse lung.

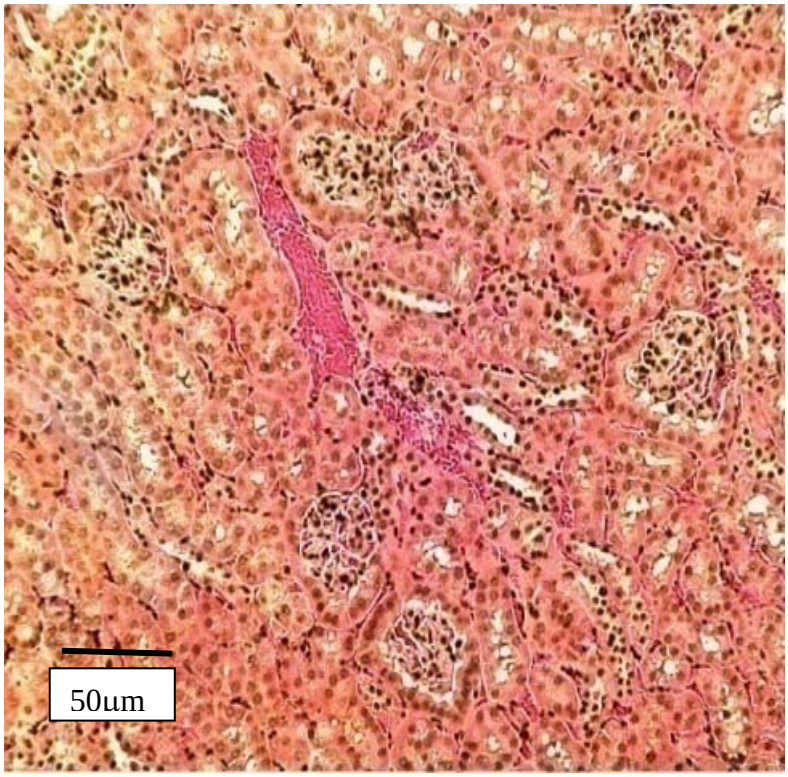

Figure 10: Arteriole branching into glomeruli. A blood fill arteriole is seen branching into a number of glomeruli for the removal of metabolic waste from the blood's serum by way of the fenestrated capillary system found in the glomeruli.

Anatomy of the Vascular Wall

With the exception of capillaries the walls of blood vessels are broken down into three concentric layers of tissue called tunics, the tunica intima, the tunica media and the tunica adventitia. The tunica intima is the innermost layer and consists of a single layer of squamous endothelial cells surrounded by sub endothelium connective tissue. The endothelial cells secrete this connective tissue in the form of types II, IV, and type V collagens. They also secrete lamin, nitrous oxide and a host of angiogenic factors as well as presenting several membrane-bound enzymatic proteins and protein receptors whose

interactions regulate metabolic and cellular behaviors. The internal elastic membrane or lamina, a thin well-defined band of elastic fibers, is the outermost part of the sub endothelial connective tissue. The elastic lamina is made of elastin and is fenestrated to allow nutrients to diffuse deep into the walls of the larger blood vessels. Capillaries consist of only this layer. In capillaries and post-capillary venules the tunic intima is intermittently surrounded by pericytes. Some investigators believe that pericytes are precursors to smooth muscle cells and other investigators believe that pericytes are specialized fibroblast.

The tunica media consists of helically arranged concentrically orientated smooth muscle cells and where it exists it is the largest of the three layers. The smooth muscle helix begins at a 30° angle to the vessel's center line in large arteries (Medvedev, Samsonov et al. 2006). This angle increases as the diameter of the blood vessel decreases until it reaches an angle of nearly 90° in arterioles as they approach the capillary beds. In addition to smooth muscle cells, there are elastic fibers, type III collagen and proteoglycans. The fibrous structures form lamellae within the amorphous gel like substance secreted by smooth muscle cells into the extracellular matrix. In larger arteries that tunica media is surrounded by an external elastic lamina. This membrane is also made of elastin but not as well defined as an internal elastic lamina.

In larger blood vessels the thickness of the muscularity prevents adequate diffusion of substances from the lumen of the blood vessel to the far-reaching smooth muscle cells and the tunica adventitia. In these cases tunica media and the tunica adventitia needs to be supplied nourishment by their own vascular system called the vasa vasorum. Because

venous blood is less oxygenated and contains a lower nutrient concentration than arterial blood, the walls of veins have more cells that cannot be supplied these factors by diffusion. Because of this reason the walls of veins are more vascularized by the vasa vasorum than those of arteries.

Sympathetic vasomotor nerves innervate the smooth muscle cells of the vascular system and are responsible for vasodilatation. Arteries in contrast to veins have higher

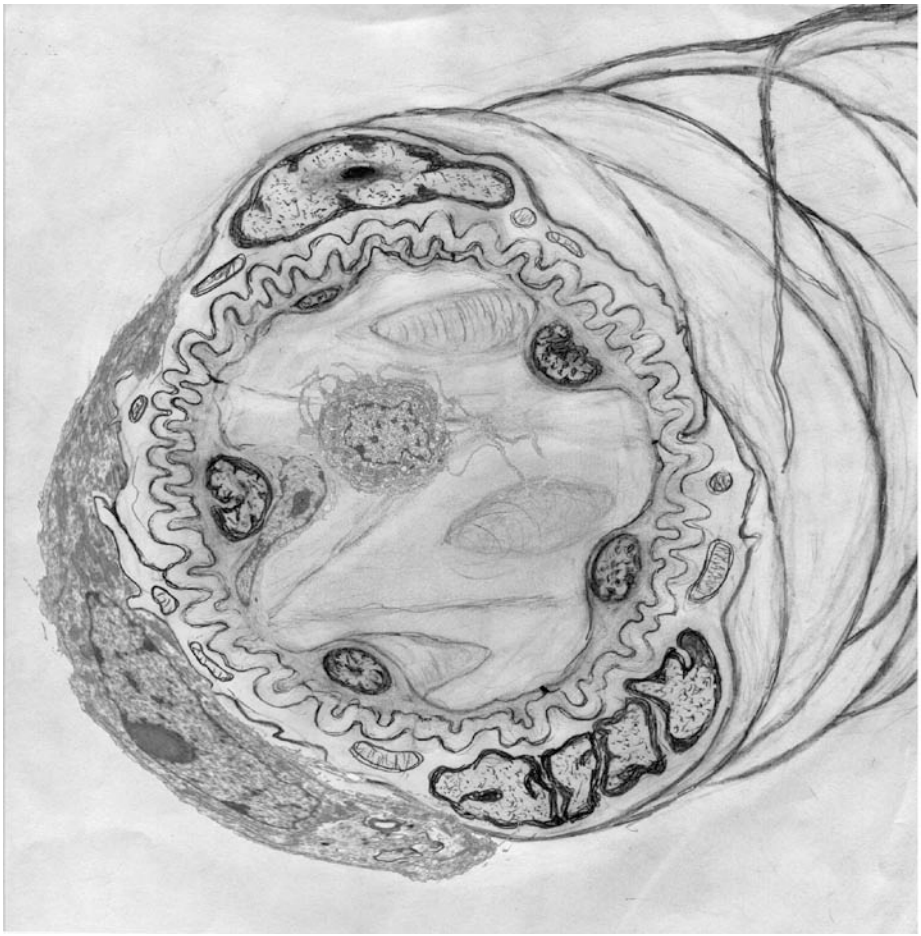

Figure 11: Illustration of small arteriole. Drawing of a small arteriole illustrating the endothelial cells lining, basal layer of connective tissue, a single layer of smooth muscle cells and a pericytes wandering upon of vessels outermost surface. (Illustration done by William Mondy)

numbers of these non-synaptic nerve endings which use norepinephrine as a neurotransmitter.

The tunica adventitia is the outermost layer of blood vessels and consists of fiber elastic connective tissue, type I collagen, fibroblasts and longitudinally orientated elastic fibers. The connective tissue found in this layer is continuous with the connective tissue of the surrounding structures.

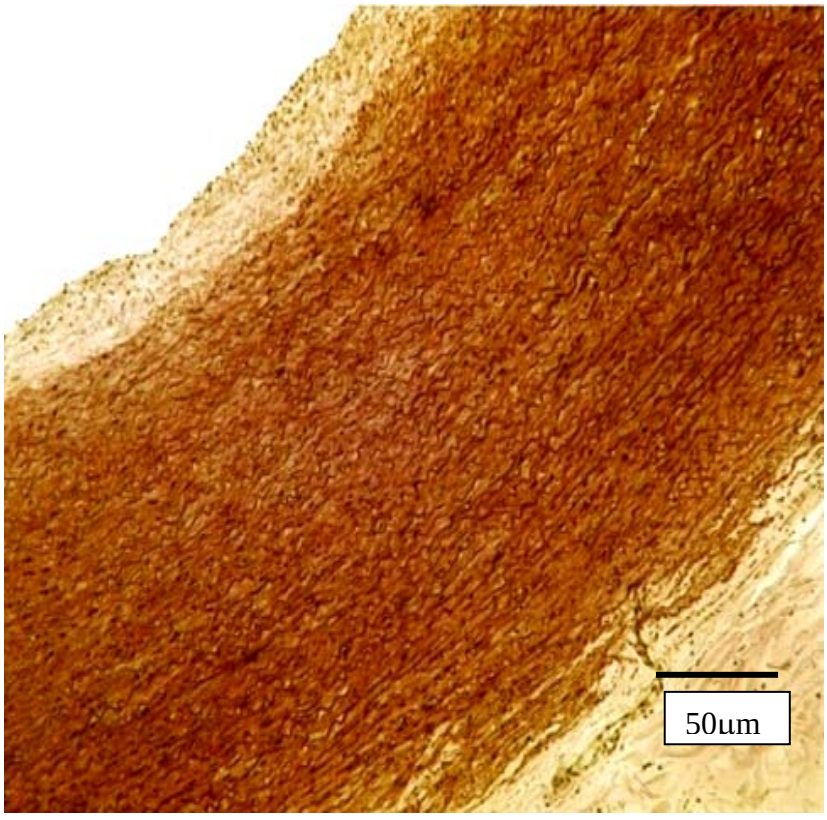

Figure 12: Wall of a human aorta. A photomicrograph of a histological section cut across the wall of a human aorta. Majority of the structure is tunic of media, consists of smooth muscle cell layers alternated of elastic connective tissue. We can see in the bottom right-hand corner this vessels owned blood supply source, the vasa vasorum, moving through the tunica externa.

You have two types of arteries that carry blood away from the heart, elastic or conducting arteries and muscular or distributing arteries. The aorta and the large arteries originating from aortic arch are elastic arteries (Figure 12). The main characteristic distinguishing them from the large blood vessels are the many concentric layers of fenestrated membranes distributed evenly through smooth muscle cells of the tunica media. The rest of the major arteries are muscular arteries characterized by tunica media consisting of mostly smooth muscle cells. (Figure 12-14)

The arteries feed into two types of arterioles, large arterioles with two to three layers of smooth muscle cells and small arterioles with one layer of smooth muscle cells (Figure 17). Specialize arterioles which regulate blood flow into capillary bed systems have

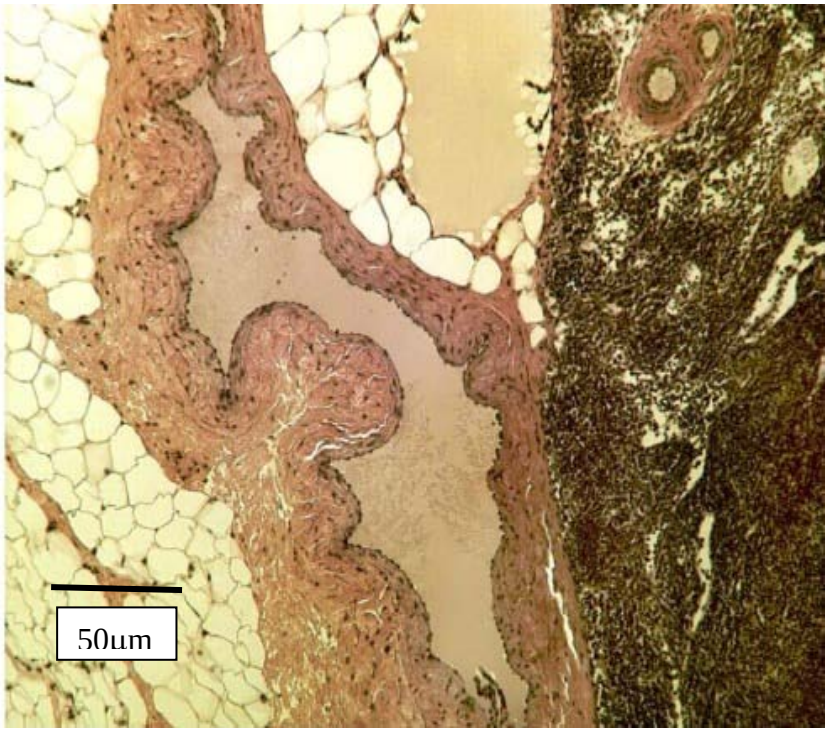

Figure 13: Photo micrograph demonstrating a large vein. Notice how it structure differs from the artery. The vein's muscular tunica media is irregular in thickness and needs not maintain a symmetrically patent lumen. In addition the tunica externa's thickness is very inconsistent and is surrounded by adipose tissue.

uniquely arranged smooth muscle cells designed to form pre-capillaries sphincters. When these sphincters are closed blood is divergent from the capillary directly into venules.

There are three types of capillaries: continuous capillaries, where the endothelial cells are connected with tight junctions. These are found in muscle, connective tissue and nervous tissue; a fenestrated capillary whose cytoplasm contains pores connecting the capillary lumen to the sub endothelial connective tissue spaces, separated by an ultrathin

Figure 14: Fluid flow through the body's tissues. Photomicrograph we can see the passageway's for all three directions of fluid flow through the body's tissues. In the lower center we had a medium-sized artery, above a medium-sized veins and to the right of the artery a very thin walled lymphatic vessel which returns interstitial fluid, that comes into the tissue from capillary bed's, back to the blood stream at a specialize entry point near the heart.

diaphragms. These are found in pancreas intestines endocrine glands and are part of a carrier mediated transport system for amino acids nucleotides glucose and other necessary metabolic molecules of that size order; sinusoidal capillaries which have endothelial cell whose boundaries are irregular and conform to the shape of the surrounding tissue structure. Sinusoidal capillaries form irregular blood pools and have diameters from 30 to 40 µ. Sinusoidal capillaries are found in the spleen, liver and bone marrow.

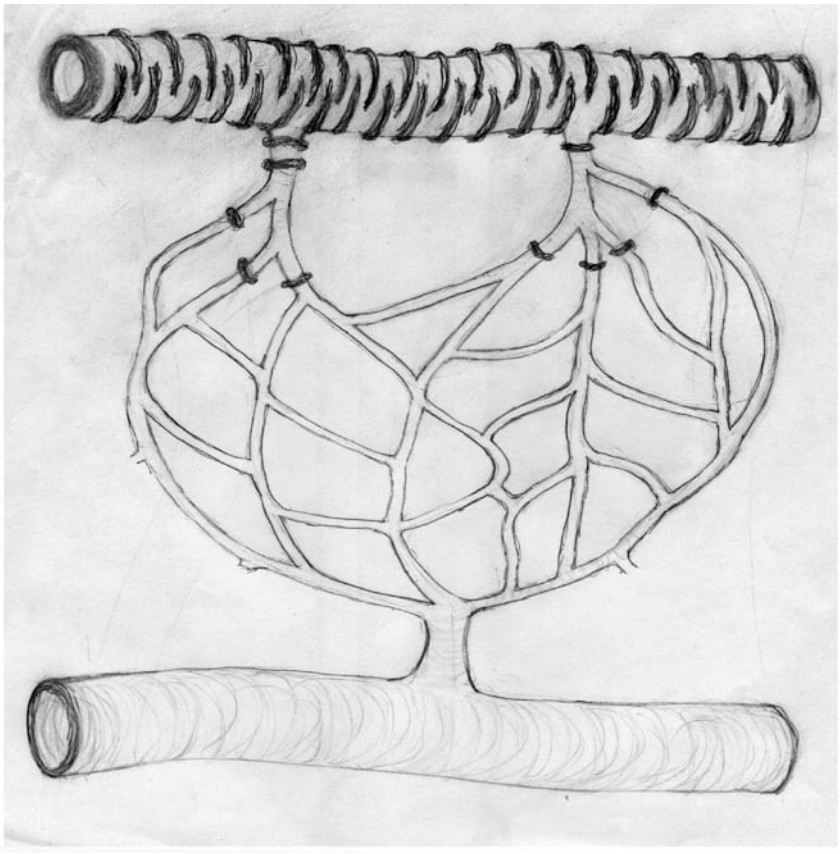

Figure 15: Capillary bed system and its associated arteriole and venules. The artery is on the top and is surrounded by pericytes with contractile properties. Pericytes at entry points to the capillary bed system create sphincters and regulate whether or not blood flows into the capillaries these sphincters. can force the blood flow to bypasses the capillaries to go directly to the venous system. (Illustration by William Mondy)

The venous return of the vascular tree system is under at much lower static pressure than the arterial supply system. Because of this their walls have less elastic membranes and many fewer layers of smooth muscle cells. The lumens of veins as well as the number of veins are much larger than those of arteries and at any given time 70% of the body's blood is in the venous system. Blood that is discharged from capillary bed systems moves into the post capillary venules. These venules range from 15 to 20 μ in diameter. Their walls, as we described earlier, are similar to capillaries except he Their tunica intima has endothelial cells with a basal lamina consisting of reticular fibers and sometimes elastic fibers, but not the fenestrated elastic lamina found and arteries. The smooth muscle cells of the tunica media are in loosely woven layers with the extracellular

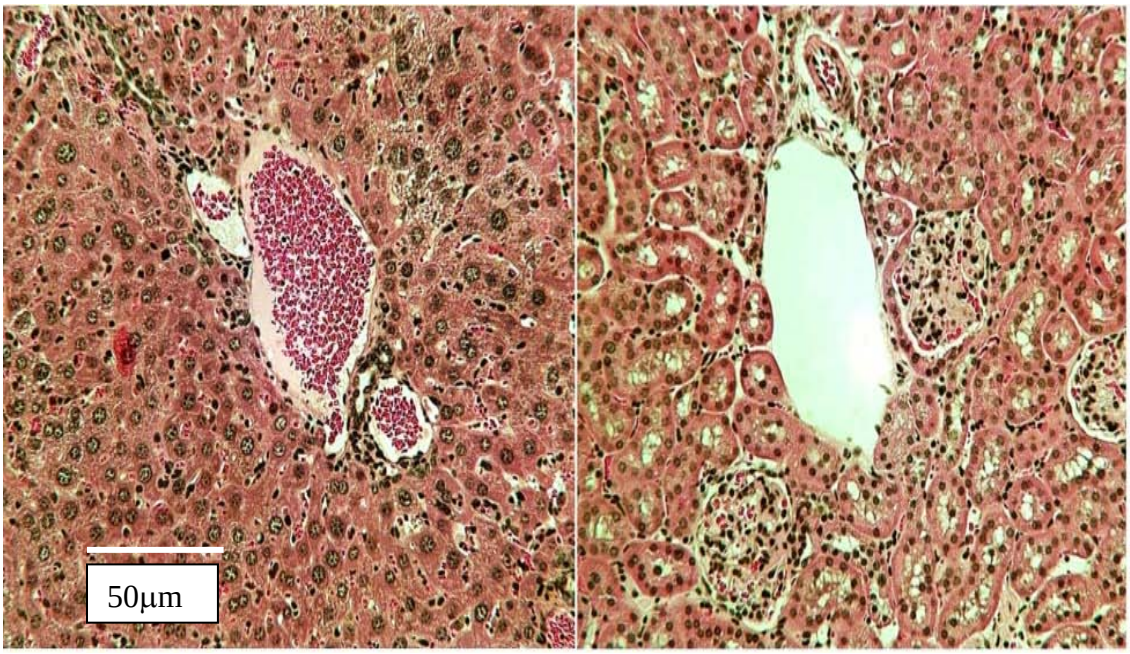

Figure 16: Capillaries of the liver and kidney. These two photomicrographs demonstrate the difference is in the capillary flow patterns in two different tissue types. On the left we have a very loosely organized sinusoidal capillaries system in the liver. On the right is the much directed capillary system of the kidneys that form specialized structures called glomeruli.

matrix of collagen secreted by the numerous fibroblasts (Figure 18). Large veins that return the blood directly to the right atrium of the heart have a much thicker sub endothelial layer and you will find in medium-size veins (Figure 18). This is due to the presence of fibroblasts and a network of elastic fibers. Well developed smooth muscle layers can only be found in the pulmonary vein and the superficial veins of the legs but the tunic of media is absent in all larger veins. This is replaced by a much larger than normal tunica adventitia abundant with elastic fibers and collagen. In specialized large veins longitudinal layers of smooth muscle cells can be found in tunica adventitia layer. Another unusual characteristic seen in the tunica adventitia of large veins is the occurrence of cardiac muscle cells in this layer as pulmonary vein approaches the heart.

Figure 17: The medulla region of the kidney. Illustrated here is a large arteriole to the left caring red blood cells in its lumen. To the right of the arteriole is a venule.

Extracellular matrix for blood vessels forms the structural framework which supports the cells that compose and maintain blood vessels. The types and amount of these material is specific to the type and size of blood vessel, and the region of the vessel wall in which the matrix occurs (Figures 18 & 19). These extracellular support structures are protein and glycoproteins with specific peptide sequences that have some effects of cell behavior, (Merzkirch, Davies et al. 2001; Santiago, Nowak et al. 2006; Polizzotti, Fairbanks et al. 2008; Weber and Anseth 2008)An examples is type I collagen, the glycoprotein tropocollagen. It occurs in nano fibers that are 1 to 12 μ in diameter.

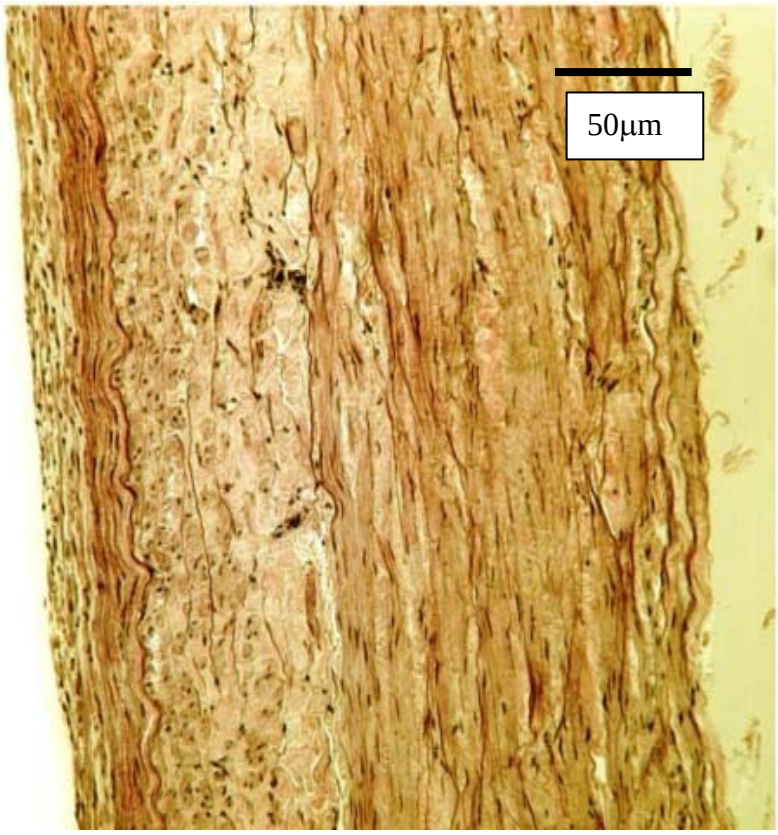

Figure 18: Longitudinal cut through a large venule wall. This photo micrograph shows a longitudinal cut through a large venule wall. You can see the organizational differences between smooth muscle cell layers of the Tunica media. Also evident in this micrograph is a very distinctive elastic component to the connective tissue layer of the tunica intima.

Its molecular structure consists of galactose and glucose, 1/3 glycine and 1/3 hydroxylproline proline. Another important example is elastin which is composed of elastic fibers, 80 -160nm in diameter. Elastin is high in glycine and contains eight other amino acids. The main amino acids are desmosine and Isodesmosine. Non polar amino acids are intermolecularly cross linked by desmosine which binds four elastin chains. We eventually want to create a scaffold design that incorporates the structures and properties of these extra cellular matrix components.

Figure 19: Large artery supplying blood to skeletal muscle. This micrograph demonstrates a relatively large artery supplying blood to skeletal muscle Seen to the right. What is distinctive about this blood vessel is the extensive amount of elastic connective tissue extending from the outer layout the tunic of media deep into the connective tissue of the tunica externa. This additional elastic tissue and its web like pattern allows for changing stress felt on the structure during muscle contraction and relaxation.

Need for New Techniques

In vitro vasculogenesis has been unable to reproduce with structural specificity the specialized morphological structure of capillary beds needed in such tissues as lung and kidney. Scaffolds have been designed and created for blood vessels but these scaffolds have been used to make large straight tubes of a constant diameter (Bergers and Song 2005; Song, Ewald et al. 2005). Not much branching and no complex of small vessels or capillaries of any sort (Stitzel, Liu et al. 2006). Many have taken an approach using mathematical models to compute the anastomosis patterning found in the vascular branching systems. Others have created models using physiological behaviors such as angiogenesis to recreate the structural branching patterns found in microvasculature. These attempts lacked the structural design millions of years of evolution has established in creating vascular structures. The realization of a need for more detailed designs is demonstrated in the recent use of lithography to pattern channels designed structurally to simulate extra cellular matrix fibers' role in guiding cellular and cytoskeleton structural alignment (Sarkar, Lee et al. 2006).

Some have created models of physiological behaviors such as angiogenesis to model the structural pattern of microvasculature(Szczerba and Szekely 2005). These attempts at modeling the branching pattern of a vascular tree, an afferent - efferent blood vascular system that includes the capillary bed, fall short in being able to reproduce the structural specificity needed for specialized tissue structure found in tissues such as lung, kidney and skin. A vascular tree scaffold is needed; one whose design can be reverse engineered to mimic the structural design of selected *invivo* vascular networks that can be

bioengineered both chemically and cellularly to promote the genesis of a replica vascular tree system which includes its capillary structures.

It is difficult to quantify the exact volume flow rate in the vasculature system using mathematic equations, $Q = V(nA)$ (Volumetric flow =Velocity X (cross sectional area)), because in the blood stream flow forces are not constant. The heart beats in rhythms that are constantly changing; the volume from a heart beat will also change; the hematocrit changes as vessel diameters vary; blood vessel branching is irregular and organ specific; the characteristics of the boundary layers are constantly changing along the blood's flow path. These are just a few of the constantly changing variables that challenge bioengineers to come up with models that can accurately reproduce just a fundamental biomechanics of circulation. Mathematically complex equations are derived in an attempt to model numerically biological structures and activities such as volume blood flow through capillary sheets of the alveolar sacs. Currently the velocity flow sensors can only determine instantaneous velocity. By the change the electrical charge measured between a pair of electrode across the diameter of a vessel blood from each other (Sun 2005), an ions deflected by a magnetic field crossing the vessel in the same plane where the electrodes are attached has a velocity at that instant of:

$$\mu = \frac{v}{\beta \ell}$$

Where v is the voltage due to the ions deflection, registered by the electrode β is the force of the magnetic field and ℓ is the diameter of the blood vessel at that instant. Another technique uses convection temperature cooling of a metal placed in contact with

the blood flow predicting what the relative rate of flow would be as compared to the rate of cooling.

Subsequent *in vitro* constructed blood vascular system will form the structure necessary for tissue engineering. This bioengineered structure will increase cell to cell adhesion interactions shown necessary for proper vessel formation (Redmond, Cahill et al. 1995; Weber, Rossi et al. 2002). These methods at determining the velocity of blood flowing through the circulatory system are an efficient at accurately providing the appropriate data for structural modeling vascular tree systems. And more efficient way is needed to mimic the structural specificity of circulatory systems found in tissues. In addition none of these methods devised consider that each organ has a unique vascular pattern that is essential for the functional morphology that characterizes the cellular structure of each organ.

Bio-CAD modeling and its application towards computer aided tissue engineering (CATE) is extremely dependent on the state of the technology in the computer imaging field, modeling software design and computer hardware technology. Neither the vascular tree system nor any part of the human anatomy can be defined mathematically or traditionally through engineering terms. Micro-CT's use of the image data acquired through x-ray slices of anatomical structures produces a high resolution reconstruction of microvascular structures. The combination of these techniques has been used in the solid freeform fabrication (SFF) of tissue scaffolding. But neither an ideal scaffold nor a functional transplantable organ structure has yet to be created. The greatest success has been seen, because of its high acellular morphology, in trabecular bone structures. But

even bone has an extremely important microvascular system which supports a cellular system which constantly senses stresses and re-models structures to suit environmental cues. The 3-D reconstructions of serial histological sections have been shown to introduce two types of artifacts the first artifact being from tissue processing which involves fixation, dehydration and embedment. Each of these steps introduces at some level a degree of distortion or loss of tissue structure. Frozen sections have been used as an attempt to elude many of these processing artifacts. But this will not correct the second type of artifact's scene in 3-D histological section reconstruction. That is the errors that occur doing the alignment of serial sections. The combining of micro CT sections with histological sections has been used to increase the detail lacking from CT sectioning while correcting for the error is in alignment of histological serial sections. These methods do not address the need for a complete microvascular system that includes a complete and accurate capillary bed reconstruction. The synthetic vascular patterns have been synthesized using constrained constructive optimization methods. But this method does not produce the organ specific microvascular patterning and needed to create tissue scaffolding capable of sustaining a tissues construct for transplant therapy. The field of computer aided tissue informatics needs the introduction of accurate renderings of these structures.

While voxel based representations of anatomical images can accurately represent many structures in 3-D voxel based images cannot be effectively use in vascular tree modeling. The 3-D volumetric model though realistic and this anatomical appearance does not have the geometric topological data to make it transferable for many engineering analysis programs. The voxel bounding service is created most popularly by the

marching cubes algorithm which produces triangle based tile is a service elements each tile is treated as a severed polygon and then on the size and the degree of detail that you want to represent the resulting models can be enormously data intensive. Attempts have been made a to integrate STL base models into computer aided design systems tissues boundary representation described by Non Uniform Rational B-Spline functions. But no one has developed software to construct the CAD-based models from medical images. Wei Sun in 2005 tested three different processing paths for their ability to bridge the gap between medical image data and CAD design models.

The first processing path uses the software MedCAD to interface medical imaging systems with CAD platforms. It uses three different file formats: International Graphic Exchange Standard (IGES), Standard for Exchange of Product (STEP) and stereolithography (STL). This software uses primitives such as planes and spheres to fit to the surface of the 2-D segmented slices during volumetric reconstruction. It also uses and limited free-form surface modeling allowing taking advantage of B-spline's. The problem with this software is it's incapability of re-creating geometrically complex anatomical structures.

The second processing path uses a reverse engineering interface approach which converts the 3-D voxel based model to point cloud data. Geomagic Studios by Raintree Inc. uses this method. Geomagic creates point clouds and applies triangular facets to its surface. The resulting surfaces can undergo further image processing removing or adding triangular facets in order to enhance or decimate the triangular surface or to remove or make addition to features. This can be used to decrease the file size dramatically.

Freeform patches of NURBS can be fitted across the outer surface of the model. Sun reported this to take a longer time to process but the results obtained appeared to be better than the other two processing paths. The third processing path uses STLs triangulated models directly imported into the integrating software. The problem with this method is that doing the transfer process errors in triangulation assignment will cause imperfections in the resulting surfaces.

If large tissue constructs for transplant therapy are to be produced using stem cell-based construction of regenerative structures microvascular structures will need to be designed that have complex hierarchical structural heterogeneity, the foundation of which must be the vascular tree lumen. Once this is realized, bioactive requirements can be incorporated in a scaffold's design and a model of the microvascular tree system as well as the larger vasculature can be produced that accurately mimics the ultrastructural requirements for the extracellular matrix which supports the cell morphology and the mechanical requirements needed in these structures. The results would be the first step in creating a bio blueprint for vascular tree production that mimics the description of the microscopic anatomy for an entire organ specific vascular tree. Including but not limited in this description will be the necessary components to regulate cell division, cell adhesion, cell motility, cell morphology and the mechanical properties.

The resulting vascular tree models will contain microvascular data that can be useful organ specific microvascular vessel primitive constructions for the creation of software capable of modeling the vascularization of organ structures on top of which scaffolding

can be designed to support the systemic cells for that specific organ. Presently no such designs have been created that mimic the actual capillary bed structure.

Scaffolding

There are so many experimental techniques being developed today to produce tissue scaffolding that can be applied to scaffolding for vascular trees systems. These scaffoldings are made porous, biodegradable by cellular enzymes or semi-made out of naturally occurring extracellular matrix molecules. Scaffolds are constructed out of forms of carbohydrate polymers such as thiolated methylacrylamide chitosan to which peptides can be covalently attached to regulate cell adhesion and other types of cell behavior.

Most promising form of scaffold production through which our method of capillary bed design a can take direct advantage of is Multi photon three dimensional nano fabrication. These systems are being developed to use two and three photon lasers guided by CAD integrated systems to create patterns in photosensitive matrixes. These laser systems can selectively activate the electronic excitation of sensitive atoms sending electrons from their ground state to excitation energy levels. The results are photopolymers whose features are only restricted by the converging lasers' focal spot size. Investigators are using this technique to create specific chemical morphological properties in micro-patterned environments. There is a need for Bio-CAD models that take full advantage of these new technologies. Our method for mimicking microvascular system uses Bio-CAD for the creation of microvascular systems that mimic organ specific capillary bed designs, merging these techniques with the dynamic cell

environments produced by state-of-the-art bioreactors. Adapted these new technologies to our new method for tissue scaffolding designs will place us at the beginning of a new and revolutionary era for tissue engineering.

Vascular Tree State of the Art

Many have taken an approach of using mathematical models to compute the anastomosis patterning found in the vascular branching systems (Volkau, Zheng et al. 2005; Volkau, Ng et al. 2008). Others have created models using physiological behaviors such as angiogenesis to recreate the structural branching patterns found in microvasculature (Szczerba and Szekely 2005; Szczerba and Szekely 2005). Morphological data has been used to construct or view 3D images of vascular tree systems (Kassab, Rider et al. 1993; Lametschwandtner, Minnich et al. 2005; Szymczak, Stillman et al. 2006; Yu, Ritman et al. 2007).

High-Quality Vessel Visualization (HQVV) is a method used on radiological data to (Hahn, Preim et al. 2001). This method uses the image processing pipeline that begins by analyzing vessels to acquiring: volume data, vessel segmentation, skeletonization and diameter analysis, and graph analysis (Selle, Preim et al. 2002; Frericks, Caldarone et al. 2004). This follows with visualization and interaction tasks that enhanced the skeleton by pruning and smoothing the visualization using filtering diameter scaling expansion and could collapse the sub trees control and quality of the visualization output.(Hahn, Preim et al. 2001). Supplementation with factors which have been determined to be necessary in the growth and differentiation of blood vessels (Chupa, Foster et al. 2000; Ehrbar, Djonov et al. 2004; Rolny, Lu et al. 2005; Teknos, Islam et al. 2005; Vogel 2005;

Pollard, Parsons et al. 2006; van Meeteren, Ruurs et al. 2006) need to be incorporated into vascular tree scaffold to help produce the desired results. In addition, a cast of cells must be directed to play their role in this production stimulating through cell adhesion the necessary proliferation and differentiation at the proper cues (Takakura 2006). Producing cytokines and chemokine necessary for the needed responses and or products required for functional vessel formation.

One state-of-the-art visualization technique allows vessel analysis to be carried out by segmentation skeletonization and graph analysis where visualization and interaction techniques that represent vascular structures in a hierarchical manner can be applied (Hahn, Evertsz et al. 2003). Smoothing is done to remove undesirable effects seen in curves and branching structures re-created using these visualization techniques. Open GL extrusions using a library of graphic primitives are used to produce recursive tree structures. Wire frame models at polygon shaped representations use or create leaf branches in some techniques. Vessels cannot be filtered based on diameter using a bottom-up or top-down approach controlling the complexity and the inclusiveness acquired vascular tree data used in constructing a model. Different emphasis can be placed on a sign variables such as radius or coded data for entire branches. This method of visualization of radiological images can be used to assist surgical procedures (Hahn, Evertsz et al. 2003).

Another useful modeling method lumps parameters together such as those measured in the fluid dynamics large blood vessels. This is a segmented at bifurcations or try vacations and each segment is characterized like an electrical circuit. Characteristics

such as resistance, induction, and tension are used mathematically to represent physiological factors such as pressure and fluid flow and consequently branch by branch anti-vascular tree system is modeled using hemodynamics. Using this method researcher can model alterations related to cardiopulmonary bypass surgeries. Changes in continuous flow, temperature, hematocrit oxygen consumption, protein concentration, can all be measured and these simulated vascular models (Lanzarone, Liani et al. 2007) Non-Uniform Rational B-Splines (NURBS) models have been created from image data and used for patient specific iso-geometric analysis (Zhang, Laufer et al. 2009). This builds on previous work using sweeping methods medial axle base mesh generation and NURBS mesh generation. In this method traditionally image processing is used to enhance the image quality. This is followed by iso-contouring and geometry editing, path extraction, path-based meshing and solid NURBS construction, from which iso-geometric analysis can be done (Zhang, Laufer et al. 2009) In order to create the blood vessel from solid NURBS's patches the vessel's geometry is first extracted. Then, using a thinning algorithm, a skeleton is created from the resulting point cloud image. A skeleton is then swept using a sweeping method, which uses a templated circle at each cross-section. Branching templates can be created demonstrating bifurcations try vacations with a number different variations (Zhang, Chapman et al. 2005). In the cross-section meshes fluid and solid regions can be identified and giving characteristics for iso-geometric behaviors.

A third design approach for modeling vasculature integrates shapes and biomedical attributes (Li, Regli et al. 2007). Normally computer aided vascular tree models come from either biomedical imaging of discrete shapes or physiological models that rely on

biological understandings of blood vessel growth. Instead of modeling solid segments with different attributes the vasculature is represented as tubular structures of varying degree of complexity. The goal being the creation of parametrically designed vascular scaffolds which can supply required nutrients and oxygen supply to larger tissue scaffolding. The biomedical models are represented using skeletons, implicit designs, boundary representations, voxel based representations, and mesh based models and volume sweep modeling. The vascular tree is represented on two scales, macro and micro, each having its limitations (Li, Regli et al. 2007). The macro scale representation uses nodes and edges to create a vascular tree in a structural hierarchy. A sweep is applied to generate a volume representation which alone cannot support a secondary tissue scaffold for functional tissue growth. The micro scale representation must be confined to a sub-boundary within the generated macro scale vasculature. This sweeping procedure to edges between nodes of micro scale vascular incorporates the basic features of vascular system and their relationships (Li, Regli et al. 2007). Features such as blood flow rate, viscosity, segment length, blood vessel radius, changes in blood pressure and resistance to blood flow are all incorporated into the functions computed in a sweeping volume representation of a vascularized structure. NURBS curves are fitted to complex branches of the microvasculature. Prior representations use straight lines to represent each edge between nodes (Li, Regli et al. 2007). Updated vascular tree systems using NURBS curves as a skeleton allows parameterization and provide smooth fitting daughter branches from each of the originating nodes(Orazi 2007).

Nanoparticle Sustained Release Systems

Nanoparticles such as quantum dots, nanotubes, and nanowires have been receiving a considerable amount of attention recently for their unique properties that offer potential use in bioengineering, therapeutics, and more specifically drug delivery and targeting (Ozkan 2004). Based on their size, colloidal drug-polymeric sustained release systems can be classified as microparticles (1 to 1,000 μm) or nanoparticles (1 to 1000 nm). Compared to the microparticles, nanoparticles offer the advantage of higher cellular uptake. In addition, nanoparticles can be administered via the intravenous and subcutaneous routes with minimal irritation.

Natural or artificial polymers that are biocompatible and biodegradable are often used for the preparation of sustained release systems. Such polymers include poly (lactic acid) (PLA), poly (lactic-co-glycolic acid) (PLGA), acrylic polymers or copolymers, hyaluronic acid derivatives, and alginates. Among the available biodegradable polymers, the PLA and PLGAs are the most widely used. Within the body, the lactide/glycolide polymer chains are cleaved by hydrolysis to form natural metabolites (lactic and glycolic acids), which are eliminated from the body through the Krebs cycle. Depending on their composition and molecular weight, the PLA and its copolymers with glycolic acid provide degradation rates ranging from months to years (UB Kompella 2001). In our model these sustained release systems will be used to encapsulate growth factors for systemic delivery to the ischemic tissue. Our primary vehicle will be in the form of alginate nanospheres. Alginate is a naturally derived polysaccharide that is typically derived from seaweed. It is a biocompatible polymer that is widely used in the food industry. Additionally applications in cell transplantation have been developed for the use

of cells such as chondrocytes and islets. Vascular endothelial growth factor (VEGF) and other growth factors are readily incorporated into nanospheres and can release growth factors anywhere from days to weeks. (Sheridan, Shea et al. 2000)

Growth Factors

Until, recently VEGF was the only growth factor proven to be specific and critical for blood vessel formation. VEGF was initially defined, characterized and purified for its ability to induce vascular leak and permeability, as well as for its ability to promote vascular endothelial cell proliferation. Compared to its more recently discovered counterparts, much more is known about VEGF. It is now quite clear that that VEGF is such a potent and critical vascular regulator that its dosage must be delicately regulated spatial, temporal, and quantitative manner to avoid vascular disease.

In the peripheral nervous system regeneration and gradual functional restoration occur following peripheral nerve injury. Recent functional and expression studies of basic fibroblast growth factor (FGF) and its receptors have emphasized a physiological role of these molecules in the peripheral nervous system. Exogenously applied basic FGF mediates rescue effects on injured sensory neurons and supports neurite outgrowth of transectioned nerves. FGFs promote mitogenesis of mesoderm- and neuroectoderm-derived cells and is involved in regulating diverse processes like proliferation and differentiation during embryonic development and mediates effects in the adult organism on maintenance and during tissue repair. (Grothe, Haastert et al. 2006)

Platelet derived growth factor (PDGF) has not been extensively studied with respect to its neurogenic potential *in vivo*. In studies investigating growth factors that could

potentially be used to regenerate dompaminergic neurons in Parkinson's disease models, PDGF is thought to be a good candidate since it appears to play an integral role in the normal development to the central nervous system. The delivery of PDGF to the cerebroventricles preceding an ischemic insult can protect against neuronal degradation. The correlations between these models and our study of treatment of ischemic stroke also make PDGF an ideal candidate for drug encapsulation and release from our bioengineered vascular tree. (Mohapel, Frielingsdorf et al. 2005)

While quite a bit of work has been done using biocompatible materials to form scaffold for blood vessel formation (Kilian, Alt et al. 2005; Stitzel, Liu et al. 2006), a material needs to be selected that can meet these specialized needs. A bioengineered vascular tree system can be a life supply line for stem cells in their development into the tissues and organ systems of the human. Using this novel system of blood vessel production will make the engineering of all types of three dimensional tissue structures possible using cell cultured in this novel stimulatory bioreactor system

The novelty of our process is that it combines image data that represents both the macroscopic and microscopic domains of tissue structures. Then it uses that data for an entirely new concept, the production of Bio-CADs that render structures which are designed down to the microscopic level to successfully interface with cells such as to support, recruit and influence their behavior, guiding their mimicking of naturally developed tissue structures. In addition, this novel process converts these Bio-CAD derived models into data files that interface with programs such as Solidworks which drive 3D fabrication and micro patterning equipment. With this process we can create

tissue scaffolds, and or molecular patterned structural pathways which replicate the Bio-CAD structural design, compelling and supporting the genesis of reversed engineered vascular tissue structures (Kobayashi, Miyake et al. 2007).

Functional Vascular Tree Scaffolds and 3D Tissue Structures

The generation of biological tissues is a natural phenomenon that requires the cells which comprise the tissues to orchestrate its engineering. Much of this process is due to interactions between cells and their surrounding environments (Davis and Senger 2005) which in itself is produced by cells. This extracellular matrix supplied by cells is a product of millions of years of adaptive evolution leading from single cellular to multicellular organisms. The key structure which allowed evolvement of multicellularity from small unicellular aquatic organisms to multicellular organisms a few hundred microns in diameter, to large animals with organs, was the evolution of a vascular system. The key structural design by which Bio-CAD can play an essential role in designing, one which once constructed can open up tissue engineering's therapeutic potential, is also the vascular tree system (Mertsching, Walles et al. 2005; Schreiner, Karch et al. 2006; Linke, Schanz et al. 2007).

Chapter Three

Reverse Engineering a Vascular Tree

Current Approach

Currently researchers are trying to produce artificial blood vessels comprised of living cells. In creating these vessels it is their aim to produce a living structure that the ability to heal wounds, remodel vasculature, produce receptor-mediated bioactivity and produce normal blood vessel yields. Techniques researchers have used to realize this aim approach the creation of structural scaffolds using natural biomaterials such as collagen and fibronectin or by using biodegradable polymers such as polyethylene glycolic acid. Investigators are taking various approaches at creating structures comprised of vascular cells that have the proper receptors capable of the appropriate responses to environmental stimuli produced in healthy *in vivo* systems. Bioreactors are used to provide a nurturing environment through the use of a pulsated flow to induce cellular reactions that will change the mechanical properties of the artificial blood vessels as they are being created *in vitro*. The pulsated flow is to simulate blood flow that the vessel would experience if it was part of a cardiovascular system. The simulated blood flow provides forces on the vascular wall and inducing the cells within to compensate by strengthening the extracellular matrix surrounding the cells. This prepares artificial blood vessel for the environmental forces that would experience once transplanted to a cardiovascular system.

To date the scaffolding being used to create blood vessels had lumens that are nearly a thousand times larger in diameter than the average capillary. This makes their use as support structures for 3-D tissue scaffolds for transplant therapy and large wound healing impractical. These so called micro- blood vessels have been created as tubes or as sheets that are later rolled into tubes. When sheets are used they are sealed with cells characteristic of its destined position in the vascular wall. These cells are destined to become endothelial cells, smooth muscle cells, fibroblasts or pericytes depending on the diameter of the proposed vessel, their position in the vascular wall and whether the destined vessel is to be part of the arteriolar or the venous system. The scaffold's can be made of natural occurring substrates or synthetic biodegradable polymers. The mechanical properties of natural substrates such as Collagen require additional support with materials like Dacron in order to produce the mechanical properties needed to support the hydrostatic pressure experienced by blood vessels and cardiovascular system. The synthetic biodegradable polymers are built with the mechanical properties necessary without additional support. A few examples of these biodegradable polymers are polyglycolic acid, polyhydroxyalkanoate, lactic acid and polyhydroxygluconate. The mechanical properties necessary for the vascular wall to function properly are approached by using micro porous patterns and photolithography produce channels to create specifically aligned vascular smooth muscle cells during the construction of the tunica media (Sarkar, 2006).

The cells used to seed scaffold structures can be autologous or allergeneic and come from numerous sources. Examples of some sources are existing blood vessels such as bovine aorta, human umbilical cord veins and the canine femoral artery. Tissue

structures such as skin, skeletal muscle, cardiac muscle, adipose tissue, bone marrow, blood including umbilical cord blood and embryonic tissues. These structures provide a range of cell types with different potentials for developmental differentiation and lifespan. The cell types include endothelial cells, smooth muscle cells, vascular smooth muscle cells, endothelial progenitor cells, smooth muscle progenitor cells, myo fibroblasts, adult stem cells from haemopoietic tissues, mesenchyme, adipose tissue and embryonic stem cells (Sales, 2005). In addition these cells can be genetically engineered to over express or fail to express proteins orchestrating a cell's ability to perform necessary roles in the development of the vascular wall production. This includes the enzyme telomerase that maintains telomeric length during cell division, allowing continuous mitotic passages without the malfunctions that occurs during the chromosome separation of cells from long lineages; significantly increase the lifespan of engineered tissues (Rhim, 2006).

Another type of scaffolding that has been seeded with cells originates from the tissue structures that have been decellularized. These acellular structures can originate from blood vessels and other tubular structure such as intestines. They are taken from animals and humans and both have met with success. But again just the fact these structures need to be manipulated by hand preclude them from being any size close to what is needed for a capillary bed structure (Kakisis, 2005; Cho, 2005; Borschel, 2005).

Without the use of any scaffolding these so-called microvessels have been created from co-cultures of fibroblasts and smooth muscle cells taken from human umbilical cords vasculature (Kakisis, 2005). These cells are allowed to grow for 30 days where

they form sheets of cells surrounded by extra cellular matrix. These sheets are then rolled into tubes and used to function as the tunica media layer (Figure) in this method of the *in vitro* engineering of a blood vessel. The tunica adventitia layer (Figure) of the blood vessel is simulated in form from pure a fibroblast culture added to the outer wall of the previously synthesized tunica media, after its stabilization in culture. After another week is stabilization the center piece supporting the rolled up sheets of cultured tissue is removed and the resulting lumen seeded with endothelial cells taken from human umbilical cord veins (Kakisis, 2005). This procedure produce well organized macrovascular like structures with very good mechanical properties.

Vascular scaffolds have been developed based on patient's arterial configuration (Uchida, 2007) but these were large structures not intended to substitute for capillary bed systems and their ability to provide a nurturing environment for organ tissues. In this case the CAD design was used to reconstruct the carotid artery diameter nearly 100,000 times that of a capillary. Although researchers here discuss a size limitation of 1 mm in diameter even so the structure is still nearly a thousand times too large to represent the capillary feature.

An entirely different approach at using scaffolding to produce microvascular structures is seen in the use of collagen I to replace injured myocardium. This method takes advantage of cryo lesions and the body's foreign body reaction which uses neutrophils and macrophages to pave the way for neovascularization, collagen deposition, and matrix metalloproteinase's (van Amerongen, 2006).

Coronary Arterial Trees

The generation of vascular tree models of the Coronary system is a popular area of research. This is due to the needy for virtual models of the human heart that can reflect perimetric changes in blood flow to create pathological conditions and model proposed surgical procedures. Some very impressive models of the coronary arterial tree have been created to combine physiological factors, imaging data and mathematical reconstructions. Research has produced correlations between the structural anatomy of coronary vessels and the dynamics of blood pressure, flow and volume. Researchers are using these correlations to develop mathematical approaches for computing blood vessel branching patterns, vessel luminal diameter and blood vessel wall thickness (Wischgoll, 2007; Kaimovitz, 2005; Szymczak, 2006). A very complete study was done on the relationship between the biological variations in branching patterns and blood perfusion in stochastically generated coronary artery trees (Denkelman, 2007). The author resolves differences between Strhler algorithm which defines ordering based on vessel diameter and Van Bavel's model which is based on the measured heterogeneousity of the vascular tree's branching pattern's. The results show that different branching rules affect the perfusion parameters and can be used to predict variation in segment length trees, vascular volume and can be used to predict corresponding physiological states of the vascular blood flow.

Based on detailed anatomical data 3-D models of vascular tree structures have been created in rectangular slab geometry using parallel simulated annealing algorithms (Kaimovitz, 2005). The results of these algorithms were optimized by setting constraints based on morphometric features of the Coronary vasculature. The resulting vascular tree

systems were then mapped on the surface of a modified sphere representation of the heart's surface adapting the tree's structure to fit the surface. Kaimovitz et al used a novel method for determining vessel diameter along bifurcations with results consistent with the morphological statistics of the measured data on corresponding structures. The more recent work coming from Ghassan S. Kassab research group have sought to model the capillary systems of the Coronary vasculature. Experimental investigation on capillary structures is not complete. Engineering a capillary system create a challenging visualization problem for a number reasons (Wischgoll, 2007), the biggest being the need for almost a mile of geometrical representations.

In order to tackle this problem geometry reduction and occlusion culling techniques were use to reduce the number of triangles set forth in a reading frame at a given time while maintaining the full complexity of the entire model. The results were increased performance of interactive visualization using novel algorithms that are anatomically based, integrating structural properties with changes in physiological conditions. The resulting models are extremely complex, with one tree containing 4.3 million vessel segments, at full resolution contained 77 million triangles. Using different collusion culling techniques and depending on the view angle, parts of the vascular tree could be rendered at very low resolution, reducing the number of triangles up to 56% (Wischgoll, 2007). Even still the culling process was expensive making rendering these vascular tree structures no easier. Computer hardware and software available at the time of this publication severely limited the ability of this research group and other groups performing similar geometrical reconstructions to render these vascular tree structures. Many tricks have been used such as a creation of occlusion buffers using OpenGL with

visualization service such as a Sun Fire V880z, applying out of core and other high-end GPU's and increasing the amount of main memory enabling the whole geometric model to be stored during computer processing.

A more image based approach in reconstructing 3D coronary vessel trees by Szymczak uses algorithms to create and extract maximums in intensity ridges to represent the outer surfaces of blood vessels captured in 2D radiological image sections (Szymczak, 2006). This method was in effective at creating a complete vasculature because of its inability to represent low intensity structures. Results are models with gaps in their structure and suspended pieces of blood vessels. With the use of filters some of these errors were removed or corrected but the resulting model nevertheless lacked a complete representation of the coronary of vessel tree sought for modeling.

Electrospinning technology is being used to create tubular scaffolds for blood vessel engineering. Anthony Atala's group at Wake Forest studied the use of type 1 collagen taken from skin and elastin taken from ligaments of the neck blended with the synthetic polymer, poly D,L - lactide - glycolide (PLGA), to create tubular vascular scaffolds less than 5 mm in diameter, through electrospinning. Atala's group found that these blends were safe for *in vivo* use, eliciting no local or systemic toxicity and demonstrated mechanical properties comparable to the native vessels that are designed to replace (Stitzel, 2006). One of the benefits of electro-spun scaffolds is their features size which is on the nano meter scale. This makes them in the same diameter range of extra cellular matrix fibers, collagen and elastin, from which they are being made and designed to simulate. Research has shown that endothelial cells and smooth muscle cells show

favorable responses to structures of the size demonstrated here in the form of improved adhesion during the process of seeding cells into scaffold structure while being cultivated in a bioreactor for cellular development. The results of this electro-spun scaffolding created vascular like tubes with mechanical properties that resist 12 times the systolic blood pressure experienced by normal vessels of the same diameter. In addition minimal inflammation occurs that soon subsides and thrombosis though not discussed in this paper has been shown to be minimized using special surface coatings or genetically engineered endothelial cells expressing factors that resist fibrin binding.

Optical lithography is being used to pattern capillary networks with the goal of creating a microvascular structure to support cell viability in 3-D engineered tissue scaffolds by providing oxygen and nutrients to its internal structures (Kobayashi, 2007). This method is similar to traditional total lithography used in the fabrication of micro electrical mechanical systems. In this case a titanium dioxide photo-mask was created on top of a chromium quartz mask with slits around 60 μ wide and 300 μ apart. The resulting mask was used to create hydrophobic patterns on a fluoro -alkyl -silate substrate using UV irradiation through the mask (Kobayashi, 2007). The patterned substrate was then cultured with endothelial cells that were attracted and attached to the hydrophobic regions. Substrate then was placed on top of Matrigel and incubated for 24 hours after which the substrate was removed transferring the patterns cells into the extracellular matrix solution Matrigel^{TM} along with the cell culture medium formulated to stimulate a vascular growth. There was some evidence that capillary type structures formed and express vascular endothelial cell cadherins at intercellular junctions.

The use of hydrogels to form structural scaffolds for cellular growth is becoming a very hot and promising procedure. Through physical, covalent or ionic interactions polymer chains are cross-linked together with the ability to absorb and maintain aqueous environment. One promising polymer is the polysaccharide chitosan which is obtained from the exoskeleton of shrimp. It is a naturally occurring poly-electrolyte which is biodegradable. Cross-linking is formed with chitosan by the repeated alternating steps of sodium hydroxide neutralization and rinsing with water. This causes the neutralization of ammonium ions to free amine groups. This removes ionic repulsions between molecules making way for hydrophobic interactions and hydrogen bonding between polymer chains (Elisseef, 2008). Good understanding of these reactions the mechanical properties of polysaccharide hydrogels can be manipulated by altering the monomeric molecular structure of polymers or the degree of neutralization of the acidic groups present in the polymer chains. In addition to mechanical properties, other physical properties can be controlled such as the amount of water present in the hydrogel, the thickness of the resulting hydrogel structure and the density of cross-links occurring between chains (Elisseef, 2008) all important parameters whose modulation can be used to regulate cell motility, cell shape, proliferation and differentiation. In addition of interrupting the neutralization process an interphase zone is created separating the neutralized hydrogel from polysaccharide chains in their pre-neutralized gel form creating a separation or enters membrane space (Elisseef, 2008). Repeated cycles of this procedure can be used to create multilayered hydrogel structures of different shapes such as tubes and spheres (Elisseef, 2008).

Problems with Current Approaches

There are different fronts attacking the vascular tree problem. Initially researchers made tube structures out of biocompatible materials already approved for use by the food and drug administration. Then they seeded these structures with any kind of cells they could get their hands on that were remotely similar to ones you would find in a vascular wall. Next they tried to find specialized cells that would differentiate into specific cell types that belonged in the blood vessel wall. Then when they could not obtain the cellular morphology expected, intense research began on the molecular factors that regulated cell morphology and behavior. Then there was a problem with the inflammatory response by the host to these devices absorbing the scaffold's structure replacing it with fibrous connective tissue and the vascular lumen losing its patency due to thrombosis. Therefore more attention was placed on material used for creating the scaffold itself. Larger vessels fed in bioreactors prior to *in vivo* implantation soon saw the internal cellular components die from lack of oxygen and nutrition before the host's tissue could react to neovascularization of the implant internal structure. So experimentation began in scaffold pore size, to trying to find a happy medium that would allow cellular attachment as well as the movement of extracellular fluid to provide needed oxygen and nutrients until microvasculature was established. This turned out to be a futile approach yielding little success but a lot was learned about cellular responses to different features sizes and material types. Recently there has been a realization of the need for more detailed designs as is demonstrated in the recent use of lithography to pattern channels designed structurally to simulate extra cellular matrix fibers' role in guiding cellular and cytoskeleton structural alignment (Sarkar, Dadhania et al. 2005).

While, as described earlier, many researchers are addressing the cellular organization found in the different layers of the vascular wall. But their methods are course and not effective at addressing the core problem for tissue engineering, even of the larger vasculature. The core problem is that lack of a capillary bed system to provide oxygen and nutrients as well as developmental factors necessary for both the basic nurturing of the surrounding cells and the support for vasculogenesis. Some excellent work is being done at combining theoretical measurements with physiological and mechanical properties to produce models of microvascular-like structures for physiological simulations. Where simulations of the larger vasculature gave some productive results for large-scale needs, the actual feature sizes of the capillary and its bed precluded the acquisition of these types of data by methods used for the macro vasculature. Of all of radiological methods used to obtain structural data on the anatomy of the cardiovascular system, only fairly recent studies used in micro computer tomography have come close to providing detailed and accurate information on the structure of complete capillary bed systems (Heinzer, Kuhn et al. 2008). But even this study has serious issues in contrasting complete capillaries systems using the present methods. A different problem, as described above, the actual size of the detailed models of capillary systems is confounding researchers using theoretical models to represent these structures. The basic problem being the incapability of computer hardware design software to handling the enormous size of models created to reflect accurately the complete capillary bed structure.

Solutions Proposed to Date

The recent use of lithography to pattern channels (Sarkar, Lee et al. 2006; Figallo, Flaibani et al. 2007) designed structurally to simulate extra cellular matrix fibers' role in guiding cellular and cytoskeleton structural alignment in the formation of a vascular wall (Medvedev, Samsonov et al. 2006) represents the first attempt at microscopically designing the structure of vascular scaffolds to structurally mimic natural vasculature. Using algorithms of constraint construction optimization computer generated model have been created to supply analytical models of hollow organs as well as finite element analysis of image generated triangular mesh models (Schreiner, Karch et al. 2006).

These are all interesting ideas but none are true solutions to the problem of building a complete and accurate model of the capillary bed system capable of being use to fabricate a vascular structure which accurately mimics the necessary interstitial relationship maintained by the capillary bed on organ by organ bases. Without this relationship it will be impossible to engineer tissue structures that can fully represent the function of any organ and without this function any such tissue is rendered useless for placement therapy.

Chapter Four

Vascular Tree Modeling

Research Design

We have a novel to approach to designing tissue scaffolds: The reverse engineering of tissue's cellular structural framework, its extracellular matrix, using its natural tissue structure as a model. Our first project is to successfully design a scaffold for the vasculogenesis of a complete vascular tree system. However, the availability, through diffusion and active transport, of molecules and atoms necessary for cell maintenance, growth and behavior is a central problem limiting 3D tissue growths. Because of this limitation, we have failed to stimulate significant 3D tissue growth in *in vitro* systems, and our attempts at the regeneration of damaged tissues result in avascular scarring. Thus far, scaffolding for vasculogenesis have consisted of crude tubular macro-designs that lack micro-capillary structures and therefore can have no direct impact on tissue genesis or regeneration. In order to make these substances available, a vascular tree scaffold needs to be designed to include a configuration that supports the growth of a properly structured capillary bed.

Using a reverse engineering approach, we designed scaffolding for vascular tree development, modeled from a natural vascular tree. Extensive literature that demonstrates techniques for creating a vascular cast exists. Through literature, we will identify the best technique for obtaining images of these microvasculature casts that can

be used to reconstruction a digital representation of a 3D micro-vascular tree. We will obtain access to these tools and use them to perform the necessary techniques to obtain images of the cast of micro-vascular system, and we will use the images to construct 3D digital model. The model will be constructed for use in stereolithography techniques.

By reverse engineering the natural designs of microvasculature tree systems, a scaffold can be designed for engineering large 3D tissue structures for clinical use. Using a reverse bioengineering approach, we will model a complete afferents-efferent blood vascular system that includes its capillary bed system, necessary for the development of the cells surrounding a 3D tissue construct. In order to accomplish this for the in-vitro micro computer tomography (micro-CT), we acquired volumetric image data to reconstruct 3D image for modeling the microvasculature. The capillary bed's design configuration must interface precise morphological specifications for the given tissue structure. This requires critical attention to the capillary bed's microscopic relationships

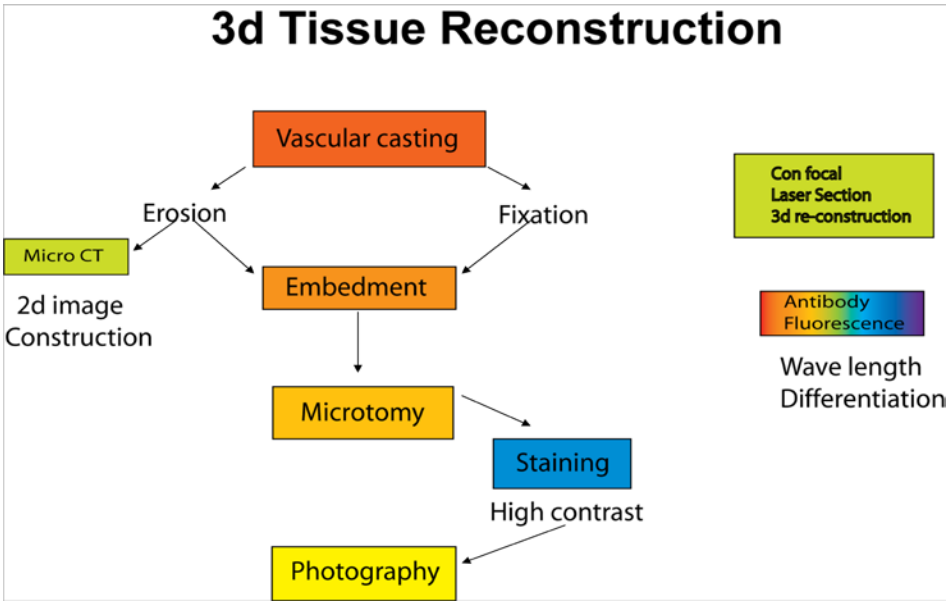

Figure 20: 3D tissue reconstruction flow chart.

with surrounding cells. The decomposition of the structural elements of the capillary bed in that specific tissue structure is required.

A vascular cast that represents the lumina of the corresponding vascular the tree system will be used for acquiring image data from the structure of the corresponding vascular tree system. Using a cast made of the lumina of the appropriate vascular tree, a scaffold can be constructed to replicate that vascular tree's framework.

New methods are needed to develop a bimolecular scaffold that supports a wide array of cellular functions and is not rejected by the host. For nearly twenty years, studies of the 3D structure of blood vessels (Schraufnagel 1987) and other luminal systems found in the body (Hojo 1993) have produced techniques that use a blend of vinyl chloride latexes, consisting of a plasticized vinyl chloride copolymer with a vinyl chloride copolymer, to create a latex replica of the microvasculature system, demonstrating the luminal surfaces of these structures.

In this initial project, and through the use of an interdisciplinary approach, the vascular tree scaffold described above will be constructed on a scaffold of its own. The vascular tree will be perfused with heparinized Ringers solution. Latex or similar resin perfused into MCA and subsequently polymerized in its lumen will serves as the subject for a computer-assisted design model (Fabris, Cadamuro et al. 2007).

For vascular casting, the selected material must begin as a viscous liquid and polymerize into a porous, fibrous, biocompatible network similar to the successful scaffold previously described. It must allow various degrees of layering, permit cell

migration, contain the necessary growth factors found in extra cellular matrix of developing blood vessels (van Meeteren, Ruurs et al. 2006), and be suitable for the engineering of an *in vitro* cellular replica of the vascular tree.

In our preliminary work, we discovered that the erosion cast was very fragile, making it very hard to keep the capillary networks intact when handling the structure. The subsequent 3D image scanning technique presented a monumental task.

The acquisition of images is needed in order to gather data for the bio-CAD 3D reconstruction of the corresponding 3D vascular tree. An entire vascular tree system can be digitally imaged and the data captured for 3D rendering. In order to create a bio-CAD rendering of a sound vascular tree system, we need to obtain data through reverse engineering that is representative of the entire vascular tree system. Only through this method can we precisely measure and completely recreate the structural dimensions of such biological systems, making functionality under its natural fluid flow condition possible.

File size limitations initially prevented us from directly obtaining the entire image data needed to capture the complete vascular tree structure from one image reconstruction technique. The area that can be imaged and reconstructed by micro-CT is also limited in size when high-resolution instrumentation is used. This makes the area of the tissue organs scanned smaller than the area of most complete vascular tree systems. Micro-CT results published in the current literature demonstrate the lack of capabilities to resolve completely and accurately the 7 to 10 μ diameter tubes that make up the capillary beds of vascular tree system. These resolution limitations of micro-computer assisted

tomography imaging systems make the complete capture of image data for the capillary bed of a vascular tree very difficult – almost impossible – even with the latest equipment.

In order to reverse engineer a vasculature tree using micro-CT image data, image data for the capillary networks that are missing because of resolution limitations will have to be supplied through other means. We will use image data obtained through the reconstruction of serial sections obtained by histological techniques, taken through a reference plane created during tomography scans. Reference points will be created in scanned tissue that corresponds with section tissues. The resulting images will be imported into bio-CAD software, where we will connect the afferent and efferent arterioles and venules and mesh structures obtained by micro-CT with mess structures obtained through the reconstruction of serial tissue sections of the capillary bed systems.

The reconstructed image data sets from micro-CT and serial section, which create a complete bio-CAD model, will give us a complete 3D layout of the inner wall of the vascular tree system of interest. Using histological data on the vessels' wall thicknesses along the length of it structure bio-CAD can be use to render, on top of the inner wall layout, a design for a structural scaffolding of the seeding migrating proliferating cells.

In the future we hope to converted image data from micro-CT and re-constituted serial tissue sections to 3D wire frame models and merged together using bio-CAD software. Three-dimensional prototyping is a very is established field of engineering that has given us the ability to bring virtual models into physical existence. The mathematical models currently being used to imitate vascular tree systems fall extremely short of accurately mimicking nature’s designed vascular trees. By using actual image data to

illustrate size dimensions and other complexities of natural structures, we can create, through reverse engineering principles, designs that mimic these natural structures. These designs can then be imported into 3D prototyping software in a created structure. However, limitations are found in the creation of microstructures. These limitations are due to the molecular structure of structural materials, the prototyping technology – which is quickly improving – and the details of the design. By using actual image data obtained directly from vascular tree systems, we can create a highly detailed model of its structure. Such structures could be extremely valuable in the 3D fabrication of scaffolds to be used for the tissue engineering of complete vascular tree systems. By combining a micro-CT study of vascular tissue with the reconstruction of thin serial tissue sections of capillary beds, the resulting bio-CAD rendering can be used as a structural design for the scaffolding on which a vascular tree can be constructed.

Before we began putting the digital model together in bio-CAD, we developed a new approach. We needed an efficient way of isolating desired capillary lumen structures from other cellular structures in the surrounding tissues, thereby decreasing the information being digitalized in the process of 3D reconstruction. This is necessary to keep down the file size of resulting data sets, lowering the computer processing hardware strains and requirements.

Merging image data obtained from micro-CT with image data obtained from the 3D reconstruction of tissue sections requires careful attention to section orientation. We must match the sectioning plane used in micro-CT acquisition of images with the sectioning plane used to obtain histological sections the vascular tree of interest. In

addition, reference points need to be created to match the micro-CT image data with the beginning of histologically reconstructed image data. In order to accomplish this, one way would be to explore the use of fluorescent dye as part of the compound used to fill and opacify the microvascular system. We can then use fluorescent microscopy to catch the image data of the serial sections. This will give us a high-contrast, 2D image of capillary lumen structures against a black background for image capture and 3D reconstruction of the capillary bed.

Tissue containing the vascular tree of interest, processed for light microscopy and using histomorphometry imaging software, the capillary bed and its arterioles and venules can be digitally selected and contrasted with the surrounding tissues. The resulting montage images could then be stacked in the Z plane and aligned in the X and Y directions using three fiduciary marks, recreating a 3D volumetric image of the original capillary bed. This image could be further processed into a virtual wire frame model. Models will be replicated and connected to the vascular tree reference points identified in the CT scan established before tissue sectioning. In order to merge the data obtained from the two different image acquisition techniques, we could create reference points in tissue for the biological reconstruction of data sets collected using two different image acquisition techniques. These reference points can be pre-selected, natural branches in the vascular tree systems that occur before micro-CT's resolution capabilities diminish. Another solution could be the use of radio opaque beads of a constant diameter, which are just above the resolution capabilities of micro-CT. These beads can be perfused into the vascular system and mixed into the radio opaque solution used micro-CT imaging. These can be introduced into the vascular tree only after a complete profusion of the pure

radio opaque solution has been completed. The beads will proceed only to a point at which the vascular tree is still resolved using micro-CT.

The reverse engineering of a vascular tree system can be a life supply line for stem cells and other cell types during their development into tissues and organ systems, whether its for regeneration or transplants. In order to build such a vasculature tree system, one must first come up with a way to design a model that replicates the dimensional complexities found in the naturally occurring system. This is what we intend to do.

Data Acquisition

The application of computer science and engineering technology into medical sciences has led to the bio-CAD refinement of many medical devices, such as artificial joints, bone implants, vascular stents and prostheses (Sun 2005). These devices are mechanical in their application and have made vast improvements over their predecessors designed before the advent of computer technology, which aided the design and manufacturing processes (Sun 2005; Witkowski, Komine et al. 2006; van Lenthe, Hagenmuller et al. 2007; Wang and Tang 2007). In contrast, the use of bio-CAD to engineer tissue structures has not yielded products with comparable success in physiological applications (Sun, Darling et al. 2004; Sun, Starly et al. 2004; Sun, Starly et al. 2005).

The generation of biological tissues is a natural phenomenon that requires the cells that comprise the tissues to orchestrate its engineering. Much of this process involves

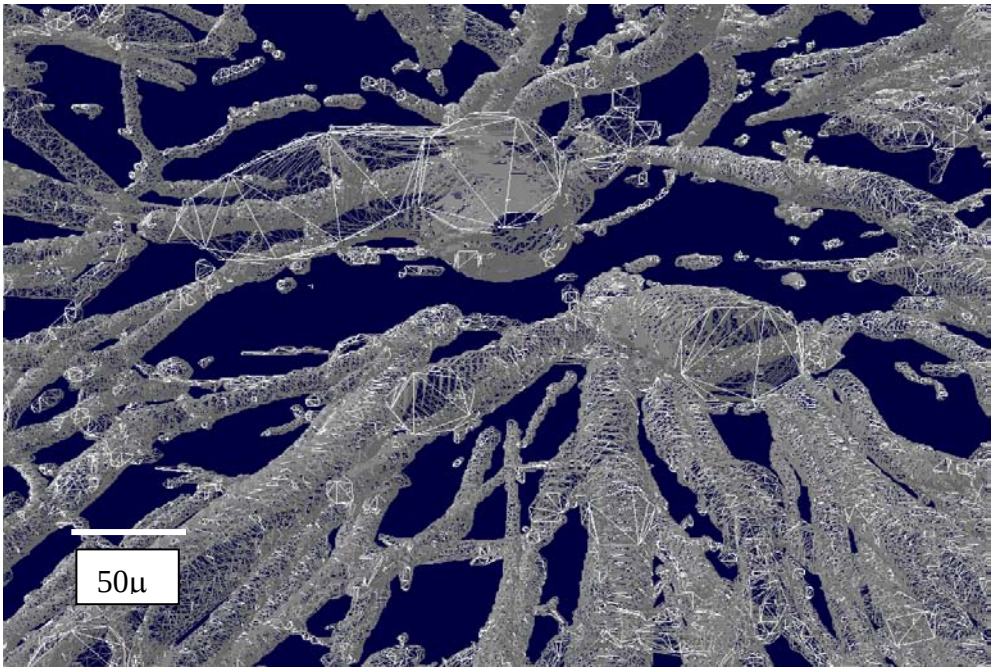

Figure 21: Microfil[tm] volumetric STL. STL constructed from Microfil-perfused vascular networks in mouse kidney. Image pixel size 8.89 µm.

interactions between cells and their surrounding environments (Davis and Senger 2005) that have evolved for millions of years, from single cellular to multicellular organisms. The key structure *in vivo* which allowed the evolution of multicellular organisms from small, unicellular aquatic organisms to large animals with complex tissue structures is the vascular system. Clearly, the reconstruction of complex tissue structures *in vitro* would allow for significant therapeutic applications. This bioengineering potential, however, will not be reached without first reconstructing the vascular tree *in vitro* (Mertsching, Walles et al. 2005; Schreiner, Karch et al. 2006; Linke, Schanz et al. 2007) from complete and accurate models of the capillary bed.

Micro-computer tomography (micro-CT) is commonly use to generate 3Dtissue structures, although there has been limited success in using this method for the reconstruction of complete and accurate capillary beds (Ikura, Shimizu et al. 2001; Badea, Hedlund et al. 2006; Badea, Hedlund et al. 2007). While micro-CT has the resolving potential to create 3D tissue structures (Sasov and Van Dyck 1998; Parkinson and Sasov 2008), limitations arise due to the nature of contrast agents used in this technique (Badea, Hedlund et al. 2006) because they allow the for the demonstration of large vessels adequately but do not result in high-resolution imaging of small vessels, such as those found in capillary beds (Elleaume, Charvet et al. 2002; Hainfeld, Slatkin et al. 2006; Litzlbauer, Neuhaeuser et al. 2006).

A technique to overcome the difficulties with micro-CT contrast agents hampering complete visualization of capillary bed systems is the utilization of corrosion cast methodology, such as Batson's methylmethacrylate corrosion casting (BMCC) (Polysciences) because of its proven success in creating durable vascular casts (Gross, Joneja et al. 1993; Krohnand Bertelsen 1997).

Viscosity issues were long ago addressed with this technique, allowing for complete perfusions of capillary beds (Lametschwandtner, Lametschwandtner et al. 1984; Lametschwandtner, Lametschwandtner et al. 1990; Simoens, De Schaepdrijver et al. 1992).

The goal of this study was to demonstrate our ability to acquire 2D micro-CT image slices that could be reconstructed into models that clearly mimic capillary beds. To accomplish this, this study compared the BMCC casting methodology (Figure 22) to the

Figure 22: Vascular corrosion cast of a whole rabbit kidney. In our search through the available literature and online resources, we found an emerging field in image construction on a microscopic level, which had previously been well developed on both macroscopic and geophysical scales.

Microfil™ contrasting agent methodology (Figure 20, 21, 23, 24) to determine which resulted in the most accurate, high-resolution imaging of capillary beds.

Our challenge is to capture images of a vascular tree's luminal cast, which are capable of being reconstructed into a digital 3D image of the cast. These images are needed to provide the data for producing a 3D bio-CAD model that reconstructs the corresponding vascular tree lumen. An entire vascular tree luminal system, including its capillary bed,

can be imaged in 3D using micro-CT scans. The micro-CT data captured is rendered into a 3D model using stereolithography.

Reverse bioengineering calls for us to create a bio-CAD model of a sound vascular tree system. Data must be representative of the entire vascular tree system, including the natural capillary bed's structural design. This way we can completely and precisely recreate the structural dimensions of the biologically engineered vascular tree system, making its functionality under its natural fluid flow condition ideally suited. Resolution and scanning limitations of micro-CT prevented us from directly obtaining all of the image data to capture the complete vascular tree structure from one micro-CT scan image reconstruction.

High-resolution micro-CT was used to completely resolve capillary bed systems. Specimens were prepared with both Microfil^{TM} microvascular (mv) method and modified Batson's #17 method. In the following section we explain the use of the modified Batson's #17 method.

Issues with Resolution and Accuracy

Because of viscosity issues, contrasting agents may not be consistently present in the capillary lumens being imaged. Less viscous contrasting agents did not produce enough contrast between the agent in the capillary lumen and the image of the surrounding tissues. Intensity thresholding has not been able to clearly contrast lumen-filled capillaries from its surrounding tissues while at the same time demonstrating the larger

vasculature. Small variations in the contrast levels of capillaries from background tissues are not clearly distinguishable when thresholding the image's intensity for larger vessels. This creates an imaging problem where the image's noise-free threshold is being sought. Capillaries become indistinguishable from surrounding tissues without introducing large amounts of background noise. After comparison, it was determined that Batson's methylmethacrylate corrosion casting, a method traditionally used in the scanning electron microscopic analysis of luminal tissue structures, was an appropriate method to represent the capillary's luminal structure during micro-CT scanning. (Table 1)

Corrosion casting defeats the issues viscosity gives us with complete perfusion. Viscosity issues have long ago been worked out with this technique and complete perfusions of capillary beds structures have been demonstrated with this technique. The corrosion casting technique also addresses the limitations of contrasting capillary structures with the surrounding tissues when using the contrasting agents described in Table 1. We compared our micro-CT of corrosion casting results with the micro-CT results we obtained using Microfil™ to fill blood vessel lumens. Microfil™ was inefficient in contrasting a complete representation of capillary structures. The micro-CT results using the Batson's corrosion casting technique gave us clean images that could then be created and stored as mesh structure in a stereolithography file format, compatible with solid works and other software-guided fabrication. Using CTan analysis and CTvol visualization software, stereolithographic images were created. The resulting volumetric images were constructed from various tissue types (Table 2) using both micro-CT scanned corrosion casts of vascular networks (Figure 29, and Chapter V) and micro-CT scanned contrast agent-filled vascular networks (Figures 24-26).

Tissue scanned with Microfil™ as a contrasting agent, even with small tissue samples (Figures 24-26), demonstrated incomplete and inaccurate capillary structures, even at high-resolution micro-CT scanning (Tables 2 and 3). Region of interest (ROI) models constructed from high-resolution micro-CT of Microfil™-prepared samples demonstrate the incomplete filling of capillary system. (See arrow points in Figure 24). Micro-CT-scanned Microfil™ specimen, post 3D reconstruction, can be adapted to show an improved microvascular structure (Figure 28) with image sweep variation of the despeckling image processing plug-in for Skyscan's CT-Analyser version 1.8.1.3.

The perfusion of mouse tissue with Batson's #17 solution is shown in figure 27. The blue pigment mixed in the Batson's casting resin allowed us, using stereo light microscopy, to visually analyze the successful vascular perfusion of the casted tissue (figure 27). This method also allowed us to be selective in our further processing of tissue for capillary bed imaging. This strategy is not apparent in past investigations.

The rabbit vascular casts were good for whole organ representations. Figure 31 is a casting of a whole rabbit lung taken from the animal casting. Figure 32 is a 3D view of a micro-CT image data set acquired from this casting using the Skyscan 1176. In order to capture high-resolution images of capillary beds, a small portion was taken from whole lung vascular casting (Figure 31) for high-resolution with micro-CT (Figure 33). Micro-CT data captured from the lung vascular cast were used to construct the 3D model presented in Figure 33c. Figures 30 shows - at increasing magnifications, a scanning electron microscopic (SEM) analysis of the vascular cast shown in 7a of figures 33 - rabbit lung. In figure 30, the capillary network surrounding an alveolar air sac

Table 1: Performance of Vascular Contrast Agents

Contrast Agents	Iodine solutions (Priebe, Aukrust et al. 1999; Badea, Hedlund et al. 2006)	Barium Sulfate ($BaSO_4$) (Langheinrich, Leithauser et al. 2004)	Nanogold particles (Hainfeld, Slatkin et al. 2006)	Osmium tetroxide (Muller 2006)	Microfil (Beeuwkes 1971; Marxen, Thornton et al. 2004)	Micropaque (Grabherr, Djonov et al. 2007)
Information	In vivo	Quickly settle out of suspension.	New Technique	Not thoroughly investigated	Radio opaque silicone rubber	Gelatin thymolBaSO4
Limitations	Rapidly metabolized	Stimulates formation of globular vacuoles in endothelium	Expensive for large specimens	Dangerous carcinogen	Viscosity –will not consistently fill capillary beds	Viscosity will not fill capillary beds unless water replaces gelatin as a solvent

Table 2: Micro-CT Image Acquisition

Skyscan1172							
	Source voltage (kV)	Source current (uA)	Image Pixel Size (µm)	Object to Source (mm)	Camera to Source (mm)	Exposure (ms)	Figures
Rabbit Kidney Microfil	59	167	5.99	110.47	214.243	1178	23
Mouse Brain Microfil	59	167	4.25	78.57	216.692	3534	26
Batson's Rabbit Skin	100	100	17.45	258.20	347.049	885	35
Batson's Rabbit Lung	100	100	5.06	93.68	217.089	1178	31
Mouse Kidney 301 Microfil	55	181	8.89	3534	3534	3534	21
Mouse Kidney 501 Microfil	55	181	8.89	3534	3534	3534	24
Skyscan1076							
Batson's Rabbit Lung Whole	89	110	35.36	121	161	158	30
Batson's Rabbit Kidney Whole	89	110	35.36	121	161	158	28

Table 3: Micro-CT Image Reconstruction

Skyscan1172					
	Section count	Result Image Width (Pixels)	Result Image Height (Pixels)	Pixel Size (µm)	Figure
Rabbit Kidney Microfil	1869	3684	2944	5.99	24, 25
Mouse Brain Microfil	1869	3592	3592	4.25	26
Batson's Rabbit Skin	3301	3968	3968	17.45	35
Batson's Rabbit Lung	1961	2160	2160	5.06	32
Mouse Kidney 301 Microfil	1788	2096	2096	8.89	21
Mouse Kidney 501Microfil	1746	2388	2388	8.89	23
Skyscan1076					
Batson's Rabbit Lung Whole	1825	1000	1000	35.38	31
Batson's Rabbit Kidney Whole	1090	1000	1000	35.38	28

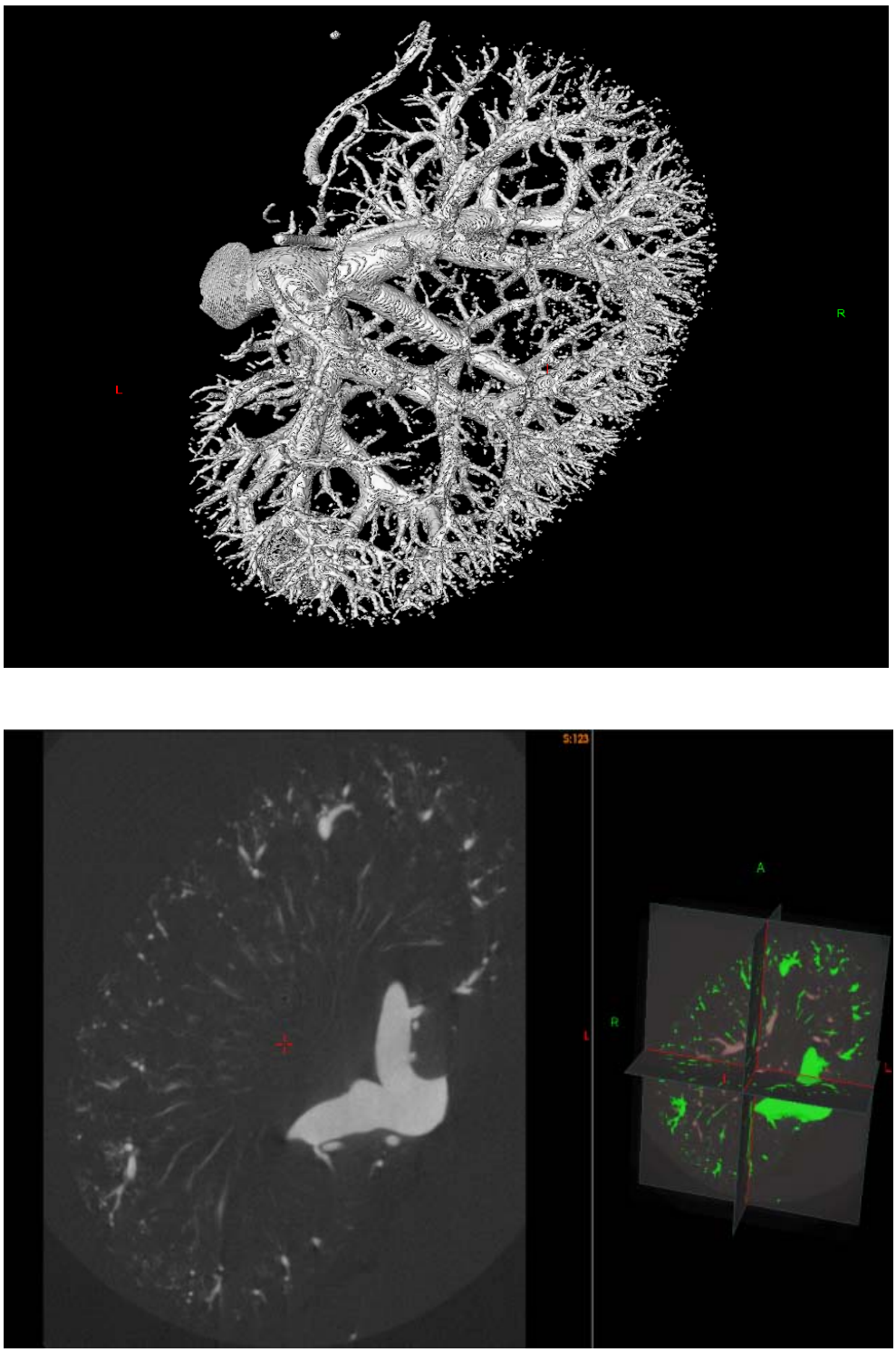

Figure 23: 3D Microfil projection. A 3D projection of mouse kidney vasculature created with Microfil contrasting agent - Micro-CT image data. Image pixel size

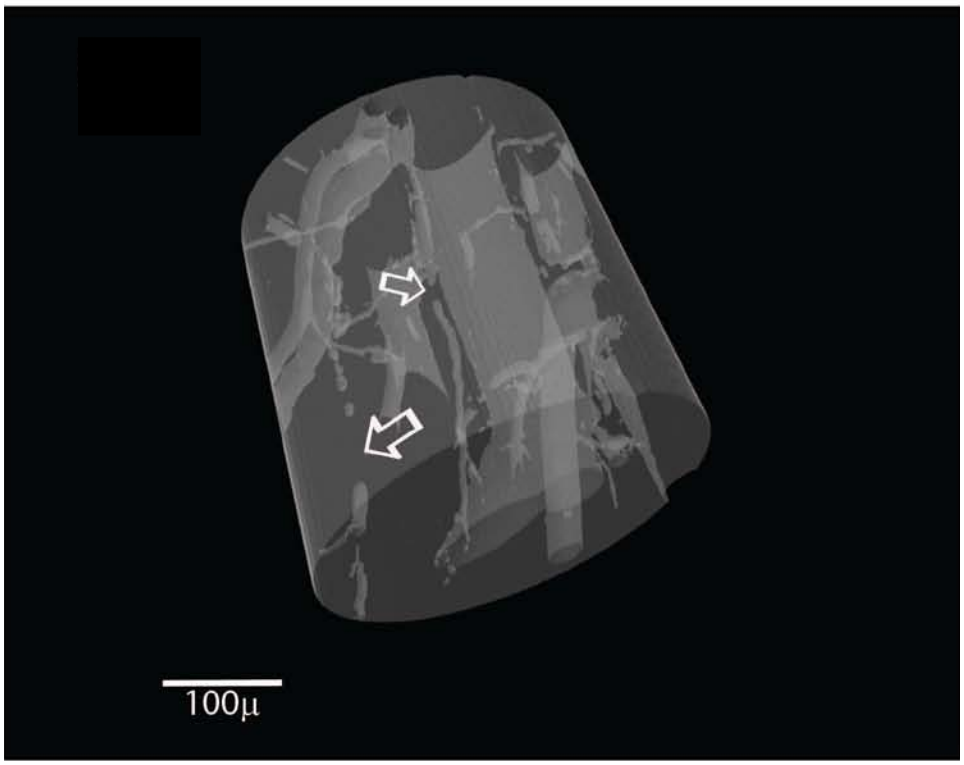

Figure 24: Microvasculature prepared with Microfil. ROI taken from a high-resolution Micro-CT reconstruction of mouse kidney microvasculature prepared with Microfil. The arrows point to the lack of a continuous capillary system. Image pixel size 8.89 µm

Figure 25: Mouse lung perfused with Batson's methylmethacrylate.

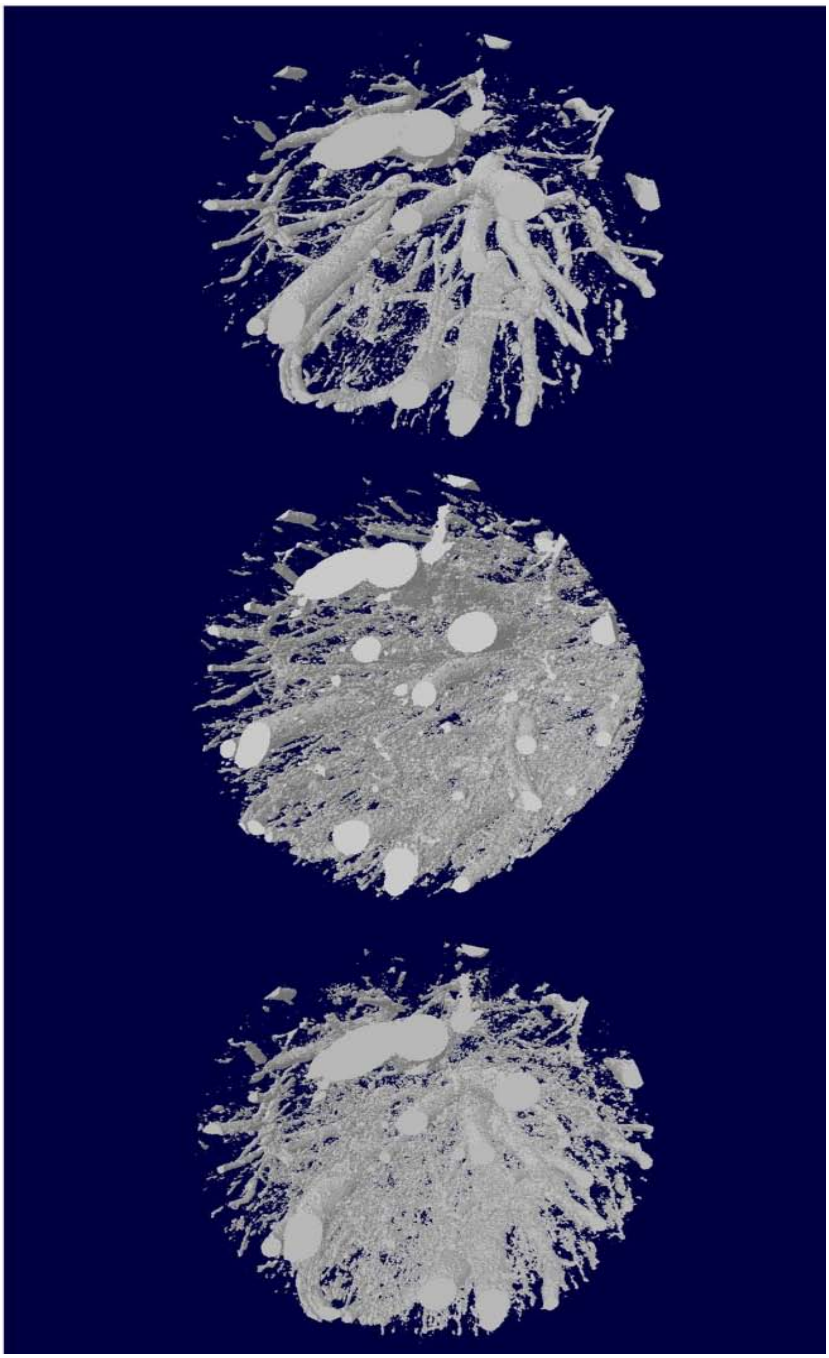

Figure 26: Inability to resolve a complete and accurate capillary system. Three images of the same region of interest at three different intensity thresholding were modeled from a micro CT scan of mouse kidney tissue contrast with Microfil in order to demonstrate the inability to resolve a complete and accurate capillary bed system using this method.

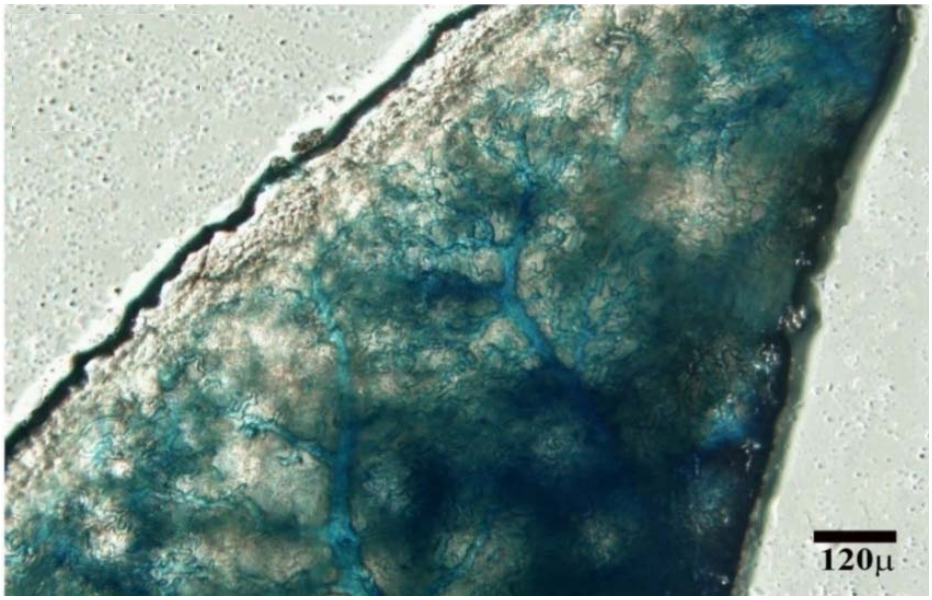

Figure 27: Lung from a mouse perfused with Batson's methylmethacrylate.

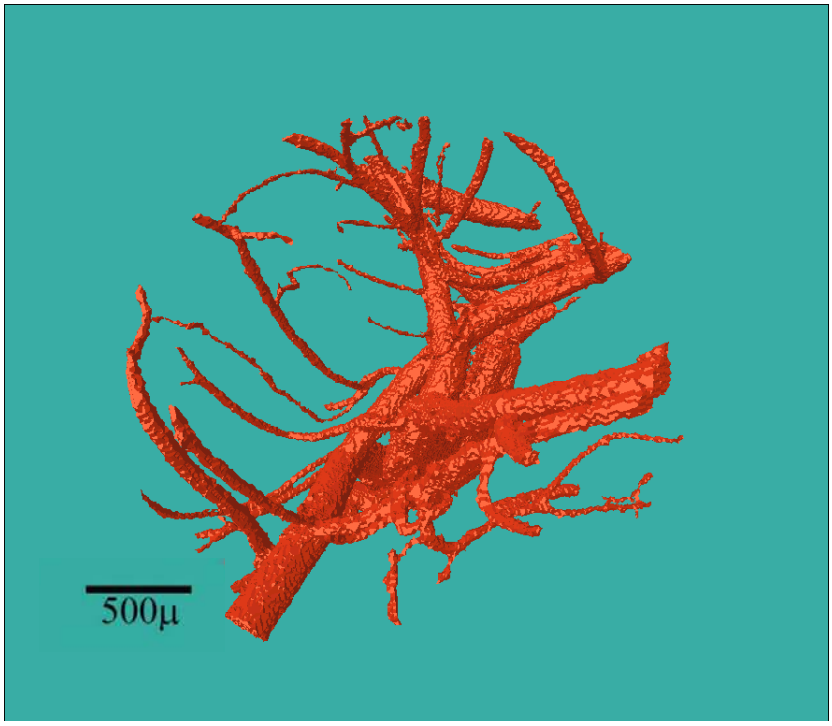

Figure 28: Microfil specimen from mouse brain. After post 3D reconstruction image sweep (CTan) processing reconstruction shows improved microvascular structure. Image pixel size 4.25 µm

becomes clearly visible. In 8c of Figure 30 shows the complexity of these networks and their association with the neighboring alveolar air space. These networks, along with their associations were not easily demonstrated with micro-CT. The pre-screening of specimens with SEM allows us to narrow our search of the casts for areas representative of the capillary bed structure desired.

The best reconstruction results for capillary structures by micro-CT were obtained with the modified Batson's procedure described in this report. Micro-CT of the rabbit skin's vasculature showed a cast with Batson's that completely filled most of the vascular tree system of the dermal and subdermal regions. Figure 30 shows, using SEM, the fine capillary detail present in the dermal vascular corrosion cast from Figure 34. Figure 36b demonstrates a 3D model created from the micro-CT images from a portion of this vascular corrosion cast. The 3D model contains these capillary structures, as well as the structures of larger blood vessels (Figure 36). This 3D model clearly represents the arteriole and venous blood supply system with continuous microvasculature and capillary beds structures demonstrated at the SEM level.

The eroding away of all tissues is characteristic of the corrosion casting technique. The lack of tissues surrounding the imaged structure reduced the background noise during the intensity profiling. The removal of tissues from the cast provided samples that contained no background material to absorb X-ray contrast levels, ultimately giving a more efficient image of the represented capillary structures.

Micro-CT scanning of corrosion casts allowed a cleaner, more complete representation of the capillary vasculature. Background noise associated with micro-CT

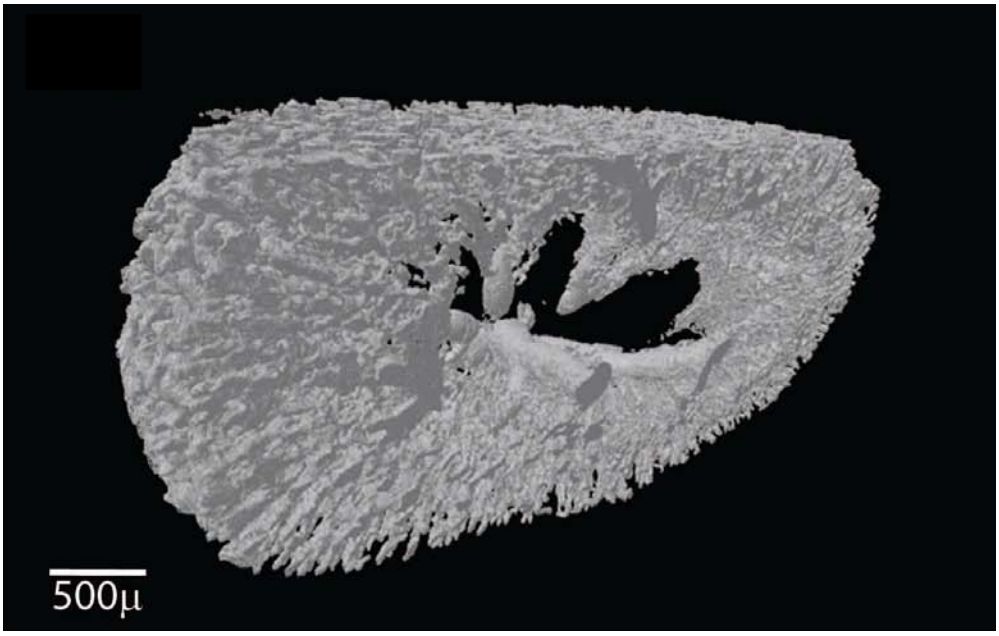

Figure 29: 3D mess model of a rabbit kidney vascular casting. Model of the vascular casting seen in figure 22, created using Micro-CT.

Image pixel size 35.36 µm.

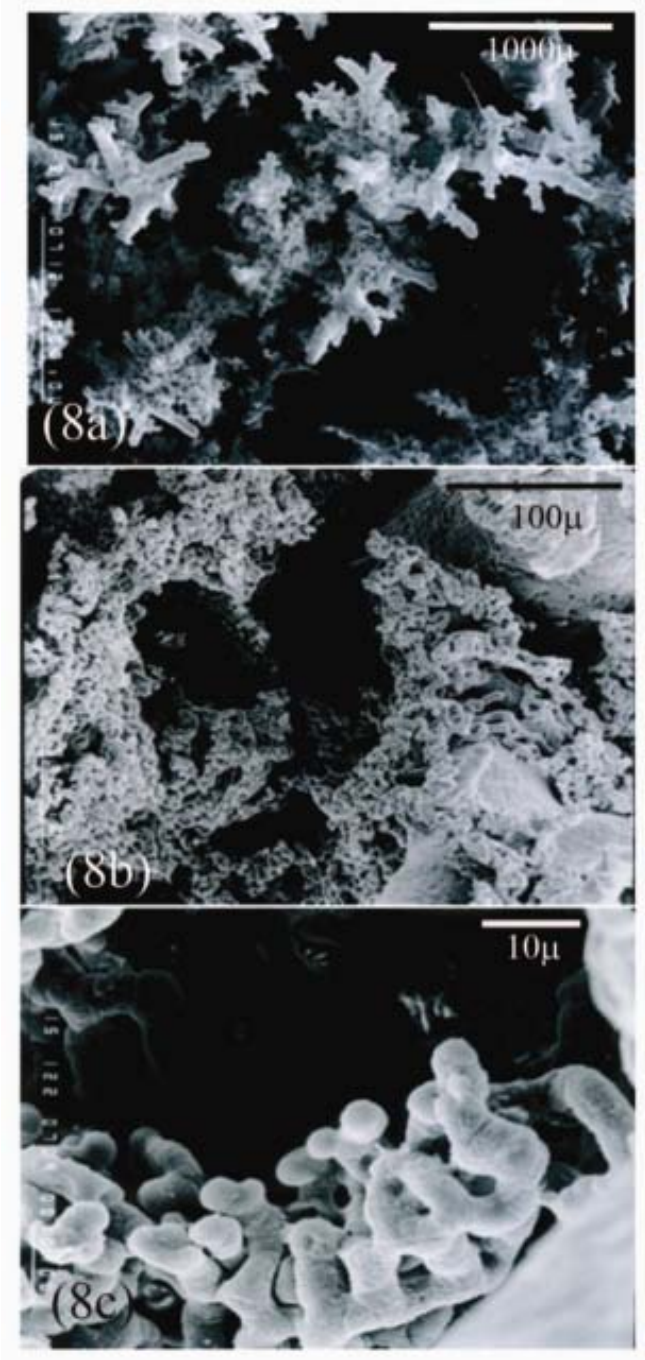

Figure 30: Scanning electron microscopy (SEM) of a vascular cast. Step-wise scanning electron microscopy (SEM) zoom into an area of the vascular cast shown in Figure 33. In 8b the capillary network around lung alveoli becomes clearly visible and 8c shows the complexity of these networks and their association with neighboring perialveolar networks.

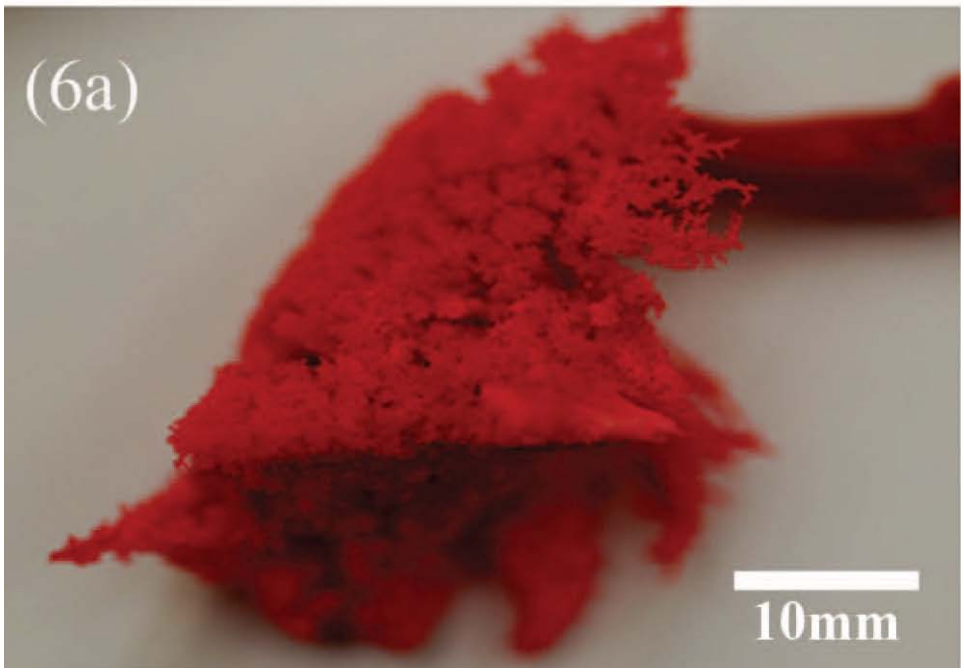

Figure 31: A corrosion cast of a whole rabbit lung

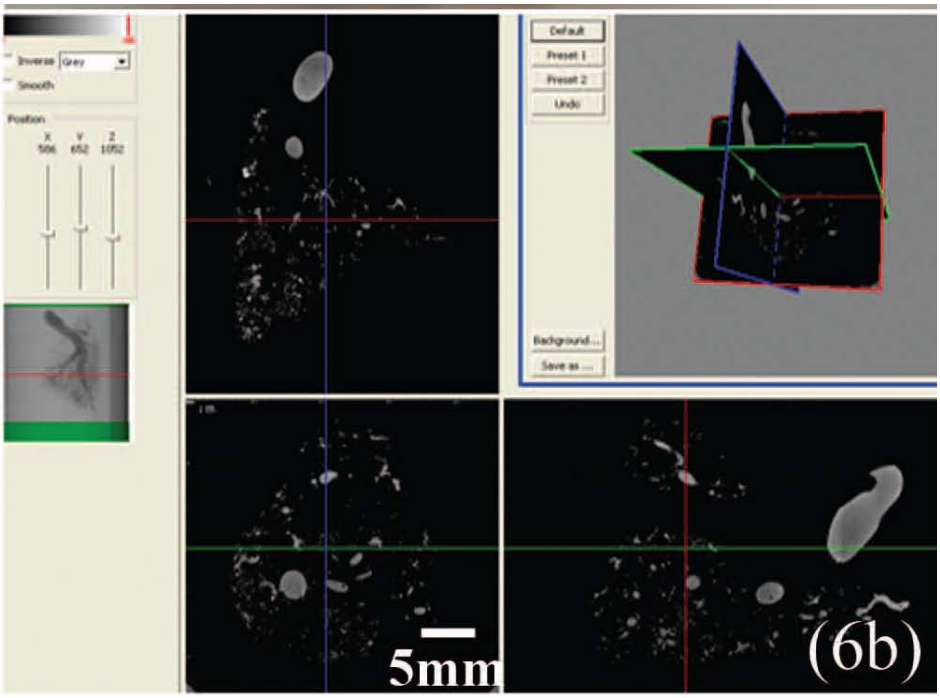

Figure 32: 3D view of a Micro-CT image data set acquired from lung casting.

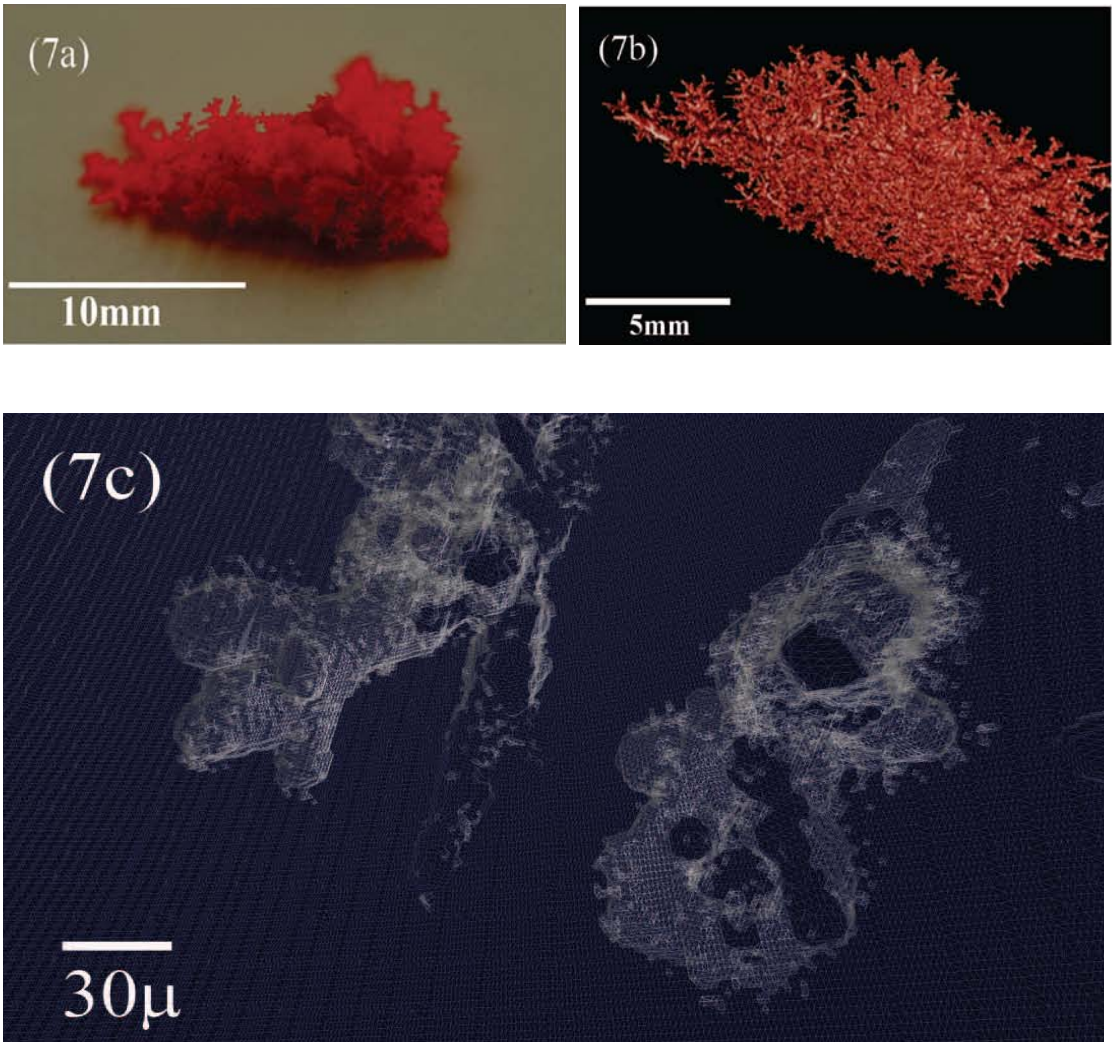

Figure 33: Capturing the capillary bed. In order to capture capillary beds a small portion was taken from a lung vascular cast for high-*resolution* Micro-CT. 7b: 3D model created from Micro-CT data captured from lung vascular cast shown in 32a. Image pixel size 5.06 μm, 7a: Selective region of interest taken from rabbit lung data set demonstrating alveolar sacs and the limitations of detail obtainable when scanning specimens with large 3D volumes and complex microstructures. The capillary structures in most areas are blended together to appear as a single structure.

images that occurs during the intensity thresholding of vessel's lumen perfused with Microfil™, with tissues present, was significantly reduced when using Batson's method. Resulting images were reconstructed in a STL file format as 3D mesh structures. The results of our experiments, using the resulting STL's for modeling complete capillary bed structures, indicated that scaffolding can be designed to directly mimic unique structural patterns of various vascular tree systems.

The *in vitro* biomedical engineering of intact, functional vascular networks, which includes the capillary structures, is needed. Capillary structures are necessary in order to make available elements and compounds for the growth, function, and maintenance of 3Dtissue structures. Using micro-CT, we studied the ability to use vascular tissues to produce data capable of aiding the design of vascular tree scaffolding that would help in the reverse engineering of a complete vascular tree system that includes capillary bed structures. We used STL models of large, data-generated CAD data of vascular structures, which contained capillary structures that mimic those in the dermal layers of rabbit skin. Using CAD software, we created from 3D STL models a bio-CAD design for the foundation of a capillary containing vascular tree scaffolding for various tissues. The resulting bio-CAD design can be used to guide the fabrication of the scaffolding by rapid prototyping techniques and 3D patterning using femtosecond laser pulses and will serve as the framework for tissue engineering of microvascular structures. Resulting microvasculature will be capable of supplying a blood source to 3D tissue scaffolds, thereby stimulating and supporting tissue genesis and regeneration.

Resolution at Different Levels with Different Devices

The area that can be imaged and reconstructed by Micro-CT is limited in size when high-resolution instrumentation is used. This makes the area that is possible to scan smaller than most complete vascular tree systems. Micro-CT results demonstrate the lack of resolving capabilities needed to clearly image the 7 to 10 μ diameter tubes that make up the capillary beds of vascular tree system. The resolution limitations of micro computer-assisted tomography imaging systems make capturing complete image data for the capillary bed of a vascular tree very difficult – almost impossible – even with the latest equipment. In the future, we will be able to have improved CT capabilities. But for now, in order to reverse engineer a vasculature tree using micro-CT image data, image data for capillary networks that are missing because of resolution limitations must be supplied by other means.

Image data from micro-CT and re-constituted serial tissue sections are converted to 3D wire frame models and merged together using CAD software. The reconstructed image data sets from micro-CT and serial section of the corresponding capillary bed are combined to complete the framework for the bio-CAD model. This framework gives us a complete 3D layout of the inner wall of the vascular tree system of interest. Using histological data on vascular wall thicknesses along the length of it structure, auto-CAD can be use to render, on top of the layout for the lumen wall, a design for a structural scaffold created for the seeding of migrating progenitor and/or stem cells.

Designs can then be imported into 3D prototyping software for the creation of structures. However, limitations are found in the creation of microstructures. These

limitations are due to the molecular structure of the structural materials, as well as the prototyping technology – which is quickly improving – and the details of the design. By using actual image data obtained directly from vascular tree systems, we create a highly detailed model of its structure. Such models are extremely valuable in the 3D fabrication of scaffolds to be used for the tissue engineering of complete vascular tree systems.

The 3D visualization of a vascular tree's complete capillary bed is the most important step in our computer-aided design process. The eroding away of all tissues, characteristic of corrosion casting, rids micro-CT images of the background noise problems seen during the intensity thresholding of micro-CT images with tissue still present. The results are images that can then be created and stored as mesh structures in a stereolithography file format, compatible with software-guided fabrication. Whereas investigators are now beginning to attempt to use our imaging strategy for the reverse engineering tissue scaffolds for large defects in soft tissues (Ballyns, Gleghorn et al. 2008), without the necessary vascular supply system native to tissue structure, attempts at engineering functional tissue structures from these types of scaffold are futile.

Micro-CT was used to capture image data directly from Batson's methylmethacrylate corrosion cast (BMCC) of the vascular tree system. Previous micro-CT investigations which illustrate complete (Robb and Hanson 2006; Bentley, Jorgensen et al. 2007; Yu, Ritman et al. 2007; Cameron, Holmes et al. 2008) 3D reconstruction of capillary bed structures demonstrate that there are major obstacle against their complete visualization (Table 1). Contrasting agents do not produce sufficient contrast between the agent in the capillary lumen and the surrounding tissues (Hainfeld, Slatkin et al. 2006; Mukundan,

Ghaghada et al. 2006; Cai, Kim et al. 2007; Kong, Lee et al. 2007; Habibi, Krishnam et al. 2008). Viscous polymers and gels consistently fill capillary beds (Marxen, Thornton et al. 2004). Low viscosity, iodine-based *in vivo* contrast agents are metabolized quickly, creating unstable images that fade rapidly from within the capillary lumina (Priebe, Aukrust et al. 1999; Kim, Kim et al. 2005; Ford, Graham et al. 2006). Reconstructing images of the whole vascular tree system at once gives rise to further problems (Muller 2006; Roberts, Neill et al. 2006). When making comparisons between micro-CT scans of a mouse kidney's vasculature contrasted with Microfil™ and a BMCC vascular cast of a rabbit kidney, we found that the ability to demonstrate the smaller vessels was restricted with Microfil™. This is caused by incomplete vascular perfusion due to metal additive used for contrasting X-ray images inducing endocytosis and vacuole formation by vascular endothelium (Figure 1) (Langheinrich, Leithauser et al. 2004; Pollard and Pascoe 2008) which is used in Microfil™. Also, it was not possible to find an intensity threshold, which eliminated background noise from the tissues surrounding blood vessels and demonstrate the complete microvascular and the larger blood vessels. In eliminating background noise, much of the contrast agent's image of the capillary's lumen is lost. Imaging of Microfil™ samples necessarily implies the sacrifice of some of the microvascular details, even at high-resolution CT scanning levels (Ritman 2005; Zavaletta, Bartholmai et al. 2007).

The use of heavy metals to increase the density of contrasting agents (Table 1) causes a toxic response by endothelial cells. The endocytosis of heavy metal-based contrasting agent by the endothelial cell encompassing the blood vessel lumina (Figure 1) (Langheinrich, Leithauser et al. 2004) creates vacuoles, which causes cytoplasmic

swelling and can lead to significant narrowing of microvascular lumina. The subsequent narrowing slows or blocks the contrast agent's profusion, resulting in the incomplete filling of the capillary beds (Beeuwkes 1980; Elleaume, Charvet et al. 2002; Bernard, Luchtel et al. 2005; Ananda, Marsden et al. 2006; Muller 2006; Kim, Park et al. 2007; Almajdub, Magnier et al. 2008) and its inaccurate micro-CT imaging.

For complete visualization of capillary bed systems, both the capillary beds and larger vessels on the opposite side of the contrasting agent’s entrance into the capillary bed system need to be filled. In order to overcome the obstacles with micro-CT contrast agents hampering complete visualization of capillary bed systems, we used BMCC corrosion casts (Figures 30, 35, 36.). The corroding away of tissue surrounding the vascular cast also allows us to examine samples with SEM before micro-CT scanning. With this added step, it can be determined whether the perfusion of the casting material has entered the necessary regions of the capillary bed structures and whether the necessary image data can be obtained from the sample chosen.

The use of the BMCC method, without adding barium sulfate or other heavy metal, prevents vacuole formation in endothelial cells of the microvascular walls, allowing capillary lumina to stay open during the perfusion with BMCC. Lowering the polymerization rate during perfusion can increase the BMCC casting media’s ability to flow through the capillary beds. Precise control of polymerization time will allow for complete filling of the blood stream with the BMCC casting media before its viscosity begins to increase to a level that limits its flow through the microvasculature. If care is

not taken in these areas, polymerization can occur in the vascular system before perfusion of the contrasting agent has completely filled the blood vasculature.

A specimen's size and thickness is an issue addressed with the eroding away of tissues, characteristic of the BMCC corrosion casting technique. With the removal of surrounding tissues, the x-ray tube can be set at lower acceleration voltages, allowing the smallest diameter of the capillaries' luminal casts, 5μm – 7μm, the ability to block the x-rays' path to exposure, making their structures resolvable. This precludes the need to add to the Batson's polymer, x-ray opaque materials, which can interfere with the perfusion.

The results here show that corrosion casting with BMCC method create representations of continuous vascular tree structures that are micro-CT detectable without the use of contrasting metals, such as barium, which have been shown to block microvascular and capillary lumina (Langheinrich, Leithauser et al. 2004; Kim, Park et al. 2007). The eroding away of tissues, characteristic of the BMCC technique gives significant reduction in background noise (See Chapter V), so this technique provides clean structures from which 3D models can then be created as mesh structures in a stereolithography file format. These files promise to be an excellent resource for further bio-CAD refinement of vascular tree-mimicking scaffolds.

The *in vitro* biomedical engineering of intact, functional vascular networks that include the capillary structures is needed in order to fully realize the true potential of tissue engineering (Germain, Remy-Zolghadri et al. 2000; Sun, Starly et al. 2004; Kannan, Salacinski et al. 2005; Sun, Starly et al. 2005; Ballyns, Gleghorn et al. 2008; Hanjaya-Putra and Gerecht 2009). Success has been limited to the stimulation of

relatively small networks of simply patterned capillary-like structures (Radisic, Park et al. 2006; Iyer, Radisic et al. 2007; Linke, Schanz et al. 2007; Radisic, Marsano et al. 2008) and short, scaffold-supported vascular-like tubes that *in vivo* have stimulated limited vasculogenesis. (Telemeco, Ayres et al. 2005; van Amerongen, Harmsen et al. 2006)

These attempts lacked the structural design millions of years of evolution has established in the creation of vascular structures (Hanjaya-Putra and Gerecht 2009). Capillary structures are necessary in order to make available elements and compounds for the growth, function, and maintenance of 3D tissue structures (Hanjaya-Putra and Gerecht 2009). Many researchers have taken the mathematical model approach to compute the anastomosis and patterning found in the vascular branching systems present in tissue structures (Bezy-Wendling, Kretowski et al. 2001; Kretowski, Rolland et al. 2003; Volkau, Zheng et al. 2005; Wischgoll, Meyer et al. 2007; Volkau, Ng et al. 2008). Other researchers have created models of physiological behaviors, such as angiogenesis, or structural measurements, such as diameter and the distance between anastomosises, to model the structural pattern of microvasculature (Hall, Ngan et al. 1997; Halpin, Evans et al. 2003; Szczerba and Szekely 2005). The best results come from researchers combining these two approaches (Li, Regli et al. 2007; Wischgoll, Choy et al. 2008). Even still, these attempts fall short of being able to reproduce, with structural specificity, a complete and accurate model of an afferent-efferent blood vascular system that includes capillary beds. In our prior study, we described the use of micro-CT) to render stereolithography (STL) models that mimic the organ-specific design of the capillary bed lumina in vascular tissues (Mondy and N. De Clerck 2009, In Press). In this paper, we describe the use of these STL vascular lumina models, rendered with micro-CT, to mimic with

computer-aided design (CAD) the organ-specific vascular tree lumina of the dermal layers in rabbit skin. Using CAD software, we created, from 3D STL, vascular tree models that contain complete and accurate designs of capillary bed lumina for the foundational use in creating bio-CAD blueprints of a capillary-containing vascular tree scaffold for skin and other tissues.

Specimen Preparations

Specimens were prepared with vascular perfusion, using modified Batson's #17 Corrosion Casting methods (Batson 1955; Pollitt and Molyneux 1990; Mondy and N. De Clerck 2009, In Press). Vascular corrosion casts, which included capillary beds, were scanned using high-resolution micro-CT to completely resolve capillary bed systems (Mondy and N. De Clerck 2009, In Press).

The ethical approval for procedures carried out on animals used in this study was obtained from University of South Florida's Institutional Animal Care and Use Committee, established in accordance with the U.S. National Instituted of Health's Guidelines for humane care and the University of Ghent's Faculty of Veterinary Medicine's Ethical Committee for Animal Experiments in Ghent Belgium.

The rabbit was a female, 1-year-old New Zealand white rabbit weighing 2.2 kg. It was euthanized by intravenous injection of 1 ml T61® (Embutramide 200 mg, Mebenzoniumiodide 50 mg, Tetracaine hydrochloride 5 mg, Dimethylformamide et aqua dest. q.s. ad 1 mL, Intervet, Mechelen, Belgium) into the marginal ear vein. The mouse was male, 8-week-old Swiss mouse, weighing 27 grams. It was killed by cervical dislocation.

Vascular Perfusion

A ventral incision was made, exposing the animal's thoracic cavity. An appropriately gauged cannula was inserted into a large artery supplying blood to the tissue. Using a three-way valve, heparinized normal saline solution was perfused through the tissues' vasculature to prevent blood clotting. Perfusion was done at a pressure of 100mm Hg ntil blood was cleared from the tissue to be vascularly casted**.** If venous perfusion was necessary, veins would be perfused at a pressure of 20-40mm Hg to prevent rupture of the vessel's wall. The valve was switched to perfuse a freshly prepared Batson's #17 solution (Batson 1955; Pollitt and Molyneux 1990), modified with the addition of methyl methacrylate, into the animal's tissues (Polysciences catalog # 07349). Batson's resin was allowed to polymerize within the animal's tissue. Curing of the polymer took two to three hours and was done with the specimen in an ice bath. This slowed polymerization and minimized distortion of the cast during this exothermic reaction. Tissue was then immersed into a 25% potassium hydroxide solution and allowed to stand for 24 to 48 hours, as necessary. The solution corroded the tissues away from the polymerized plastic in the vascular tree lumina.

Modified Batson's Formula

A freshly prepared Batson's #17/methyl methacrylate working solution consisted of 50ml of Base Monomer, 7.5ml of solution B Batson's #17 catalyst, 10 drops Promoter solution C, 20ml of methyl methacrylate monomer (MMA BDH Chemicals) and 5mg of one of the color dyes for visualization.

Scanning Electron Microscopy Preparation

The vascular cast needed very little additional processing for SEM. Gold/palladium sputter coating was used to provide an electron interactive surface for surface structure visualization. Imaging and photography of vascular castings were performed using the Hitachi S570.

Micro-CT Scanning of Specimens

The Skyscan 1172 high-resolution micro-CT and the 1076 IN-VIVO micro-CT scanners were both used to gather the necessary image data to reconstruct vascular tree structures for scaffold design. The instruments were produced by Skyscan, Belgium. Skycan1076 is designed for the *in vivo* scanning of whole animals and has an image field of 68 mm. The 1076 was used on rabbit lung and kidney for complete scans of their larger vasculatures.

For microvasculature representations, the Skyscan 1172 was used for its ability to move both the sample stage and the x-ray camera. This allows us magnification adjustments where we can optimize the spatial resolution and image quality. Smaller specimens were prepared from both the Batson's and the Microfil™ microvasculature preparations and scanned on the 1172. The specimens used to obtain the images created in this paper are listed in tables 2 and 3, along with the operating and equipment specifications utilized.

Data Merging and Model Creation

We have approached the challenges micro-CT presents with regards to accurately resolving complete capillary structures by 3D scanning corrosion casts of vascular

structures with micro-CT (Mondy and N. De Clerck 2009, In Press). Reconstruction in stereolithography (STL) format allows the compatibility of subsequent 3D models with most CAD software.

Rhinoceros 4.0, 32 bit, 3DMax and Geomagic 64 bit CAD software programs were tested for their possibility of loading and modifying stereolithographic (STL) mesh models obtained from the CTan processing of micro-CT data sets. Our aims were the bio-CAD modification of models, ease of software manipulation of models' structures, and design applications with the ability to create capillary bed-containing vascular scaffolds.

Our novel method for engineering tissue structures is built around the computer-aided designing of vascular scaffolding that mimics actual vascular tissue structures on a micrometer scale. The realization of a need for more detailed designs is demonstrated in the recent use of lithography to pattern channels designed structurally to simulate extracellular matrix fibers' role in guiding cellular and cytoskeleton structural alignment (Sarkar, Dadhania et al. 2005).

The recent use of lithography to pattern channels (Sarkar, Lee et al. 2006; Figallo, Flaibani et al. 2007) designed structurally to simulate extracellular matrix fibers' role in guiding cellular and cytoskeleton structural alignment in the formation of a vascular wall (Medvedev, Samsonov et al. 2006) represents the first attempt at microscopically designing the structure of vascular scaffolds to structurally mimic natural vasculature. Using algorithms of constraint construction optimization, computer-generated models have been created to supply analytical models of hollow organs, as well as finite element analysis of image-generated triangular mess models (Schreiner, Karch et al. 2006).

In order to accurately engineer a complete vascular tree system that includes capillary bed structures, we sought a method to reconstruct capillary bed systems using micro-CT. Reverse bioengineering approaches have been used to visualize vascular tree systems (Kassab, Rider et al. 1993; Wischgoll, Meyer et al. 2007; Yu, Ritman et al. 2007). A complete afferent-efferent blood vascular system that includes a capillary bed has yet to be reverse engineered.

Given that the vasculature is a living and dynamic structure, constructing a geometrically similar structure based on these micro-CT derived 3D images is just our first step in our goal of reverse engineering a vascular tree. Using these 3D images to guide fabrication, scaffolding can be produced by rapid prototyping and 3D femtosecond laser pulses patterning. With the attachment of bioactive peptide motifs, like RGD, guided cell behaviors can be induced in these vascular tree scaffolds (Salinas and Anseth 2008; Weber and Anseth 2008). The resulting structure becomes dynamic and serves as a framework for tissue-engineered vasculature. This vasculature will be capable of supplying a blood source to 3D tissue scaffolds, stimulating tissue regeneration.

The resolution of a CT scanner is not the same as the voxel size of the scan. It is quite likely that the resolution of the scanner is preventing us from resolving capillaries in some cases. Vessels that have diameters smaller than the point spread function will be reduced in intensity and difficult to detect. The extent to which the contrast agent filled the capillaries can be verified on histological sections in order to rule this out as an explanation.

Using a single scaffold or by combining scaffolds produced for different cellular tissue structures, we have the framework to reverse engineer any of the tissue structures produced in nature. Using this type of reverse bioengineering approach, we can create designs that merge macroscopic with microscopic data. They can mimic the extracellular environments (Shoichet, Yu et al. 2007; Rydholm, Held et al. 2008; Salinas and Anseth 2008) conducive to the functional framework specific to vessel's structural location and the tissue structure (Yu, Kazazian et al. 2007; Polizzotti, Fairbanks et al. 2008; Rydholm, Held et al. 2008) hosting the vasculature.

Data Size Issues

The 2D data sets created from micro-CT scans were very large and are listed in tables 1 and 2. The file sizes of the resulting 3D STL models constructed with CTan were dependent on the 2D image resolution and the intensity threshold (Table 5). Initially, the system requirements for building 3D STL models from these data sets crashed our computer system or required anywhere from a few hours to several days to process. The computer's RAM was increased from 1 GB to 3 GB and finally to 8 GB, and the central processing unit upgraded from single to dual core. Increasing the RAM memory and using a dual core processor gave us the results reported here. Initially, the image data sets had to be divided into smaller sets and limited volumes of interest (VOI) selected in order to construct models at the full resolution of the micro–CT scans. After the computer upgrades were made, complete data sets could be constructed into 3D STL files (Tables 4and 5). But models of complete data set were too difficult to be constructed because of their sizes (Table 5).

Only 3D STL files less than 300 MB could be opened in Rhinoceros. This made it useless for the 3D modeling of most image data sets. The smallest subsets taken from data sets and modeled in 3D were from corrosion cast of rabbit skin. This data set was selected because the vascular structure of the skin was less dense than the other tissue samples scanned (Mondy and N. De Clerck 2009, In Press). The black background was more than 80% of the image and was eliminated with image compression, allowing us to produce small files sizes without losing the high resolution obtained at the micro-CT scanning level. (See Table 5)

In testing for the most efficient manual settings for the intensity thresholding, levels providing models with most capillary bed from corrosion cast micro-CT data, we compared our results with models created with algorithmic computations (Table 5). Small regions of interest were processed from rabbit skin's data set in order to decrease the model size, significantly speeding speed up processing (Figures 44 - 53 and Tables 4&5). This was not worked out with an efficient intensity threshold, which demonstrated complete capillary structures (Figures 37 - 39 and Tables 4 and 5). The choice was made to increase RAM and work on models that created larger files.

Table 4: Models Construction from 2D Micro-CT Images

3D Stereo Lithography Models Construction from 2D Micro-CT Images Using CTan Software				
Data set:	2D Images, #/Size	3D Model Size Mb	DPI	Pixel
Rabbit Whole Lung Low Res	1828/2.9 GB Bitmap	7,880	1308	1308^2
Rabbit Lung small volume Hi-Res	1961/109MB	1,997	5019	2160^2
Rabbit Kidney	1097/1.02GB Bitmap	24,000	1308	1000^2
Rabbit Kidney Hi-Res	1870/3.77GB	77,316	4241	3684X2944
Complete Rabbit Skin scan	3308/1.05GB	5.37 GB	1455	3968^2
Mouse Brain	1869/7.6 GB	10,500	5974	3144^2

Table 5: Stereo Lithography Models

3D Stereo Lithography Models Construction of Corrosion Cast of Rabbit Skin Vasculature Micro-CT Software						
Data set:	2D Images/Size	CTan STL	Brightness Lower Index	Brightness upper Index	CTvol: Size Facets /Vertexes(Million)	3D Image Quality
Bottom ½ OF TOP 1/3 C1	541/101 MB	5,500 MB	Maximum Threshold		111,810/335,430	Never Loaded
Bottom ½ OF TOP 1/3 C1	541/101 MB	300 MB	Global Threshold		25,789/77,366	Noisy Surface
Bottom ½ OF TOP 1/3 C1	541/101 MB	810 MB	Just under Max. Threshold		10,179/30,537	Good Image
Bottom ½ OF TOP 1/3 C2	541/101 MB	32 MB	60%	62%	Incomplete Model	Incomplete Model
Bottom ½ OF TOP 1/3 C3A	541/101 MB	689 MB	7.8%	62%	14.11 /	Good Image
Top ½ OF TOP 1/3 C3A	449/103 MB	690 MB	7.8%	62%	14.13/42.39	Good Image
Top ½ OF TOP 1/3 C3B	449/103 MB	657 MB	7.8%	182	13.49/40.46	Good Image
Top ½ OF TOP 1/3 C3C	449/103 MB	564 MB	7.8%	94.5%	11.56/34.67	Good Image
Top ½ OF TOP 1/3 C3D	449/103 MB	2.47 GB	7.8%	100%	50.67/152.01	Good Image
Top ½ OF TOP 1/3 C3E	449/103 MB	1.01 GB	7.8%	97.4%	20.65/61.94	Good Image
Top ½ OF TOP 1/3 C3F	449/103 MB	1.39 GB	6%	93%	28.56/85.67	Good Image
Top ½ OF TOP 1/3 C3G	449/103 MB	838 MB	3.9%	93%	17.16/51.47	Good Image
Bottom 1/3	1401/322 MB	2.48 GB	7.8%	93%		Good Image
Middle 1/3	1001/230 MB	1.09 GB	7.8%	93%		Good Image
Top 1/3	901/205 MB	1.05 GB	7.8%	93%		Good Image
Complete data set	3308/1.05 GB	5.37 GB	7.8%	93%		No Model

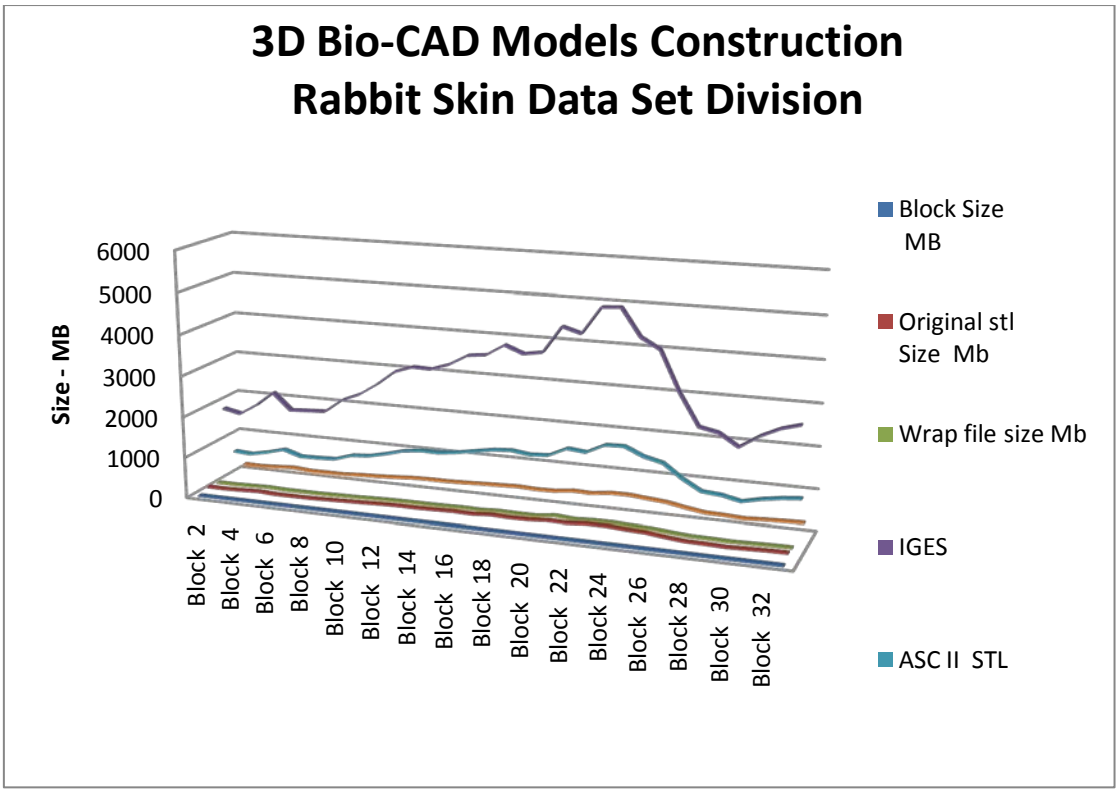

Figure 34: 3D Bio-CAD model's file size comparisons

Using the original hardware setup, the top third of the vascular cast data set created from micro-CT scans of the rabbit skin's corrosion cast had to be constructed in halves. With the addition of 2 GB of extra RAM, each third could be constructed separately (Table 5). The final hardware setup with 8 GB Dual Core intel 2.14Ghz processor and the ATI FireGL 5100 Graphic Processing Unit (GPU) allowed the whole data set to be used in the construction of a model, although the model could not be opened without significantly reducing the intensity threshold (Table 5 and Figures 36 and 37).

With the upgraded hardware and the results seen on small models made from small regions of interest (ROI) in limited numbers of micro-CT 2D images (Figures 43 - 52), we decided to stitch the entire model together in small blocks (Tables 5, 6) and Figures 53 -60. In order to make the initial models more manageable for software and hardware, they were reduced in size through the reduction of the intensity threshold used to make the initial STL 3D models. The results were models that were incomplete when opened in CAD program (Figure 36 -39). The CAD software was used to remove floating unusable area (Figure 38), repair holes and bridge gaps in the design (Figure 39).

The entire data set was created from the rabbit skin's micro-CT scanning and was divided into 33 blocks; each block had approximately 101 2D slice images. Each block was post-processed using CAD for the optimization of its structure and for stitching it to its neighboring blocks. The results were hollow designs stitched together in thirds capable of containing fluid. The thirds were then stitched together to form the whole scanned vascular structure (Figure 58&59). Although there were some broken or

incomplete areas, continuous capillary structures were clearly modeled using the CAD software (Figures 47-60)

In our long-range goal to reverse engineer a vascular tree, we must first design our structure. In our first study on this subject, (Mondy and N. De Clerck 2009, In Press) we used the direct 3D visualization of the structural patterns comprising the lumen of complete vascular tree systems for the skin, lung, brain and kidney tissues. In our second paper on the reverse engineering journey, we replicate one of these structural patterns in a bio-CAD design. The first stage in meeting our goal is to engineer a bio-CAD design to direct the micro-fabrication of vascular scaffolds. The model will simulate the extracellular matrix environment and stimulate needed cell type-specific behaviors. In doing this, the cells will themselves become engineers and our design will be the "blueprint" guiding them in the development of vasculature wall structures with characteristics specific to the cell phenotype and position as it relates to vessel diameter and the wall location.

The Skyscan 1172 high-resolution micro-CT and the 1076 INVIVO Micro-CT scanners were both used to gather the necessary image data to reconstruct vascular tree structures for scaffold design (Mondy and N. De Clerck 2009, In Press). Skycan1076 with an image field of 68 mm was used for its ability to handle large specimens. The 1172, with its smaller specimen stage and higher resolving capabilities, was used for resolving the microvasculature castings (Mondy and N. De Clerck 2009, In Press). The Skyscan 1172 has the ability to move both the sample stage and the x-ray camera. This allows us magnification adjustments where we can optimize the spatial resolution and

image quality. The 3D reconstruction of 2D micro-CT data sets into 3D Models with stereolithography (STL) file formatting was done using Skyscan's Computer Tomography Analyser (CTan). The resulting models were visualized in 3D using Skyscan's Computer Tomography visualization (CTvol) software.

Post-slice set reconstruction of the micro-CT scans data sets were used to construct 3D models of the imaged vascular structures using a HP xw4300 workstation with Windows XP Professional. An Intel Pentium 4 640 Supporting Hyper thread technology 3.0 GHz/2 800 FSB was used with 3GB Duo channel DDR2 640 memory and an ATI FireGL 5100 Graphic Processing Unit (GPU)

A custom machine was modified to aid in the graphic designing of vascular tree scaffold. Its specifications were: a MSI Motherboard with Intel P965 Express Chipset and an Intel Core 2 Pentium 4 CPU; 6400 @ 2.13 GHz; Microsoft Vista, for 64 bit operating system With 8 Gigabytes of Duo channel DDR2 800 and an ATI FireGL 5100 Graphic Processing Unit (GPU)

Chapter Five

Case Studies and Applications

Computer aided designs (CAD) of the lumina of micro vascular tree system's can be modeled from micro CT scans including complete and accurate capillary bed structures. This study focuses on using CAD to model large vascular tree system that include complete and accurately render capillary luminal. Micro CT scan results are divided into smaller subsets capable of being rendered into files manageable by CAD software and desktop computer hardware. Using Intensity threshold, image contrast is adjusted for Batson's corrosion cast's without surrounding tissues, to demonstrate complete capillary structures. One subset at a time the complete vascular tree system is rendered into 3 dimensional (3D) stereo lithography (STL) models. The marginal areas of bordering subsets are duplicated for stitching together adjoining subsets. Each STL is then modeled in CAD software, meshing errors repaired and significantly reduced in file size by triangle decimation. During this processing the marginal areas of each subset, later be rejoined, are unaltered. Processed sections of the vascular tree system are stitched together forming the complete vascular tree structure of the dermal skin anatomy(Zhang, Laufer et al. 2009).

In vitro biomedical engineering of intact, functional vascular networks, which include the capillary structures, is a prerequisite for adequate vascular scaffold production. Capillary structures are necessary since they provide the elements and compounds for the

growth, function, and maintenance of 3D tissue structures. Computer-aided modelling of stereolithographic (STL) micro-computer tomography (micro-CT) 3D models is a technique that enables to mimic the design of vascular tree systems containing capillary beds, found in tissues. In our first paper (Mondy and N. De Clerck 2009, In Press), using micro-CT, we studied the possibility to use vascular tissues to produce data capable of aiding the design of vascular tree scaffolding, which would help in the reverse engineering of a complete vascular tree system including capillary bed structures. In this paper we used STL models of large datasets of Computer-Aided Design (CAD) data of vascular structures which contained capillary structures that mimic those in the dermal layers of rabbit skin. Using CAD software we created from 3D STL models a bio-CAD design for the development of capillary-containing vascular tree scaffolding for skin. This method is designed to enhance a variety of therapeutic protocols including, but not limited to, organ and tissue repair, systemic disease mediation and cell/tissue transplantation therapy. Our successful approach to *in vitro* vasculogenesis will allow the bioengineering of various other types of 3D tissue structures, and as such greatly expands the potential applications of biomedical engineering technology into the fields of biomedical research and medicine.

Using CAD software, we created from 3D STL vascular tree models containing complete and accurate designs of capillary bed lumina for the foundational use in creating bio-CAD blueprints of capillary-containing vascular tree scaffolding for skin and other tissues. The results from this study clearly indicated that accurate and complete high-resolution models of vascular trees can be produced in bio-CAD and that direct modeling methods can be used to construct a complete and accurate high-resolution CAD

of capillary lumina (Mondy and N. De Clerck 2009, In Press). These modeling results are a basis for the further designing of a "bio blueprint" to guide, using micro-prototyping techniques such as the 3D chemical patterning of photo-cross linkable multilayered hydrogels (Yu, Kazazian et al. 2007; Elisseeff 2008), the more complete structural fabrication of a vascular scaffolding, scaffolding that will support, nurture and guide the celluarization of microvascular and macrovascular structures and serve as a nurturing framework. This framework supports the further engineering and design of organ-specific, functional tissue structures from chemically and mechanically engineered extra cellular matrixes, using micro-rapid prototyping and 3D laser pulse patterning for the regulation of tissue-specific cellular morphologies (Elisseeff, Ferran et al. 2006; Linke, Schanz et al. 2007; Garagorri, Fermanian et al. 2008).

Creating the Bio-CAD Model

In our long range goal to reverse engineer a vascular tree we must first design our structure. In our first study on this subject (Mondy and N. De Clerck 2009, In Press) we used the direct 3D visualization of the structural patterns comprising the lumen of complete vascular tree systems for the skin, lung, brain and kidney tissues. In this second paper on our reverse engineering journey we replicate one of these structural patterns, the microvasculature of the skin, in a bio-CAD design (Tables 6 & 7). The first stage in meeting our goal is to engineer a bio-CAD design to direct the micro fabrication of vascular scaffolds. The model will simulate the extracellular matrix environment and stimulate needed cell type specific behaviors. In doing this the cells will themselves become engineers and our design as the 'blueprint' guiding them in the development of

vasculature wall structures with characteristics specific to the cell phenotype and position as it relates to vessel diameter and the wall location.

3D Model Acquisition/Stereolithography File Format

The Skyscan 1172 high-resolution micro-CT and the 1076 INVIVO Micro-CT scanners were both used to gather the necessary image data to reconstruct vascular tree structures for scaffold design (Mondy and N. De Clerck 2009, In Press). Skycan1076 with an image field of 68 mm was used for its ability to handle large specimens. The 1172, with its smaller specimen stage and higher resolving capabilities was used for resolving the microvasculature castings (Mondy and N. De Clerck 2009, In Press). The Skyscan 1172 has the ability to move both the sample stage and the x-ray camera. This allows us magnification adjustments where we can optimize the spatial resolution and image quality. The 3D reconstruction of two dimensional (2D) micro-CT data sets into 3D Models with Stereo Lithography (STL) file formatting was done using Skyscan's Computer Tomography Analyser (CTan). The resulting models were visualized in 3D using Skyscan's Computer Tomography visualization (CTvol) software.

The 2D data sets created from micro-CT scans were very large and are listed in Tables 6 and 7. The file sizes of the resulting 3D STL models constructed with CT were dependent on the 2D image resolution and the intensity threshold (see Table 7). Initially, the system requirements for building 3D STL models from these data sets crashed our computer system or required from a few hours to days to process. The computer's RAM was increased from 1 GB to 3 GB and finally to 8 GB, and the central processing unit upgraded from single to dual core. Increasing the RAM memory and using a dual core

processor yielded the results reported here. Initially, the image data sets had to be divided into smaller sets and limited volumes of interest (VOI) selected in order to construct models at the full resolution of the micro–CT scans. After the computer upgrades, the above complete data sets could be constructed into 3D STL files (see Tables 6&7). However, models of complete data sets were too difficult to be constructed because of their sizes (see Table 7)

Only 3D STL files less than 300 MB could be opened in Rhinoceros, which was useless for the 3D modeling of most image data sets. The smallest subsets taken from data sets and models in 3D were from corrosion casts of rabbit skins. This data set was selected because the vascular structure of the skin was less dense than those of the other tissue samples scanned (Mondy and N. De Clerck 2009, In Press). The black background accounted for more than 80% of the image and was eliminated with image compression, allowing us to produce small-sized files without losing the high resolution obtained at the micro-CT scanning level.

Initial Processing

In our search for the most efficient manual settings for the intensity threshold levels providing models with the largest capillary bed portion from corrosion cast micro-CT data, we compared our results with models created with algorithmic computations (see Table 8). Small regions of interest were processed from data sets of rabbit skin in order to decrease the model size, which resulted in significantly lower processing times (see Figures 43 - 53 and Tables 5&7). This approach did yield an efficient intensity threshold

which allowing complete capillary structures (Figures43-53and Tables 4& 5). Therefore, we opted to increase RAM instead and work with models of larger file size.

Using the original hardware setup, the top third of the vascular cast data sets created from micro-CT scans of corrosion casts of rabbit skin, had to be constructed in halves. Addition of 2 GB of extra RAM allowed us to construct each third separately (see Table 8). The final hardware setup with an 8 GB Dual Core Intel 2.14Ghz processor and the ATI Fire GL 5100 Graphic Processing Unit (GPU) allowed us to use the whole data set to construct a model although the model could not be opened without significantly reducing the intensity threshold (Table 5). Figures 38 and 39 show magnification of selected areas, showing (Circled area in 38) incomplete structures where surface structures were loss while image intensity was adjusted to decrease STL file size. Figure 37 shows a STL model of complete rabbit skin vascular cast imported from micro-CT software into CAD software.

Intensity thresholding was set at a level that maximized the amount of data present while obtaining an image whose size could be open and then manipulate for modifications. A lot of vascular structure is not continuous due to lowering intensity levels to reduce the model's file size; even so this model was too large to be efficiently modified using our final hardware setup. Figure 37 is a STL model of same micro-CT data set processed at a lower intensity level to produce a CAD model whose structure could be fully modified in the CAD software program. Note the significant amount of microvascular structure seen in 36 missing from 37. Figure 39 shows steps to repair large hole created in model by lowering threshold of complete data set.

In constructing models from the 2D data sets we found that the automatic intensity threshold setting did not give us an optimal STL model for data representation. We experimented with intensity settings on one data sets from corrosion cast made from the lung, kidney and skin in order to establish a range of settings that would give us a complete model without introducing unnecessary information. By setting an intensity higher than necessary, even though background noise may not have been introduced, the size of the STL file was significantly increased. Because we were at the limits of our computer system's hardware and software limitations we had to cut its costs in constructing 3D models from these data sets. Once we found an acceptable range we chose the data set for rabbit skin vascular cast to fine tune the range for the intensity threshold settings that would give us the 3D STL modeling results we need.

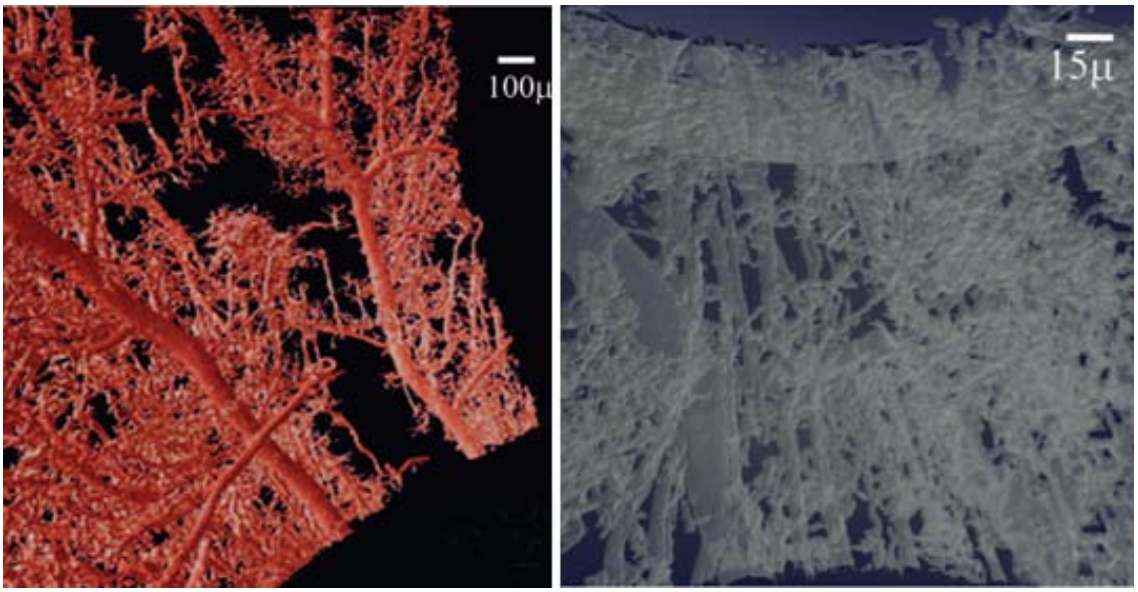

Figure 35: 3D models created from Micro-CT images of skin vascular casting. Selective region of selected from rabbit skin data set demonstrating continuous capillary structure. The detailed topological data obtainable when scanning such a large specimen in not only due to the Batson's method, but also the shallow nature of skins vascular tree structure in the z plane.

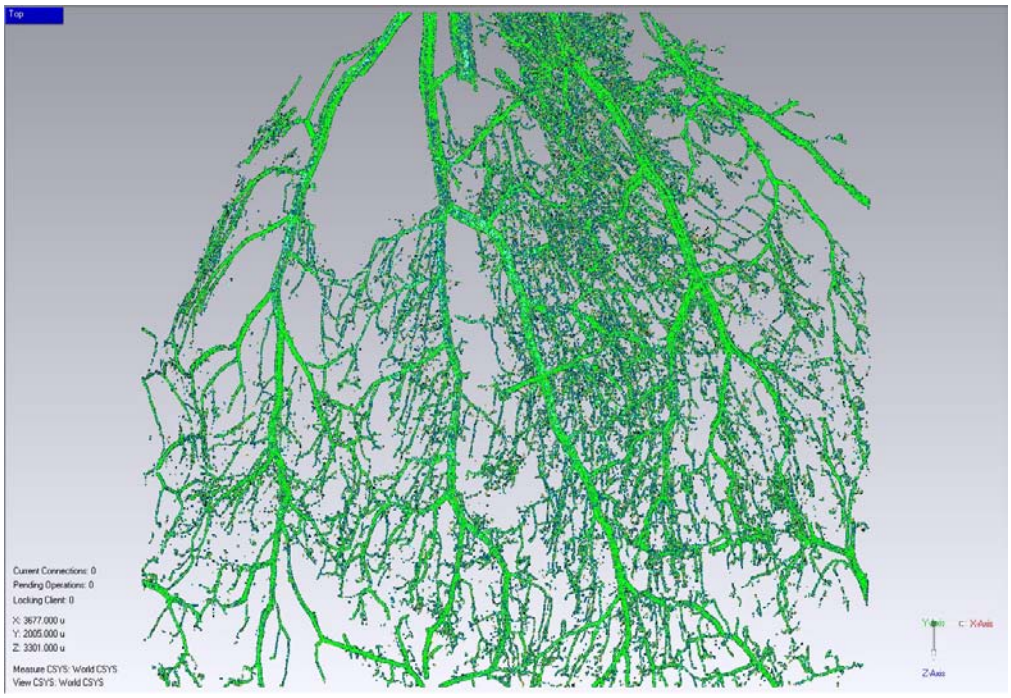

Figure 36: Bio-CAD model constructed using a complete Micro CT data. Data set consisting of over 3300 2-D images and capillary bed structures are incomplete because the image's intensity level was limited in order to produce a 3D model with a file size capable of being constructed.

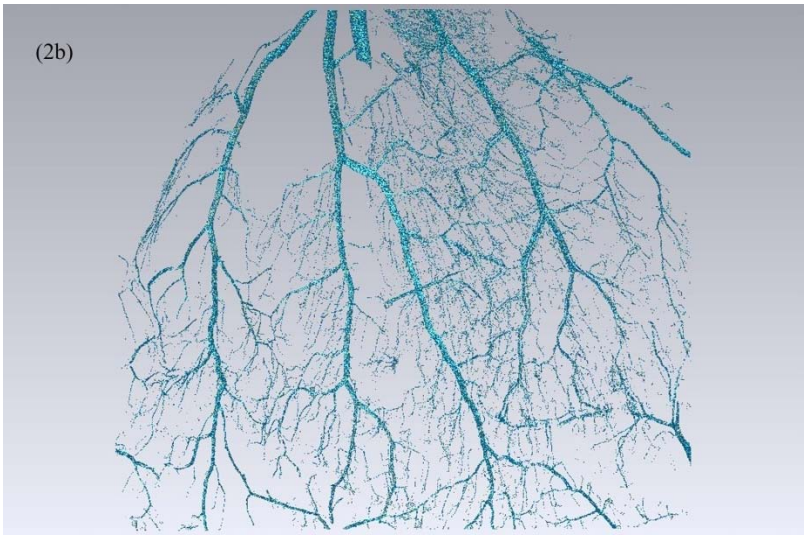

Figure 37: Reduced intensity threshold. A model from the same data set as 36 whose intensity threshold was reduced even further to remove most of the image data suspended with no connection.

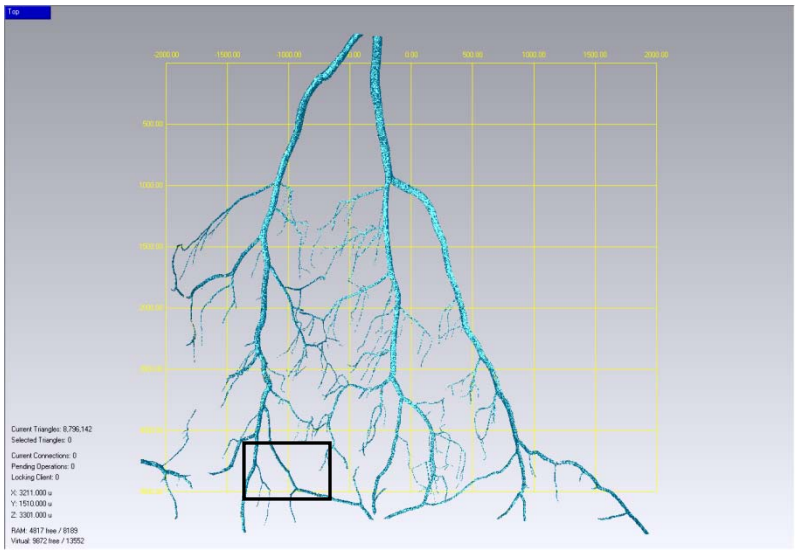

Figure 38: Suspended image data. This reconstruction demonstrates the vascular tree model from Figure 36 where all suspended image data has been selected and deleted. The area within the rectangle above is represented in the first image below.

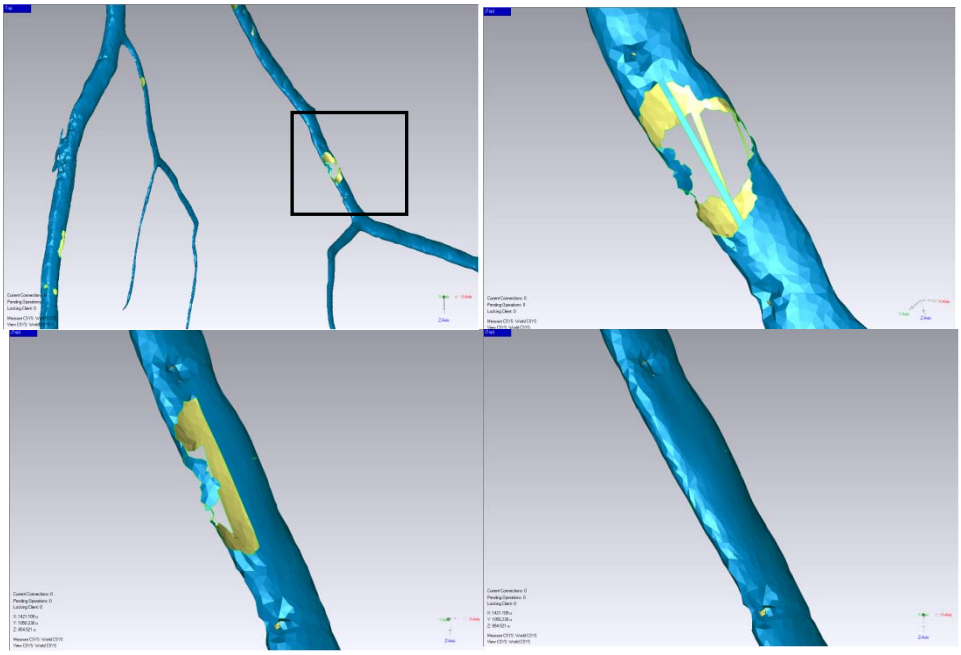

Figure 39: Laborious repair method. A demonstration of the laborious repair method needed for the larger holes that appear in models whose intensity was reduced in order to produce a model with a manageable file size. The area within the rectangle found on the first figure above demonstrates the location of the hole being repaired in the larger model.

CAD Modeling

Initial models were reduced in size by reducing the intensity threshold in order to make them manageable by software and hardware. This approach resulted in incomplete models when opened in the CAD program (Figure 37). CAD software was used to remove the superfluous floating area (Figure 38), repair holes and bridge gaps in the design (Figure 39).

Using the upgraded hardware and starting from the results with small models obtained from small regions of interest (ROI) in limited numbers of micro-CT 2D images (Figures 42, 43, &46-50) we decided to stitch the entire model together from small blocks of images (Tables 6&7 and Figures 55-57).

The entire data set created from the rabbit skin's micro-CT scanning was divided into 33 blocks; each block had approximately 101 2D slice images (see Appendix Table 1) and was post-processed using CAD for optimization of its structure and stitching to its neighbouring blocks. The results were hollow and structural designs that were stitched together in thirds (Table 7&8) capable of containing fluid. The thirds were then stitched together to form the whole scanned vascular structure (Figure 56). Although there were some broken or incomplete areas, continuous capillary structures were clearly modelled using the CAD software (Figures 51-52)

Figures 42 is a 2D image section of the model in Figures 45 and 46. This section shows a region of interest from the rabbit skin's vascular cast modeled in CTan software, before modeling in 3Dvol software (Figures 45 & 46), figures 47 and 48 show the same model imported into the CAD software, Geomagic, as STL created in micro-CT software.

The trimming away of the empty areas around vasculature shown here in Figure 42is the first steps in the creation of the blue model in Figures 51. Figure 49 is the CAD model from Figure 47 and 48 after removing floating pieces and smoothing its surface. Figure 50 is a high magnification taken from one portion of Figure 49. Figures 54 and 55 illustrates eight and eleven blocks of STL models respectively, stitched together and processed during the design and assembly of one third of the complete micro-CT scans acquired from the vascular tree lumen casting. The insert on the top right-hand corner of Figure 51 shows a magnification of the inside of an anastomosis at a processed opening of one of the modeled 2D image blocks. (Table 5&8)

Figure 54 illustrates a comparison of CAD models. The top created by stitching together separately processed CAD models and the bottom created by engaging one third of the data set at an intensity level that brought into view as much as possible of the capillary bed structures with as little noise as possible. The segmented model was stitched from eleven models, each model segment constructed from a STL consisting of 101 2D micro-CT images. The bottom image is of a CAD model created from one single STL constructed from 800 of the same 2D micro-CT images used in the top design. Insert shows the complete micro-CT scan stitched together in three sections of eleven models as each prepared as the one shown at the top of this figure. Figures 57 and 58 show the entire data set modeled results of stitching together 33 separately built STL models. The 75% decimation of the complete segmented model illustrated in Figure 59, maintains its capillary consistency while reducing its file size two thirds.

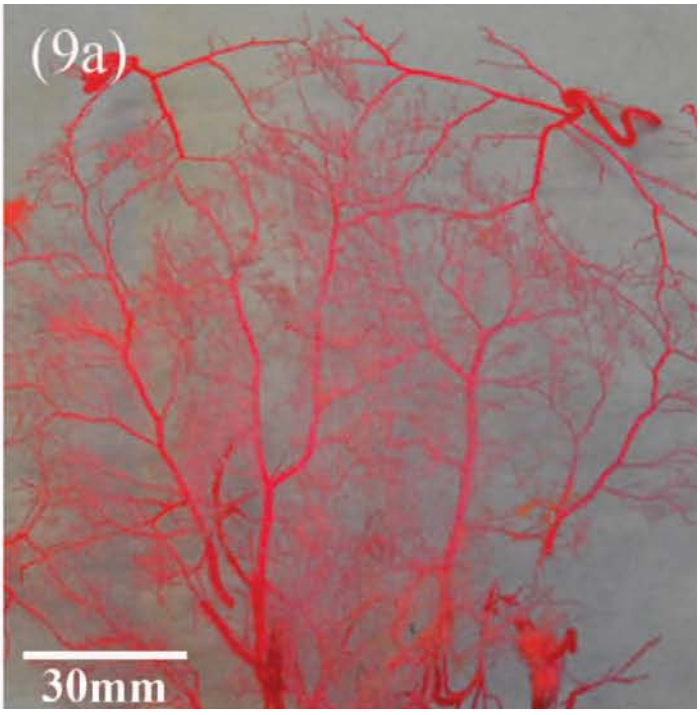

Figure 40: Rabbit skin casting. Vascular tree casting taken from the dermal and sub-dermal regions of dorsal rabbit skin.

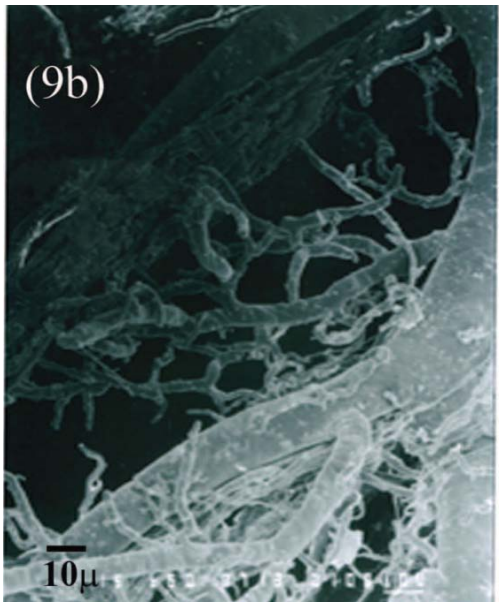

Figure 41: Scanning electron micrograph of skin casting. This micrograph shows a portion of vascular casting in figure 41. It captures the capillary bed's anastomosis with neighboring blood vessels.

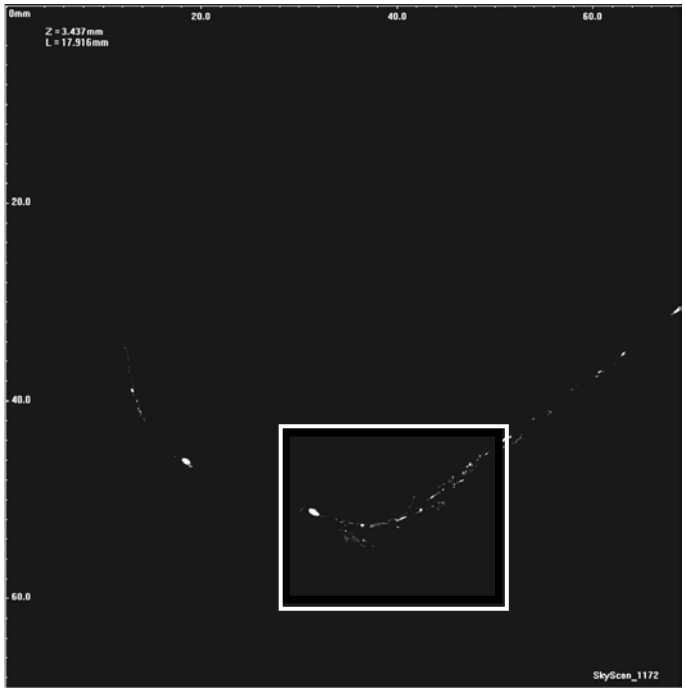

Figure 42: A single 2-D image slice from the micro-CT data set. Acquired from the rabbit skin vascular cast used to build the 3-D models demonstrated in this manuscript, It demonstrates the size of the ROI modeled in Figure 46 - 48.

Figure 43: Cutting it down. One of the 2-D image slices used to create the region of interest model demonstrated in Figures 46 through 49. This image can be seen highlighted in the square on Figure 43. This gives a perspective on the size in reference to the size of the original area captured by the micro-CT the

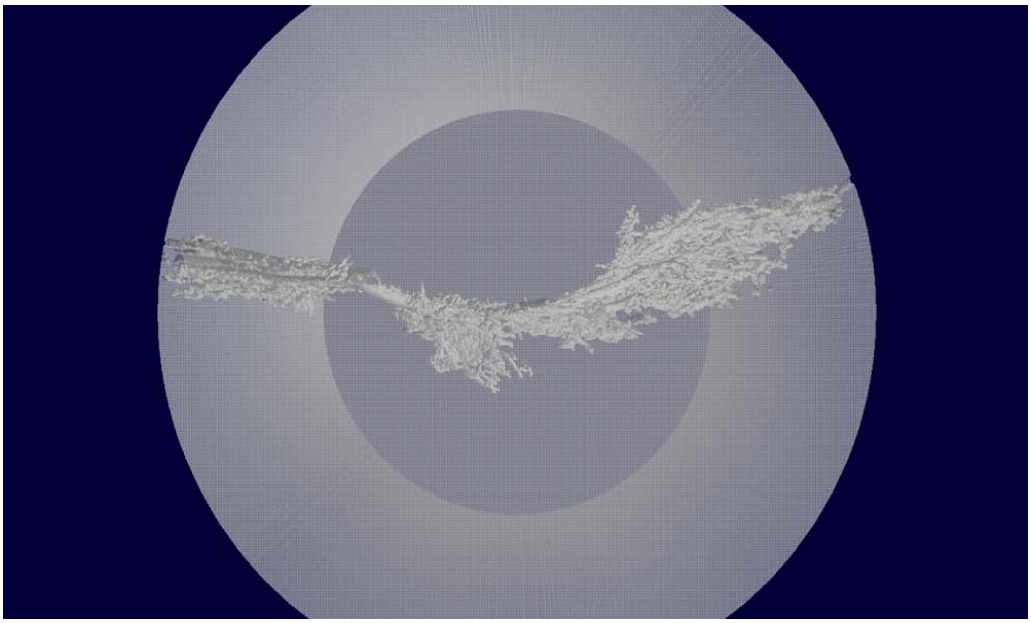

Figure 44: A 3D cylindrical region of interest STL model. Constructed using CTvol software this same model is demonstrated, after importing into Geomagic CAD software, in Figure 45.

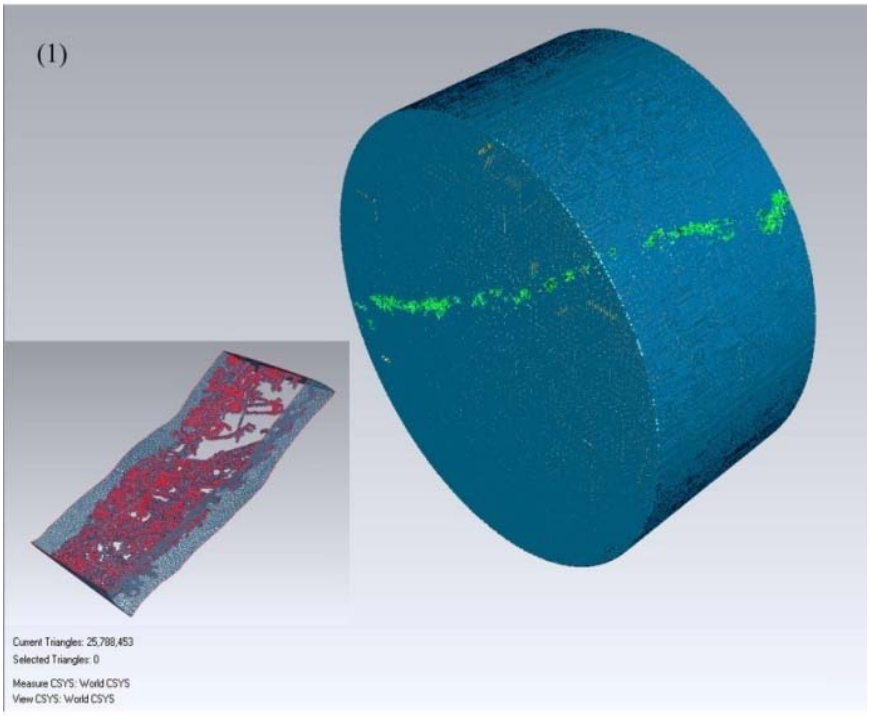

Figure 45: From STL to CAD. A cylindrical region of interest model acquired from micro-CT image data rendered in Geomagic CAD software. The boundary region, demonstrated in the lower left-hand corner, can be selectively removed, allowing visual access to the selectively modeled

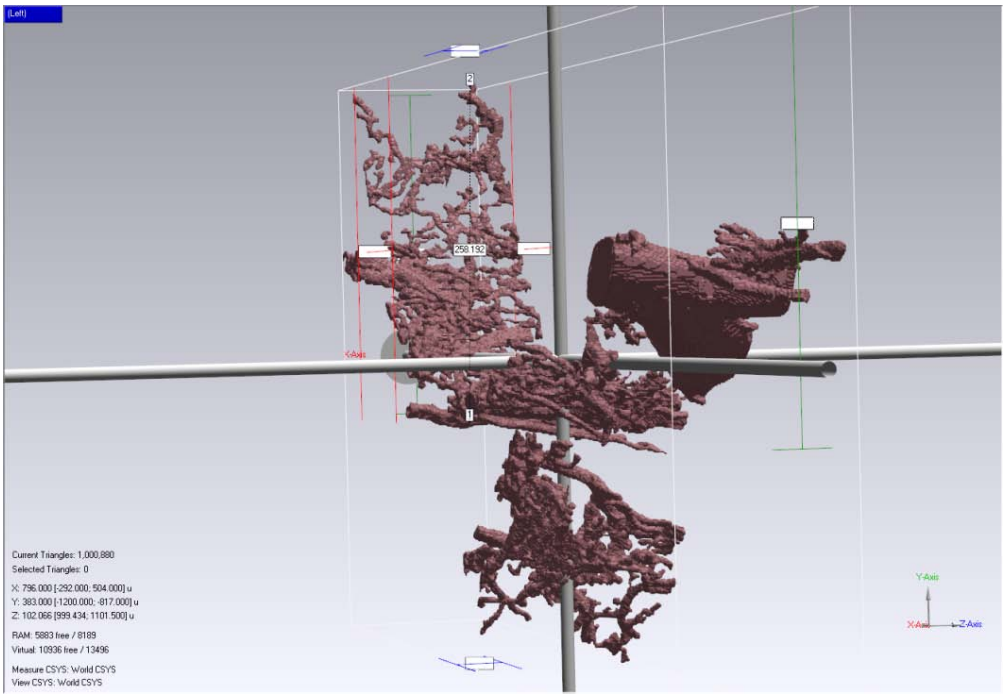

Figure 46: CAD model of Figure 47. Constructed from a very small region of interest the small ROI allows optimization of intensity thresholding resulting in a STL with a manageable file size allowing for further image processing. The model's dimensions are marked with values listed in the lower left corner.

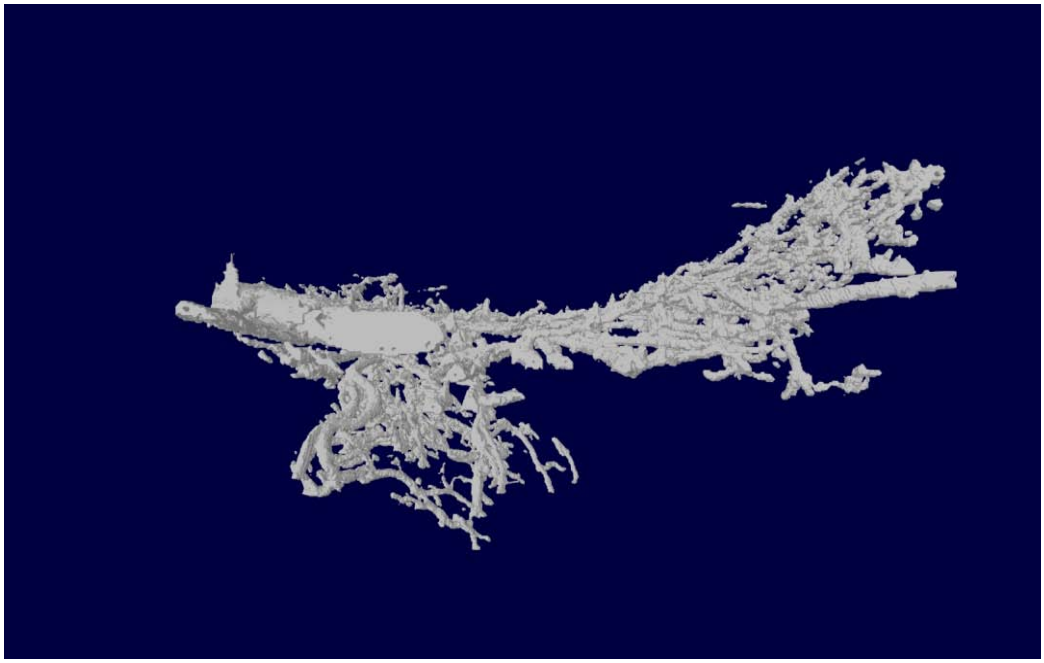

Figure 47: STL model of region of interest demonstrated in Figure 43.

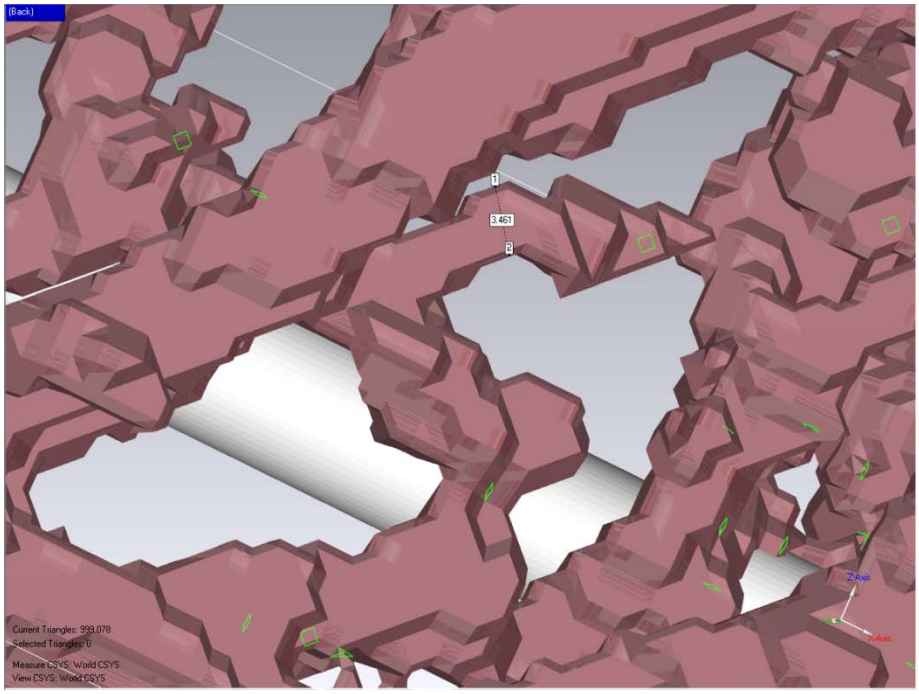

Figure 48: Demonstrating model's surface at high magnification. Here we see an unprocessed model of a luminal cast of continuous capillary structures. Diameters of one capillary lumen measured and labeled in microns.

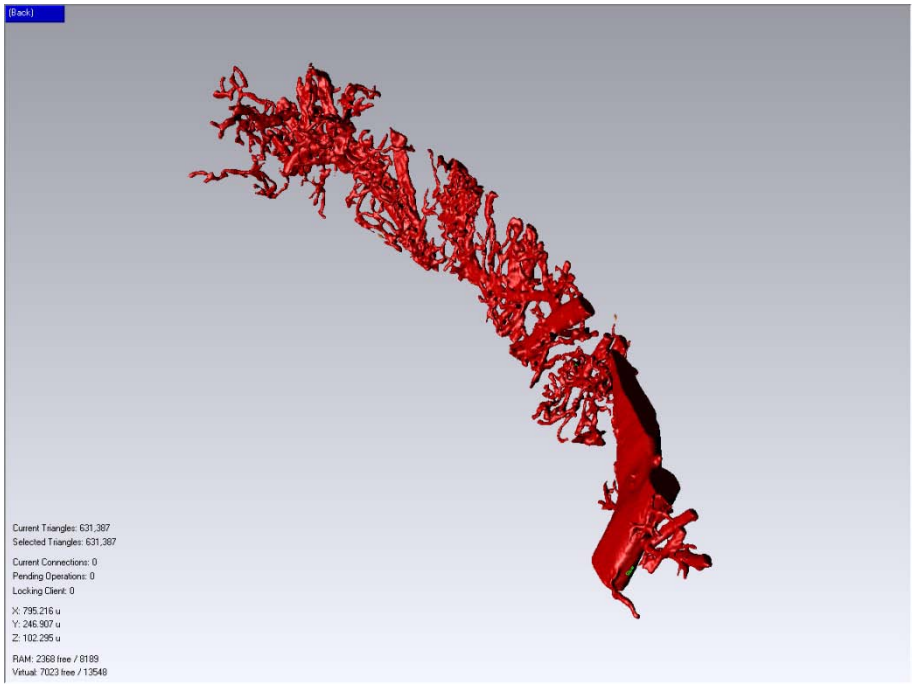

Figure 49: Smoothing the surface. We show here the CAD model from Figure 47 after removing floating pieces and smoothing its surface.

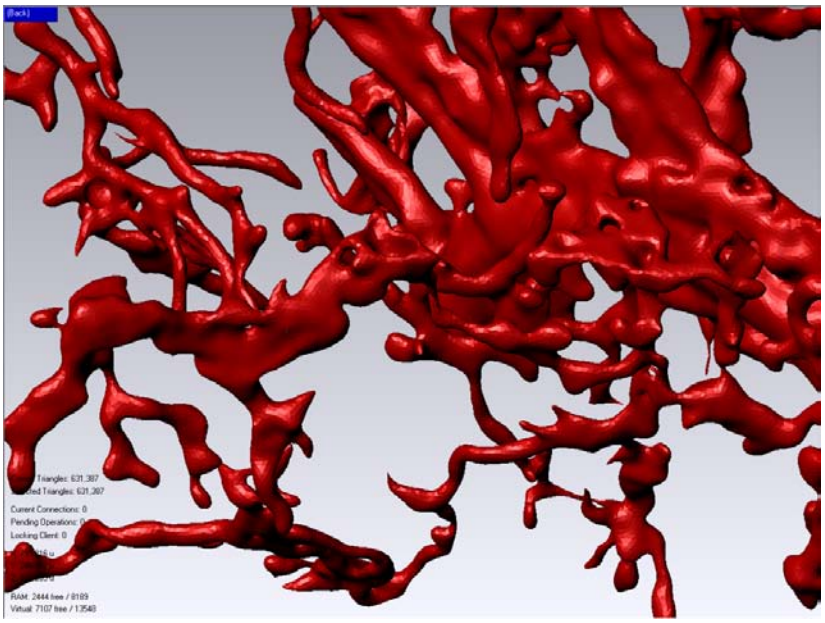

Figure 50: High magnification taken from one portion of Figure 49.

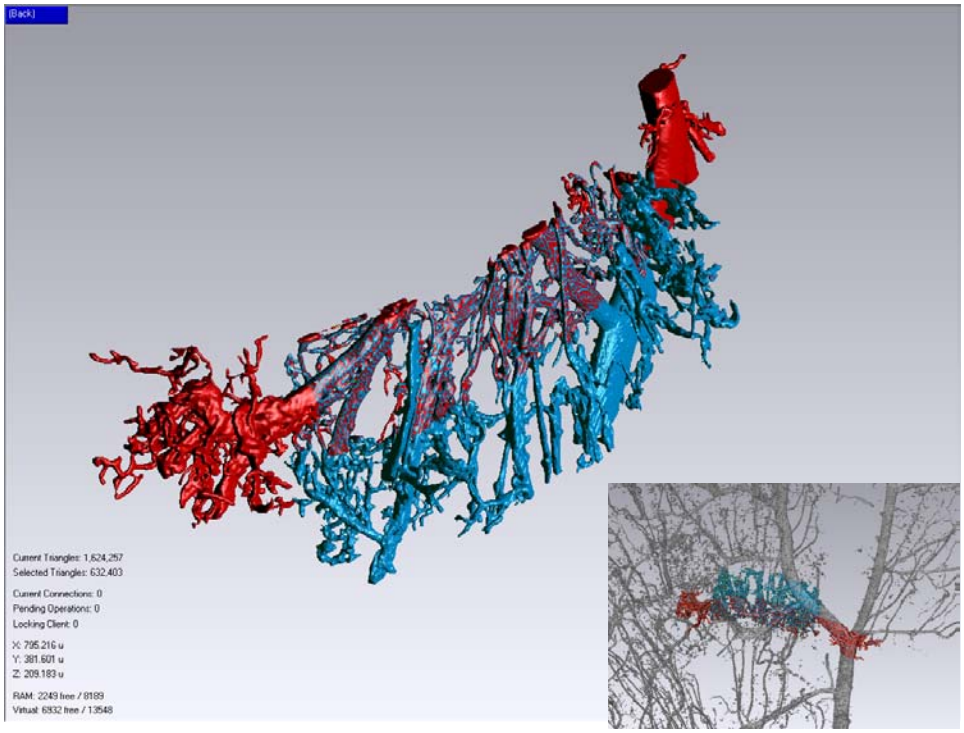

Figure 51: Combining models. This is a combination of two CAD models created from two separate STL models; one red and one blue. The blue model is show in Figure 44. These small ROIs were taken from micro-CT scan of vascular cast made of the vascular lumen of rabbit skin. Insert shows where they are found on part of the complete micro-CT scan demonstrated in Figure 37.

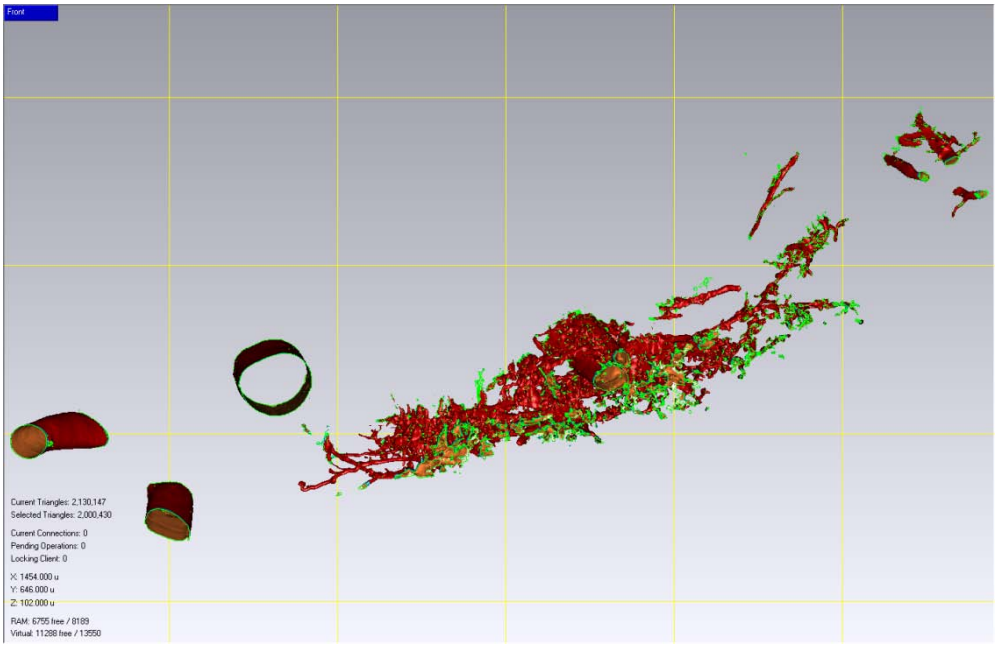

Figure 52: The first 101 images. The complete CT scan of the rabbit skins vascular cast were used to create an STL model for use in the construction of the CAD design shown here. CAD underwent processing that allowed for the complete scan of the vascular system cast to be 'stitched' together.

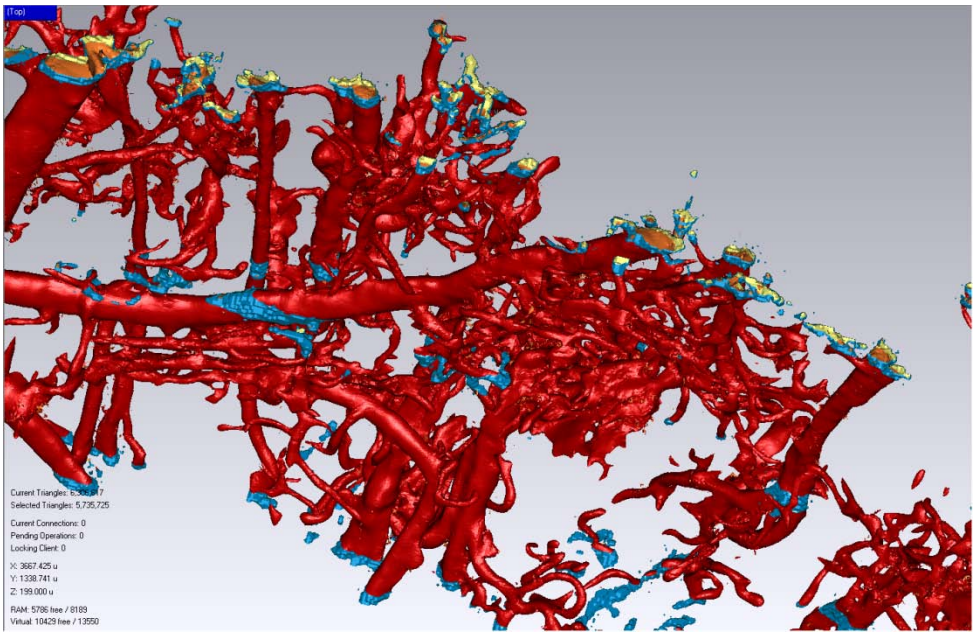

Figure 53: Two blocks of 101. 2D micro-CT slices built into two separate STLs and imported into CAD software where they were processed and stitched together. Insert shows a magnification of an area of the models in blue, modified for joining the two STL models together.

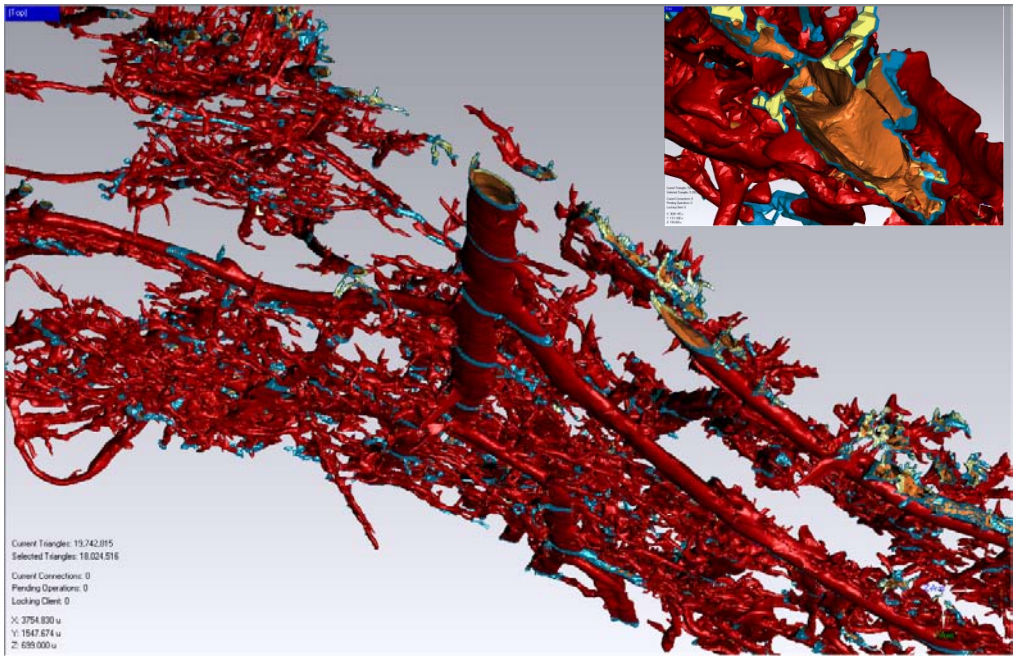

Figure 54: Eight independently constructed 3D models. Stitched together to form a single model, the blue areas indicate the zones were models overlapped in the adjoining process.

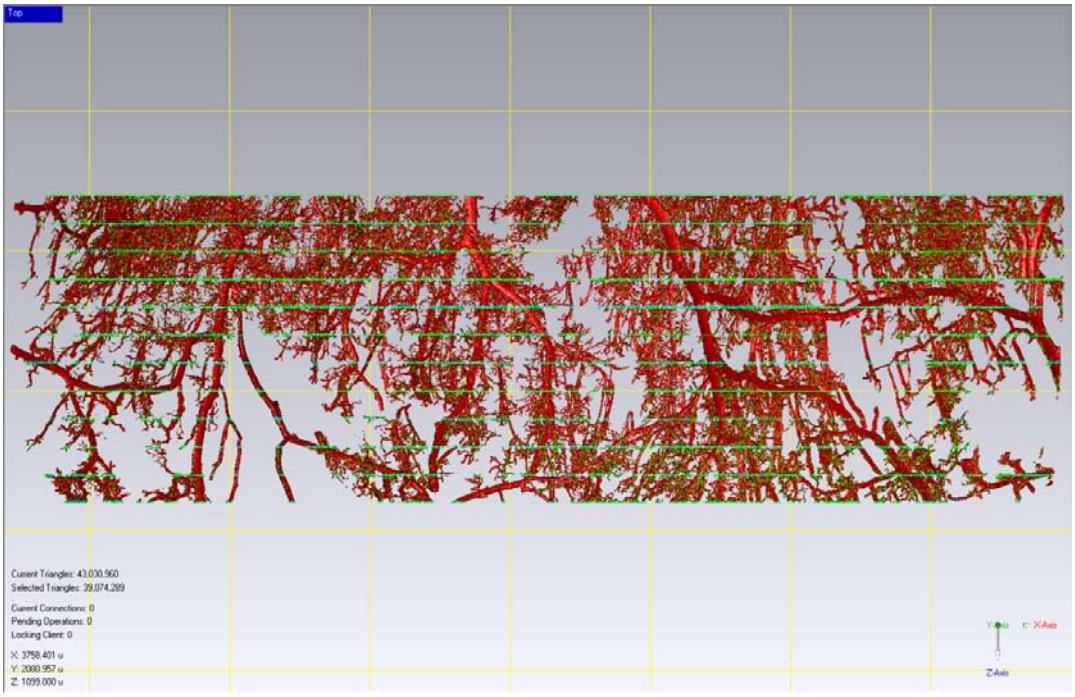

Figure 55: Eleven independently constructed 3D models. One third of the complete micro-CT scanned data is shown here consisting of 11 independently constructed models join to neighboring models after undergoing image processing.

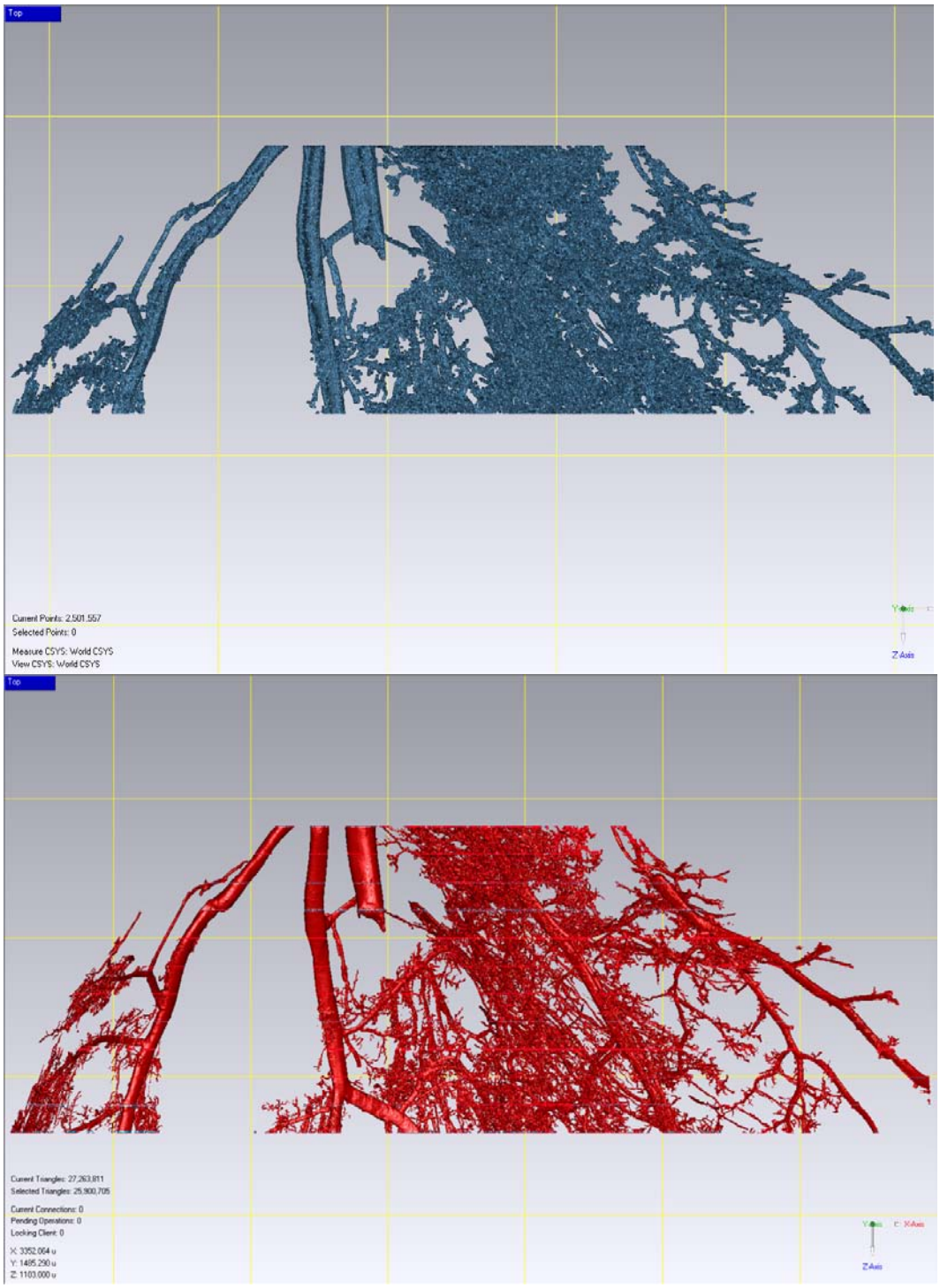

Figure 56: One piece at a time. Here we see illustrated a comparison between the top third of the complete scan created through stitching together 11 separately (red model) prepared STL models, with the model created from a single data set containing the top third of the 2D images.

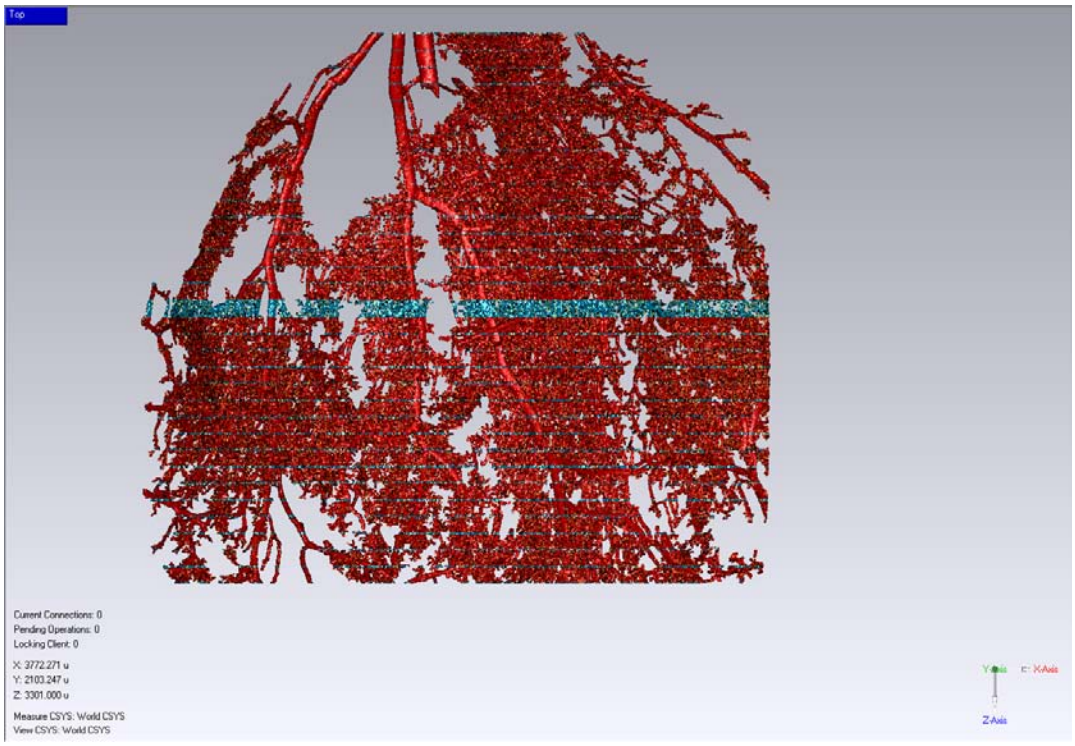

Figure 57: The whole thing. 33 separately built STL models stitched together to form a model of the complete image data set acquired through the micro-CT scanning of the rabbit skin's vascular cast.

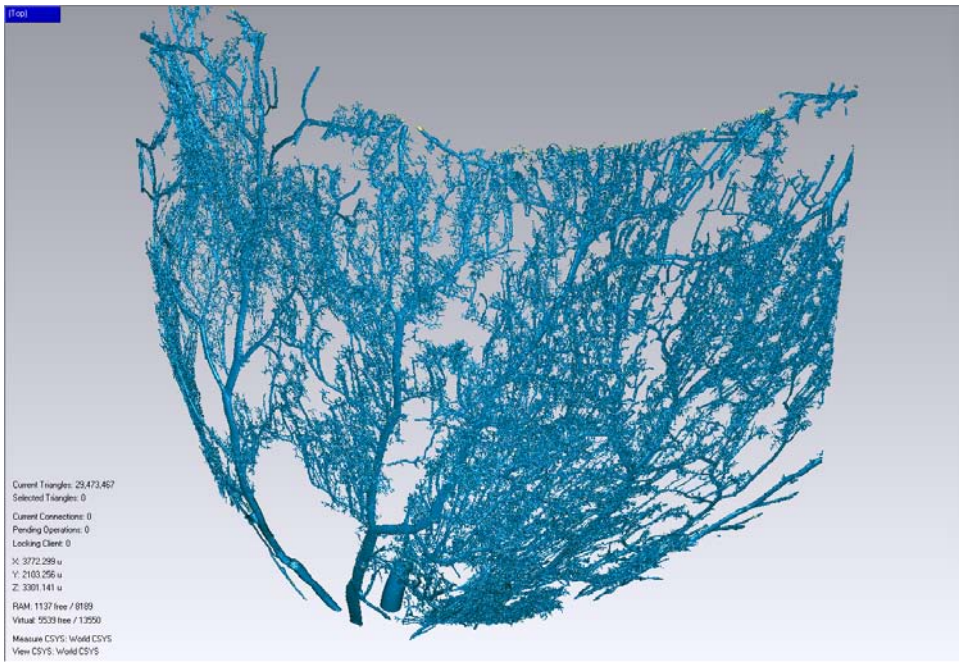

Figure 58: From a different perspective. The model of the complete data set is shown stitched together from three sets of 11 independently constructed STL models assembled in stages along the z axis.

Table 6: Rabbit Skin Vascular – 3D Bio- CAD Model Construction Blocks

Rabbit Skin Vasculature – 3D Bio-CAD Model Construction Blocks/Data Set Division (Constant gray scale indexing 5.1%-100%)			
Block of 101 images	Block Size MB	Original STL Size Mb	Wrap file size Mb
1	22.9	106	81
2	22.9	106	81
3	22.7	102	77
4	22.8	116	88
5	22.9	134	102
6	22.7	112	85
7	22.8	113	86
8	22.7	116	88
9	22.8	130	98
10	22.9	143	108
11	23.1	159	121
12	23.2	177	134
13	23.3	186	140
14	23.2	185	139
15	23.3	194	146
16	23.4	207	156
17	23.3	195*	147
18	23.5	229	173
19	23.4	215	162
20	23.4	220	167
21	23.6	254	223
22	23.6	247	187
23	23.8	283	213
24	23.8	285	214
25	23.6	255*	192
26	23.5	237	179
27	23.2	184	139
28	23.9	142	107
29	22.8	137	103
30	22.7	121	91
31	22.6	137	104
32	22.7	149	113
33	22.3	156	119

Table 7: 3D CAD Models of Rabbit Skin Vascular Cast

3D CAD Models of Rabbit Skin Vascular Cast Stitched from Smaller 3D CAD Models Blocks (WRP-some processing)			
Region of vascular cast	Number of Blocks)	File Size GB	Number of Triangles
Bottom Third Stitched	11	1.6	42,649,000
Middle Third Stitched	11	1.8	47,982,000
Top Third Stitched	11	1.0	27,263,000
Thirds Stitched Whole	33	4.4	117,894,000

Table 8: A Comparison of a Single Model's File Size

Rabbit Skin 2D image properties	
Jpeg compression of 3968 x 3968kb image file size to 231 Kb (Black background given value of zero)	
File Format Conversions	Size
Original CTan STL	810,416 Bites
IGS	7,808,265 Bites
Wrap wrp	363,295 Bites
Auto CAD dxf	3,290,924 Bites
GeomView oogl	651,924 Bites
Whorl VRML2 wrl	775,195 Bites
ASCII STL	497,022 Bites

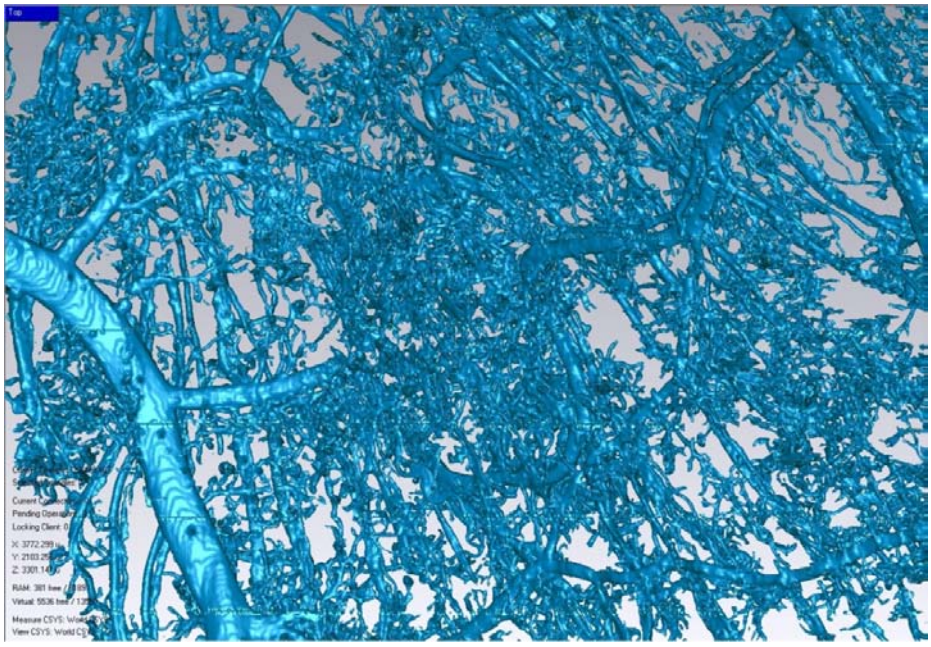

Figure 59: A decimated view. A closer view of the models demonstrated above after being decimated by 75% of the model's triangles.

Chapter Six

Conclusion/Future Work

Our successful approach to designing vascular scaffolds uses an interdisciplinary approach to enhancing a variety of therapeutic protocols including but not limited to: organ and tissue repair, systemic disease mediation and cell/tissue transplantation therapy. The results of these methods takes us closer to the bioengineering of various types of three-dimensional tissue structures, greatly expanding the potential application of biomedical engineering technology into the areas of biomedical research and medicine.

Using a single scaffold or by combining scaffolds produced for different cellular tissue structures, we have the framework to reverse engineer any of the tissue structures produced in nature. Using this type of reverse bioengineering approach, we can create designs that merge macroscopic with microscopic data to mimic the extracellular environments (Shoichet, Yu et al. 2007; Rydholm, Held et al. 2008; Salinas and Anseth 2008) conducive to the functional framework specific to vessel's structural location - and the tissue structure (Yu, Kazazian et al. 2007; Polizzotti, Fairbanks et al. 2008; Rydholm, Held et al. 2008) hosting the vasculature.

Future design approach should cater to specific cell phenotypes and their corresponding position as ***it*** relates to vessel type, diameter and location. Location specific vascular interrelationships characteristic for the tissue type to be supported by the resulting vasculature should be a primary concern for future bio-CAD models. Structural

data must be acquired with the specifications necessary to provide an environment that meets the vascular/physiological needs for nurturing the growth and maintenance of 3D tissue structures. This structural environment must be designed to support the needed cell behaviors of precise cell types in order to guide genotypical expression and location specific structural development.

In order for such models to be useful in the fabrication of microvascular scaffolding for tissue engineering purposes they must include the unique branching pattern seen in the capillary beds, nurturing the specialized tissue structure found in organs such as lung, kidney and skin. A vascular tree scaffold is needed whose design mimics the structural design of organ specific vascular networks. A vascular tree scaffold bioengineered both chemically and cellularly, to promote the genesis of a replica vascular tree system that includes its organ specific capillary structures. (Mondy and N. De Clerck 2009, In Press). These modeling results are a basis for the further designing of a 'bio blueprint' to guide using micro-prototyping techniques such as the 3D chemical patterning of photo cross linkable multilayered hydrogels (Yu, Kazazian et al. 2007; Elisseeff 2008). Using these methods a more complete structural fabrication of a vascular scaffolding capable to support, nurture and guide the celluarization of microvascular and macro vascular structures and serve as a nurturing framework. This framework will support the further design and engineering of organ specific, functional tissue structures from chemically and mechanically engineered extra cellular matrixes, using micro rapid prototyping and 3D laser pulse patterning for the regulation of tissue specific cellular morphologies(Elisseeff, Ferran et al. 2006; Linke, Schanz et al. 2007; Garagorri, Fermanian et al. 2008).

References

Aharinejad, S. and A. Lametschwandtner (1992). "Microangioarchitecture of the guinea pig gallbladder and bile duct as studied by scanning electron microscopy of vascular corrosion casts." J Anat 181 (Pt 1): 89-100.

al-Awqati, Q. and M. R. Goldberg (1998). "Architectural patterns in branching morphogenesis in the kidney." Kidney Int 54(6): 1832-42.

Almajdub, M., L. Magnier, et al. (2008). "Kidney volume quantification using contrast-enhanced in vivo X-ray micro-CT in mice." Contrast Media & Molecular Imaging 3(3): 120-126.

Ananda, S., V. Marsden, et al. (2006). "The visualization of hepatic vasculature by X-ray micro-computed tomography." J Electron Microsc (Tokyo) 55(3): 151-155.

Anseth, K. S., C. N. Bowman, et al. (1996). "Mechanical properties of hydrogels and their experimental determination." Biomaterials 17(17): 1647-57.

Badea, C. T., L. W. Hedlund, et al. (2006). "Tumor imaging in small animals with a combined micro-CT/micro-DSA system using iodinated conventional and blood pool contrast agents." Contrast Media & Molecular Imaging 1(4): 153-164.

Badea, C. T., L. W. Hedlund, et al. (2007). "Tomographic digital subtraction angiography for lung perfusion estimation in rodents." Medical Physics 34(5): 1546-1555.

Ballyns, J. J., J. P. Gleghorn, et al. (2008). "Image-guided tissue engineering of anatomically shaped implants via MRI and micro-CT using injection molding." Tissue Engineering Part A 14(7): 1195-1202.

Batson, O. V. (1955). "Anatomic variations in the abdomen." Surg Clin North Am (Philadelphia No): 1727-37.

Beeuwkes, R., 3rd (1971). "Efferent vascular patterns and early vascular-tubular relations in the dog kidney." Am J Physiol 221(5): 1361-74.

Beeuwkes, R., 3rd (1980). "The vascular organization of the kidney." Annu Rev Physiol 42: 531-42.

Bentley, M. D., S. M. Jorgensen, et al. (2007). "Visualization of three-dimensional nephron structure with microcomputed tomography." Anat Rec (Hoboken) 290(3): 277-83.

Bergers, G. and S. Song (2005). "The role of pericytes in blood-vessel formation and maintenance." Neuro-oncol 7(4): 452-64.

Bergers, G. and S. Song (2005). "The role of pericytes in blood-vessel formation and maintenance." Neuro Oncol 7(4): 452-64.

Bernard, S., D. L. Luchtel, et al. (2005). "Structure and size of bronchopulmonary anastomoses in sheep lung." Anat Rec A Discov Mol Cell Evol Biol 286(1): 804-13.

Berry, J. L., S. K. Yazdani, et al. (2006). "Acellular vascular scaffolds for tissue engineered blood vessels." Journal of Biomechanics 39(Supplement 1): S578-713.

Bezy-Wendling, J., M. Kretowski, et al. (2001). "Toward a better understanding of texture in vascular CT scan simulated images." IEEE Trans Biomed Eng 48(1): 120-4.

Boccafoschi, F., J. Habermehl, et al. (2005). "Biological performances of collagen-based scaffolds for vascular tissue engineering." Biomaterials 26(35): 7410-7.

Bolourani, P., G. B. Spiegelman, et al. (2006). "Delineation of the Roles Played by RasG and RasC in cAMP-dependent Signal Transduction during the Early Development of Dictyostelium discoideum." Mol. Biol. Cell 17(10): 4543-4550.

Bolourani, P., G. B. Spiegelman, et al. (2006). "Delineation of the roles played by RasG and RasC in cAMP-dependent signal transduction during the early development of Dictyostelium discoideum." Mol Biol Cell 17(10): 4543-50.

Bonner, J. T. and D. S. Lamont (2005). "Behavior of cellular slime molds in the soil." Mycologia 97(1): 178-84.

Bryant, S. J., R. J. Bender, et al. (2004). "Encapsulating chondrocytes in degrading PEG hydrogels with high modulus: engineering gel structural changes to facilitate cartilaginous tissue production." Biotechnol Bioeng 86(7): 747-55.

Bryant, S. J., C. R. Nuttelman, et al. (1999). "The effects of crosslinking density on cartilage formation in photocrosslinkable hydrogels." Biomed Sci Instrum 35: 309-14.

Burdick, J. A. and K. S. Anseth (2002). "Photoencapsulation of osteoblasts in injectable RGD-modified PEG hydrogels for bone tissue engineering." Biomaterials 23(22): 4315-23.

Cai, Q. Y., S. H. Kim, et al. (2007). "Colloidal gold nanoparticles as a blood-pool contrast agent for x-ray computed tomography in mice." Investigative Radiology 42: 797-806.

Cameron, B. M., D. R. Holmes, 3rd, et al. (2008). "Patient specific physical anatomy models." Stud Health Technol Inform 132: 68-73.

Cao, X. and M. S. Shoichet (2002). "Photoimmobilization of biomolecules within a 3-dimensional hydrogel matrix." Journal of Biomaterials Science-Polymer Edition 13(6): 623-636.

Cheah, C. M., C. K. Chua, et al. (2003). "Integration of laser surface digitizing with CAD/CAM techniques for developing facial prostheses. Part 2: Development of molding techniques for casting prosthetic parts." Int J Prosthodont 16(5): 543-8.

Chen, V. J. and P. X. Ma (2004). "Nano-fibrous poly(-lactic acid) scaffolds with interconnected spherical macropores." Biomaterials 25(11): 2065-2073.

Choi, Y. J., S. K. Choung, et al. (2005). "Evaluations of blood compatibility via protein adsorption treatment of the vascular scaffold surfaces fabricated with polylactide and surface-modified expanded polytetrafluoroethylene for tissue engineering applications." J Biomed Mater Res A 75(4): 824-31.

Chupa, J. M., A. M. Foster, et al. (2000). "Vascular cell responses to polysaccharide materials: in vitro and in vivo evaluations." Biomaterials 21(22): 2315-22.

Couet, F., N. Rajan, et al. (2007). "Macromolecular biomaterials for scaffold-based vascular tissue engineering." Macromol Biosci 7(5): 701-18.

Davis, G. E. and D. R. Senger (2005). "Endothelial extracellular matrix - Biosynthesis, remodeling, and functions during vascular morphogenesis and neovessel stabilization." Circulation Research 97(11): 1093-1107.

Draper, J. S., H. D. Moore, et al. (2004). "Culture and characterization of human embryonic stem cells." Stem Cells Dev 13(4): 325-36.

Ehrbar, M., V. G. Djonov, et al. (2004). "Cell-demanded liberation of VEGF121 from fibrin implants induces local and controlled blood vessel growth." Circ Res 94(8): 1124-32.

Elisseeff, J. (2008). "Hydrogels: structure starts to gel." Nat Mater 7(4): 271-3.

Elisseeff, J., K. Anseth, et al. (1999). "Transdermal photopolymerization of poly(ethylene oxide)-based injectable hydrogels for tissue-engineered cartilage." Plast Reconstr Surg 104(4): 1014-22.

Elisseeff, J., A. Ferran, et al. (2006). "The role of biomaterials in stem cell differentiation: applications in the musculoskeletal system." Stem Cells Dev 15(3): 295-303.

Elisseeff, J., W. McIntosh, et al. (2001). "Controlled-release of IGF-I and TGF-beta1 in a photopolymerizing hydrogel for cartilage tissue engineering." J Orthop Res 19(6): 1098-104.

Elleaume, H., A. M. Charvet, et al. (2002). "Performance of computed tomography for contrast agent concentration measurements with monochromatic x-ray beams: comparison of K-edge versus temporal subtraction." Phys Med Biol 47(18): 3369-85.

Fabris, L., M. Cadamuro, et al. (2007). "[105] Arterial And Peribiliary Vasculogenesis During Liver Development Is Modulated By Angiogenic Growth Factors Expressed By Ductal Plate Cells And Hepatoblasts." Journal of Hepatology 46(Supplement 1): S46-S47.

Fang, Z., B. Starly, et al. (2005). "Computer-aided characterization for effective mechanical properties of porous tissue scaffolds." Computer-Aided Design 37(1): 65-72.

Figallo, E., M. Flaibani, et al. (2007). "Micropatterned biopolymer 3D scaffold for static and dynamic culture of human fibroblasts." Biotechnology Progress 23(1): 210-216.

Ford, N. L., K. C. Graham, et al. (2006). "Time-course characterization of the computed tomography contrast enhancement of an iodinated blood-pool contrast agent in mice using a volumetric flat-panel equipped computed tomography scanner." Investigative Radiology 41(4): 384-390.

Frericks, B. B., F. C. Caldarone, et al. (2004). "3D CT modeling of hepatic vessel architecture and volume calculation in living donated liver transplantation." Eur Radiol 14(2): 326-33.

Garagorri, N., S. Fermanian, et al. (2008). "Keratocyte behavior in three-dimensional photopolymerizable poly(ethylene glycol) hydrogels." Acta Biomater 4(5): 1139-47.

Gattas-Asfura, K. M., E. Weisman, et al. (2005). "Cinnamate-functionalized gelatin: Synthesis and "Smart" hydrogel formation via photo-cross-linking." Biomacromolecules 6(3): 1503-1509.

Germain, L., M. Remy-Zolghadri, et al. (2000). "Tissue engineering of the vascular system: from capillaries to larger blood vessels." Med Biol Eng Comput 38(2): 232-40.

Grabherr, S., V. Djonov, et al. (2007). "Postmortem Angiography: Review of Former and Current Methods." Am. J. Roentgenol. 188(3): 832-838.

Grigoriy A. Mun, Z. S. N. V. V. K. G. S. A. E. M. S. K. P. (2002). "Collapse of Poly(methacrylic acid) Hydrogels in Response to Simultaneous Stimulation by an Electric Field and Complex Formation." Macromolecular Rapid Communications 23(16): 965-967.

Gross, P. M., M. G. Joneja, et al. (1993). "Topography of short portal vessels in the rat pituitary gland: a scanning electron-microscopic and morphometric study of corrosion cast replicas." Cell Tissue Res 272(1): 79-88.

Grothe, C., K. Haastert, et al. (2006). "Physiological function and putative therapeutic impact of the FGF-2 system in peripheral nerve regeneration--lessons from in vivo studies in mice and rats." Brain Res Rev 51(2): 293-9.

Habibi, R., M. S. Krishnam, et al. (2008). "High-spatial-resolution lower extremity MR angiography at 3.0 T: Contrast agent dose comparison study." Radiology 248(2): 680-692.

Hahn, H. K., C. J. G. Evertsz, et al. (2003). "Fractal properties, segment anatomy, and interdependence of the human portal vein and the hepatic vein in 3D." Fractals-Complex Geometry Patterns and Scaling in Nature and Society 11(1): 53-62.

Hahn, H. K., B. Preim, et al. (2001). Visualization and interaction techniques for the exploration of vascular structures. IEEE Visualization ACM: 395--402.

Hahn, M. S., J. S. Miller, et al. (2006). "Three-dimensional biochemical and biomechanical patterning of hydrogels for guiding cell behavior." Advanced Materials 18(20): 2679-+.

Hainfeld, J. F., D. N. Slatkin, et al. (2006). "Gold nanoparticles: a new X-ray contrast agent." Br J Radiol 79(939): 248-53.

Hall, P., M. Ngan, et al. (1997). "Reconstruction of vascular networks using three-dimensional models." Ieee Transactions on Medical Imaging 16(6): 919-929.

Halpin, T., K. Evans, et al. (2003). Reverse engineering physical schemas to logical models. Database Modeling. San Francisco, Morgan Kaufmann: 297-305.

Hanjaya-Putra, D. and S. Gerecht (2009). "Vascular engineering using human embryonic stem cells." Biotechnol Prog 25(1): 2-9.

Heinzer, S., G. Kuhn, et al. (2008). "Novel three-dimensional analysis tool for vascular trees indicates complete micro-networks, not single capillaries, as the angiogenic endpoint in mice overexpressing human VEGF(165) in the brain." Neuroimage 39(4): 1549-58.

Hojo, T. (1993). "Scanning electron microscopy of styrene-methylethylketone casts of the airway and the arterial system of the lung." Scanning Microsc 7(1): 287-93.

Hojo, T. (1993). "Scanning Electron Microscopy Of Styrene-Methylethylketone Casts Of The Airway And The Arterial System Of The Lung." Scanning Microscopy, Vol. 7,(No. 1): 287 -293.

Horiuchi, K., K. Suzuki, et al. (2005). "Intraoperative monitoring of blood flow insufficiency during surgery of middle cerebral artery aneurysms." Journal of Neurosurgery 103(2): 275-283.

Howlett, A. R. and M. J. Bissell (1993). "The influence of tissue microenvironment (stroma and extracellular matrix) on the development and function of mammary epithelium." Epithelial Cell Biol 2(2): 79-89.

Hunt, J. A. and M. S. Shoichet (2002). "Biomaterials: drug delivery systems." Current Opinion in Solid State & Materials Science 6(4): 281-281.

Hurley, L. A. and S. N. Stein (1957). "Embedding of Corrosion Casts of the Vascular Tree - Technic for Production of Transparent Plastic Anatomic Models." Laboratory Investigation 6(2): 162-170.

Ikura, H., K. Shimizu, et al. (2001). "Ultra high-resolution CT of the human lung specimen: Synchrotron radiation CT and micro focus X-ray CT." Radiology 221: 206-206.

Imreh, M. P., S. Wolbank, et al. (2004). "Culture and expansion of the human embryonic stem cell line HS181, evaluated in a double-color system." Stem Cells Dev 13(4): 337-43.

Iyer, R. K., M. Radisic, et al. (2007). "Synthetic oxygen carriers in cardiac tissue engineering." Artif Cells Blood Substit Immobil Biotechnol 35(1): 135-48.

J. Nam , B. S., A. Darling and W. Sun (2004). "Computer Aided Tissue Engineering for Modeling and Design of Novel Tissue Scaffolds." Journal of Computer-Aided Design and Application 1 (1-4) 633 - 640.

Jirkovska, M., L. Kubinova, et al. (1998). "Spatial arrangement of fetal placental capillaries in terminal villi: a study using confocal microscopy." Anatomy and Embryology 197(4): 263-272.

Jorgensen, S. M., D. R. Eaker, et al. (2008). "Reproducibility of global and local reconstruction of three-dimensional micro-computed tomography of iliac crest biopsies." IEEE Trans Med Imaging 27(4): 569-75.

Kannan, R. Y., H. J. Salacinski, et al. (2005). "The roles of tissue engineering and vascularisation in the development of micro-vascular networks: a review." Biomaterials 26(14): 1857-75.

Karen, P., M. Jirkovska, et al. (2003). "Three-dimensional computer reconstruction of large tissue volumes based on composing series of high-resolution confocal images by GlueMRC and LinkMRC software." Microscopy Research and Technique 62(5): 415-422.

Karen, P., M. Jirkovska, et al. (2003). "Three-dimensional computer reconstruction of large tissue volumes based on composing series of high-resolution confocal images by GlueMRC and LinkMRC software." Microsc Res Tech 62(5): 415-22.

Kassab, G. S., C. A. Rider, et al. (1993). "Morphometry of pig coronary arterial trees." Am J Physiol 265(1 Pt 2): H350-65.

Khalil, S. and W. Sun (2007). "Biopolymer deposition for freeform fabrication of hydrogel tissue constructs." Materials Science and Engineering: C 27(3): 469-478.

Kilian, O., V. Alt, et al. (2005). "New blood vessel formation and expression of VEGF receptors after implantation of platelet growth factor-enriched biodegradable nanocrystalline hydroxyapatite." Growth Factors 23(2): 125-33.

Kim, D., S. Park, et al. (2007). "Antibiofouling polymer-coated gold nanoparticles as a contrast agent for in vivo X-ray computed tomography imaging." J Am Chem Soc 129(24): 7661-5.

Kim, E. Y., S. S. Kim, et al. (2005). "Sulcal hyperintensity on fluid-attenuated inversion recovery imaging in acute ischemic stroke patients treated with intra-arterial thrombolysis: iodinated contrast media as its possible cause and the association with hemorrhagic transformation." J Comput Assist Tomogr 29(2): 264-9.

Kobayashi, A., H. Miyake, et al. (2007). "In vitro formation of capillary networks using optical lithographic techniques." Biochemical and Biophysical Research Communications 358(3): 692-697.

Kong, W. H., W. J. Lee, et al. (2007). "Nanoparticulate carrier containing water-insoluble iodinated oil as a multifunctional contrast agent for computed tomography imaging." Biomaterials 28: 5555-5561.

Kretowski, M., Y. Rolland, et al. (2003). "Fast algorithm for 3-D vascular tree modeling." Computer Methods and Programs in Biomedicine 70(2): 129-136.

Krohn, J. and T. Bertelsen (1997). "Corrosion casts of the suprachoroidal space and uveoscleral drainage routes in the human eye." Acta Ophthalmol Scand 75(1): 32-5.

Kyriakis, J. M. and J. Avruch (2001). "Mammalian mitogen-activated protein kinase signal transduction pathways activated by stress and inflammation." Physiological Reviews 81(2): 807-869.

Lagerveld, B. W., R. D. ter Wee, et al. (2007). "Vascular fluorescence casting and imaging cryomicrotomy for computerized three-dimensional renal arterial reconstruction." BJU International 100(2): 387-391.

Lametschwandtner, A., U. Lametschwandtner, et al. (1984). "Scanning electron microscopy of vascular corrosion casts--technique and applications." Scan Electron Microsc(Pt 2): 663-95.

Lametschwandtner, A., U. Lametschwandtner, et al. (1990). "Scanning electron microscopy of vascular corrosion casts--technique and applications: updated review." Scanning Microsc 4(4): 889-940; discussion 941.

Lametschwandtner, A., B. Minnich, et al. (2005). "Analysis of microvascular trees by means of scanning electron microscopy of vascular casts and 3D-morphometry." Ital J Anat Embryol 110(2 Suppl 1): 87-95.

Langheinrich, A. C., B. Leithauser, et al. (2004). "Acute rat lung injury: Feasibility of assessment with micro-CT." Radiology 233(1): 165-171.

Lanzarone, E., P. Liani, et al. (2007). "Model of arterial tree and peripheral control for the study of physiological and assisted circulation." Medical Engineering & Physics 29(5): 542-555.

Levesque, S. G. and M. S. Shoichet (2006). "Synthesis of cell-adhesive dextran hydrogels and macroporous scaffolds." Biomaterials 27(30): 5277-5285.

Li, J., W. C. Regli, et al. (2007). "An approach to integrating shape and biomedical attributes in vascular models." Computer-Aided Design 39(7): 598-609.

Linke, K., J. Schanz, et al. (2007). "Engineered liver-like tissue on a capillarized matrix for applied research." Tissue Eng 13(11): 2699-707.

Litzlbauer, H. D., C. Neuhaeuser, et al. (2006). "Three-dimensional imaging and morphometric analysis of alveolar tissue from microfocal X-ray-computed tomography." Am J Physiol Lung Cell Mol Physiol 291(3): L535-545.

Liu, X., Y. Won, et al. (2006). "Porogen-induced surface modification of nano-fibrous poly(l-lactic acid) scaffolds for tissue engineering." Biomaterials 27(21): 3980-3987.

Luo, Y. and M. S. Shoichet (2004). "Light-activated immobilization of biomolecules to agarose hydrogels for controlled cellular response." Biomacromolecules 5(6): 2315-2323.

Ma, Z., M. Kotaki, et al. (2005). "Surface engineering of electrospun polyethylene terephthalate (PET) nanofibers towards development of a new material for blood vessel engineering." Biomaterials 26(15): 2527-36.

MacWilliams, H. K. and J. T. Bonner (1979). "The prestalk-prespore pattern in cellular slime molds." Differentiation 14(1-2): 1-22.

Maeda, Y. (1970). "Influence of ionic conditions on cell differentiation and morphogenesis of the cellular slime molds." Dev Growth Differ 12(3): 217-27.

Maeda, Y. and I. Takeuchi (1969). "Cell differentiation and fine structures in the development of the cellular slime molds." Dev Growth Differ 11(3): 232-45.

Marxen, M., M. M. Thornton, et al. (2004). "MicroCT scanner performance and considerations for vascular specimen imaging." Med Phys 31(2): 305-13.

Medvedev, A., V. Samsonov, et al. (2006). "Rational structure of blood vessels." Journal of Applied Mechanics and Technical Physics 47(3): 324-329.

Mertsching, H., T. Walles, et al. (2005). "Engineering of a vascularized scaffold for artificial tissue and organ generation." Biomaterials 26(33): 6610-7.

Merzkirch, C., N. Davies, et al. (2001). "Engineering of vascular ingrowth matrices: are protein domains an alternative to peptides?" Anat Rec 263(4): 379-87.

Mithieux, S. M., J. E. J. Rasko, et al. (2004). "Synthetic elastin hydrogels derived from massive elastic assemblies of self-organized human protein monomers." Biomaterials 25(20): 4921-4927.

Mohapel, P., H. Frielingsdorf, et al. (2005). "Platelet-derived growth factor (PDGF-BB) and brain-derived neurotrophic factor (BDNF) induce striatal neurogenesis in adult rats with 6-hydroxydopamine lesions." Neuroscience 132(3): 767-76.

Mondy, W. L., D. Cameron, Jean-Pierre Timmermans, and A. S. N. De Clerck, C. Casteleyn, L. A. Piegl (2009, In Press). " Micro-CT of Corrosion Casts for Use in the Computer Aided Design of Microvasculature " Tissue Engineering:.

Mukundan, S., K. B. Ghaghada, et al. (2006). "A liposomal nanoscale contrast agent for preclinical CT in mice." American Journal of Roentgenology 186(2): 300-307.

Muller, B. e. a. (2006). "Blood vessels staining in the myocardium for 3D visualization down to the smallest capillary " Nuclear Instruments and Methods in Physics Research B (246): 254-261

Nelson, C. M. and M. J. Bissell (2006). "Of extracellular matrix, scaffolds, and signaling: tissue architecture regulates development, homeostasis, and cancer." Annu Rev Cell Dev Biol 22: 287-309.

Nicholl, S. M., W. J. Tanski, et al. (2004). "Sphingosin-1-phosphate (S1P) induces g alpha i coupled, P[I3-K/ras dependent SMC migration." Faseb Journal 18(4): A594-A594.

Opitz, F., K. Schenke-Layland, et al. (2007). "Phenotypical Plasticity of Vascular Smooth Muscle Cells-Effect of In Vitro and In Vivo Shear Stress for Tissue Engineering of Blood Vessels." Tissue Eng.

Opitz, F., K. Schenke-Layland, et al. (2004). "Tissue engineering of ovine aortic blood vessel substitutes using applied shear stress and enzymatically derived vascular smooth muscle cells." Ann Biomed Eng 32(2): 212-22.

Orazi, L. (2007). "Constrained free form deformation as a tool for rapid manufacturing." Computers in Industry 58(1): 12-20.

Ozkan, M. (2004). "Quantum dots and other nanoparticles: what can they offer to drug discovery?" Drug Discovery Today 9(24): 1065-1071.

Park, S. H., T. G. Kim, et al. (2008). "Development of dual scale scaffolds via direct polymer melt deposition and electrospinning for applications in tissue regeneration." Acta Biomaterialia 4(5): 1198-1207.

Parkinson, C. R. and A. Sasov (2008). "High-resolution non-destructive 3D interrogation of dentin using X-ray nanotomography." Dent Mater 24(6): 773-7.

Polizzotti, B. D., B. D. Fairbanks, et al. (2008). "Three-dimensional biochemical patterning of click-based composite hydrogels via thiolene photopolymerization." Biomacromolecules 9(4): 1084-7.

Pollard, R. E. and P. J. Pascoe (2008). "Severe reaction to intravenous administration of an ionic iodinated contrast agent in two anesthetized dogs." Javma-Journal of the American Veterinary Medical Association 233(2): 274-278.

Pollard, S. M., M. J. Parsons, et al. (2006). "Essential and overlapping roles for laminin alpha chains in notochord and blood vessel formation." Dev Biol 289(1): 64-76.

Pollitt, C. C. and G. S. Molyneux (1990). "A scanning electron microscopical study of the dermal microcirculation of the equine foot." Equine Vet J 22(2): 79-87.

Prasad, C. K. and L. K. Krishnan "Regulation of endothelial cell phenotype by biomimetic matrix coated on biomaterials for cardiovascular tissue engineering." Acta Biomaterialia In Press, Corrected Proof: 78.

Priebe, H., A. Aukrust, et al. (1999). "Stability of the X-ray contrast agent iodixanol=3,3',5,5'-tetrakis(2,3-dihydroxypropylcarbamoyl)- 2,2',4,4',6, 6'-hexaiodo-N,N'-(2-hydroxypropane-1,3-diyl)-diacetanili de towards acid, base, oxygen, heat and light." J Clin Pharm Ther 24(3): 227-35.

Radisic, M., A. Marsano, et al. (2008). "Cardiac tissue engineering using perfusion bioreactor systems." Nat Protoc 3(4): 719-38.

Radisic, M., H. Park, et al. (2006). "Biomimetic approach to cardiac tissue engineering: oxygen carriers and channeled scaffolds." Tissue Eng 12(8): 2077-91.

Redmond, E. M., P. A. Cahill, et al. (1995). "Perfused transcapillary smooth muscle and endothelial cell co-culture--a novel in vitro model." In Vitro Cell Dev Biol Anim 31(8): 601-9.

Ritman, E. L. (2004). "Micro-computed tomography-current status and developments." Annu Rev Biomed Eng 6: 185-208.

Ritman, E. L. (2005). "Micro-computed tomography of the lungs and pulmonary-vascular system." Proc Am Thorac Soc 2(6): 477-80, 501.

Ro, T., H. Handels, et al. (1995). "3D Visualization of microvascular blood vessel networks." Computers & Graphics 19(1): 89-96.

Robb, R. A. and D. P. Hanson (2006). "Biomedical image visualization research using the Visible Human Datasets." Clin Anat 19(3): 240-53.

Roberts, J. P., A. Neill, et al. (2006). "The use of a micro-bubble contrast agent to allow visualization of the biliary tree." Clinical Transplantation 20(6): 740-742.

Rolny, C., L. Lu, et al. (2005). "Shb promotes blood vessel formation in embryoid bodies by augmenting vascular endothelial growth factor receptor-2 and platelet-derived growth factor receptor-beta signaling." Exp Cell Res 308(2): 381-93.

Roztocil, E., S. M. Nicholl, et al. (2007). "Sphingosine-1-phosphate-induced oxygen free radical generation in smooth muscle cell migration requires Galpha12/13 protein-mediated phospholipase C activation." J Vasc Surg 46(6): 1253-1259.

Rydholm, A. E., N. L. Held, et al. (2008). "Modifying network chemistry in thiol-acrylate photopolymers through postpolymerization functionalization to control cell-material interactions." J Biomed Mater Res A 86(1): 23-30.

Salinas, C. N. and K. S. Anseth (2008). "The influence of the RGD peptide motif and its contextual presentation in PEG gels on human mesenchymal stem cell viability." J Tissue Eng Regen Med 2(5): 296-304.

Santiago, L. Y., R. W. Nowak, et al. (2006). "Peptide-surface modification of poly(caprolactone) with laminin-derived sequences for adipose-derived stem cell applications." Biomaterials 27(15): 2962-2969.

Sarkar, S., M. Dadhania, et al. (2005). "Vascular tissue engineering: microtextured scaffold templates to control organization of vascular smooth muscle cells and extracellular matrix." Acta Biomater 1(1): 93-100.

Sarkar, S., G. Y. Lee, et al. (2006). "Development and characterization of a porous micro-patterned scaffold for vascular tissue engineering applications." Biomaterials 27(27): 4775-4782.

Sasov, A. and D. Van Dyck (1998). "Desktop X-ray microscopy and microtomography." J Microsc 191(2): 151-158.

Schipper, J., G. J. Ridder, et al. (2004). "Individual prefabricated titanium implants and titanium mesh in skull base reconstructive surgery. A report of cases." Eur Arch Otorhinolaryngol 261(5): 282-90.

Schraufnagel, D. E. (1987). "Microvascular corrosion casting of the lung. A state-of-the-art review." Scanning Microsc 1(4): 1733-47.

Schraufnagel, D. E. (1987). "Microvascular Corrosion Casting Of The Lung.A State-Of-The-Art Review." Scanning Microscopy, Vol. 1, (No. 4,): 1733-1747.

Schreiner, W., R. Karch, et al. (2006). "Optimized arterial trees supplying hollow organs." Med Eng Phys 28(5): 416-29.

Schreiner, W., R. Karch, et al. (2006). "Optimized arterial trees supplying hollow organs." Medical Engineering & Physics 28(5): 416-429.

Schroeder, C., W. C. Regli, et al. (2005). "Computer-aided design of porous artifacts." Computer-Aided Design 37(3): 339-353.

Selle, D., B. Preim, et al. (2002). "Analysis of vasculature for liver surgical planning." IEEE Trans Med Imaging 21(11): 1344-57.

Sheridan, M. H., L. D. Shea, et al. (2000). "Bioabsorbable polymer scaffolds for tissue engineering capable of sustained growth factor delivery." Journal of Controlled Release 64(1-3): 91-102.

Shoichet, M. S., L. M. Y. Yu, et al. (2007). "Peptide modification of biomaterials enhances cellular interactions and guidance." Biopolymers 88(4): 518-518.

Simms, H. M., C. M. Bowman, et al. (2008). "Using living radical polymerization to enable facile incorporation of materials in microfluidic cell culture devices." Biomaterials 29(14): 2228-36.

Simoens, P., L. De Schaepdrijver, et al. (1992). "Morphologic and clinical study of the retinal circulation in the miniature pig. A: Morphology of the retinal microvasculature." Exp Eye Res 54(6): 965-73.

Sodian, R., P. Fu, et al. (2005). "Tissue engineering of vascular conduits: fabrication of custom-made scaffolds using rapid prototyping techniques." Thorac Cardiovasc Surg 53(3): 144-9.

Solari, C. A., S. Ganguly, et al. (2006). "Multicellularity and the functional interdependence of motility and molecular transport." PNAS 103(5): 1353-1358.

Solari, C. A., J. O. Kessler, et al. (2006). "A hydrodynamics approach to the evolution of multicellularity: flagellar motility and germ-soma differentiation in volvocalean green algae." Am Nat 167(4): 537-54.

Song, S., A. J. Ewald, et al. (2005). "PDGFRbeta+ perivascular progenitor cells in tumours regulate pericyte differentiation and vascular survival." Nat Cell Biol 7(9): 870-9.

Sreerekha, P. R. and L. K. Krishnan (2006). "Cultivation of endothelial progenitor cells on fibrin matrix and layering on dacron/polytetrafluoroethylene vascular grafts." Artificial Organs 30(4): 242-249.

Stitzel, J., J. Liu, et al. (2006). "Controlled fabrication of a biological vascular substitute." Biomaterials 27(7): 1088-1094.

Sun, W. (2005). "Bio-CAD." Computer-Aided Design 37(11): 1095-1096.

Sun, W., A. Darling, et al. (2004). "Computer-aided tissue engineering: overview, scope and challenges." Biotechnology and Applied Biochemistry 39: 29-47.

Sun, W. and P. Lal (2002). "Recent development on computer aided tissue engineering -- a review." Computer Methods and Programs in Biomedicine 67(2): 85-103.

Sun, W., B. Starly, et al. (2004). "Computer-aided tissue engineering: application to biomimetic modelling and design of tissue scaffolds." Biotechnology and Applied Biochemistry 39: 49-58.

Sun, W., B. Starly, et al. (2005). "Bio-CAD modeling and its applications in computer-aided tissue engineering." Computer-Aided Design 37(11): 1097-1114.

Szczerba, D. and G. Szekely (2005). "Computational model of flow-tissue interactions in intussusceptive angiogenesis." J Theor Biol 234(1): 87-97.

Szczerba, D. and G. Szekely (2005). "Simulating vascular systems in arbitrary anatomies." Med Image Comput Comput Assist Interv Int Conf Med Image Comput Comput Assist Interv 8(Pt 2): 641-8.

Szymczak, A., A. Stillman, et al. (2006). "Coronary vessel trees from 3D imagery: A topological approach." Medical Image Analysis 10(4): 548-559.

Takahashi, T., Y. Kawahara, et al. (1996). "Increasing cAMP antagonizes hypertrophic response to angiotensin II without affecting Ras and MAP kinase activation in vascular smooth muscle cells." FEBS Letters 397(1): 89-92.

Takahashi, T., Y. Kawahara, et al. (1996). "Increasing cAMP antagonizes hypertrophic response to angiotensin II without affecting Ras and MAP kinase activation in vascular smooth muscle cells." FEBS Lett 397(1): 89-92.

Takakura, N. (2006). "Role of hematopoietic lineage cells as accessory components in blood vessel formation." Cancer Sci 97(7): 568-574.

Teknos, T. N., M. Islam, et al. (2005). "The effect of tetrathiomolybdate on cytokine expression, angiogenesis, and tumor growth in squamous cell carcinoma of the head and neck." Arch Otolaryngol Head Neck Surg 131(3): 204-11.

Telemeco, T. A., C. Ayres, et al. (2005). "Regulation of cellular infiltration into tissue engineering scaffolds composed of submicron diameter fibrils produced by electrospinning." Acta Biomaterialia 1(4): 377-385.

UB Kompella, N. B., SP Ayalasomayajula (2001). "Poly(lactic acid) nanoparticles for sustained release of budesonide." Drug Delivery Technology 1: 24-35.

Um, S. H., J. B. Lee, et al. (2006). "Enzyme-catalysed assembly of DNA hydrogel." Nature Materials 5(10): 797-801.

van Amerongen, M. J., M. C. Harmsen, et al. (2006). "The enzymatic degradation of scaffolds and their replacement by vascularized extracellular matrix in the murine myocardium." Biomaterials 27(10): 2247-2257.

van Lenthe, G. H., H. Hagenmuller, et al. (2007). "Nondestructive micro-computed tomography for biological imaging and quantification of scaffold-bone interaction in vivo." Biomaterials 28(15): 2479-2490.

van Meeteren, L. A., P. Ruurs, et al. (2006). "Autotaxin, a secreted lysophospholipase D, is essential for blood vessel formation during development." Mol Cell Biol 26(13): 5015-22.

Vogel, G. (2005). "Developmental biology. The unexpected brains behind blood vessel growth." Science 307(5710): 665-7.

Volkau, I., T. T. Ng, et al. (2008). "On geometric modeling of the human intracranial venous system." IEEE Trans Med Imaging 27(6): 745-51.

Volkau, I., W. Zheng, et al. (2005). "Geometric modeling of the human normal cerebral arterial system." IEEE Trans Med Imaging 24(4): 529-39.

Wang, C. C. L. and K. Tang (2007). "Woven model based geometric design of elastic medical braces." Computer-Aided Design 39(1): 69-79.

Wang, Y., H. J. Kim, et al. (2006). "Stem cell-based tissue engineering with silk biomaterials." Biomaterials 27(36): 6064-82.

Weber, E., A. Rossi, et al. (2002). "Focal adhesion molecules expression and fibrillin deposition by lymphatic and blood vessel endothelial cells in culture." Microvasc Res 64(1): 47-55.

Weber, L. M. and K. S. Anseth (2008). "Hydrogel encapsulation environments functionalized with extracellular matrix interactions increase islet insulin secretion." Matrix Biol.

Weber, L. M., K. N. Hayda, et al. (2007). "The effects of cell-matrix interactions on encapsulated beta-cell function within hydrogels functionalized with matrix-derived adhesive peptides." Biomaterials 28(19): 3004-11.

Wei, G., Q. Jin, et al. (2007). "The enhancement of osteogenesis by nano-fibrous scaffolds incorporating rhBMP-7 nanospheres." Biomaterials 28(12): 2087-2096.

Weihe, S., M. Wehmoller, et al. (2000). "Synthesis of CAD/CAM, robotics and biomaterial implant fabrication: single-step reconstruction in computer aided frontotemporal bone resection." International Journal of Oral and Maxillofacial Surgery 29(5): 384-388.

Welsh, E. R. and D. A. Tirrell (2000). "Engineering the extracellular matrix: a novel approach to polymeric biomaterials. I. Control of the physical properties of artificial protein matrices designed to support adhesion of vascular endothelial cells." Biomacromolecules 1(1): 23-30.

Wenner, E. L., D. M. Knott, et al. (1983). "Invertebrate communities associated with hard bottom habitats in the South Atlantic Bight." Estuarine, Coastal and Shelf Science 17(2): 143-158.

Williamson, M. R., R. Black, et al. (2006). "PCL-PU composite vascular scaffold production for vascular tissue engineering: attachment, proliferation and bioactivity of human vascular endothelial cells." Biomaterials 27(19): 3608-16.

Wischgoll, T., J. S. Choy, et al. (2008). "Validation of image-based method for extraction of coronary morphometry." Ann Biomed Eng 36(3): 356-68.

Wischgoll, T., J. Meyer, et al. (2007). "A Novel Method for Visualization of Entire Coronary Arterial Tree." Annals of Biomedical Engineering 35(5): 694-710.

Wischgoll, T., J. Meyer, et al. (2007). "A novel method for visualization of entire coronary arterial tree." Ann Biomed Eng 35(5): 694-710.

Witkowski, S., F. Komine, et al. (2006). "Marginal accuracy of titanium copings fabricated by casting and CAD/CAM techniques." Journal of Prosthetic Dentistry 96(1): 47-52.

Woodward, J. D. and J. N. Maina (2005). "A 3D digital reconstruction of the components of the gas exchange tissue of the lung of the muscovy duck, Cairina moschata." Journal of Anatomy 206(5): 477-492.

Woodward, J. D. and J. N. Maina (2008). "Study of the structure of the air and blood capillaries of the gas exchange tissue of the avian lung by serial section three-dimensional reconstruction." J Microsc 230(Pt 1): 84-93.

Yu, K. C., E. L. Ritman, et al. (2007). "System for the analysis and visualization of large 3D anatomical trees." Comput Biol Med 37(12): 1802-20.

Yu, L. M. Y., K. Kazazian, et al. (2007). "Peptide surface modification of methacrylamide chitosan for neural tissue engineering applications." Journal of Biomedical Materials Research Part A 82A(1): 243-255.

Zavaletta, V. A., B. J. Bartholmai, et al. (2007). "High resolution multidetector CT-aided tissue analysis and quantification of lung fibrosis." Acad Radiol 14(7): 772-87.

Zhai, X. Y., H. Birn, et al. (2003). "Digital three-dimensional reconstruction and ultrastructure of the mouse proximal tubule." J Am Soc Nephrol 14(3): 611-9.

Zhang, E. Z., J. G. Laufer, et al. (2009). "In vivo high-resolution 3D photoacoustic imaging of superficial vascular anatomy." Phys Med Biol 54(4): 1035-46.

Zhang, L., B. E. Chapman, et al. (2005). "Automatic detection of three-dimensional vascular tree centerlines and bifurcations in high-resolution magnetic resonance angiography." Invest Radiol 40(10): 661-71.

Zourob, M., J. E. Gough, et al. (2006). "A micropatterned hydrogel platform for chemical synthesis and biological analysis." Advanced Materials 18(5): 655-+.

Zrzavý, J., S. Mihulka, et al. (1998). "Phylogeny of the Metazoa Based on Morphological and 18S Ribosomal DNA Evidence." Cladistics 14(3): 249-285.

Bibliography

A. Manelli SSEBMR. 2007. 3D analysis of SEM images of corrosion casting using adaptive stereo matching. Microscopy Research and Technique 70(4):350-354.

Akahane T, Yaegashi H, Kurokawa Y, Satomi S, Takahashi T. 1997. Systemic-to-pulmonary vascular malformation of lung visualized by computer-assisted 3-D reconstruction. Histopathology 31(3):252-257.

Aper T, Schmidt A, Duchrow M, Bruch HP. 2007. Autologous Blood Vessels Engineered from Peripheral Blood Sample. European Journal of Vascular and Endovascular Surgery 33(1):33-39.

Arrigoni C, Camozzi D, Remuzzi A. 2006. Vascular tissue engineering. Cell Transplant 15 Suppl 1:S119-25.

Auger FA, Laflamme K, Grenier G, Remy-Zolghadri M, Germain L. 2004. Recent optimization of a tissue engineered blood vessel: the LOEX experience. International Congress Series 1262:126-128.

Bidaut LM, Laurent C, Piotin M, Gailloud P, Muster M, Fasel JHD, Rufenacht DA, Terrier F. 1998. Second-generation three-dimensional reconstruction for rotational three-dimensional angiography. Academic Radiology 5(12):836-849.

Boccafoschi F, Rajan N, Habermehl J, Mantovani D. 2007. Preparation and characterization of a scaffold for vascular tissue engineering by direct-assembling of collagen and cells in a cylindrical geometry. Macromol Biosci 7(5):719-26.

Boerboom RA, Krahn KN, Megens RTA, van Zandvoort MAMJ, Merkx M, Bouten CVC. 2007. High resolution imaging of collagen organisation and synthesis using a versatile collagen specific probe. Journal of Structural Biology 159(3):392-399.

Bousse A, Boldak C, Toumoulin C, Yang G, Laguitton S, Boulmier D. 2006. Coronary extraction and characterization in multi-detector computed tomography. ITBM-RBM 27(5-6):217-226.

Cao Y, Mitchell G, Messina A, Price L, Thompson E, Penington A, Morrison W, O'Connor A, Stevens G, Cooper-White J. 2006. The influence of architecture on degradation and tissue in growth into three-dimensional poly(lactic-co-glycolic acid) scaffolds in vitro and in vivo. Biomaterials 27(14):2854-2864.

Cavalli F, Gamba A, Naldi G, Semplice M, Valdembri D, Serini G. 2007. 3D simulations of early blood vessel formation. Journal of Computational Physics 225(2):2283-2300.

Chalopin C, Finet G, Magnin IE. 2001. Modeling the 3D coronary tree for labeling purposes. Medical Image Analysis 5(4):301-315.

Cheah CM, Chua CK, Leong KF, Chua SW. 2003a. Development of a Tissue Engineering Scaffold Structure Library for Rapid Prototyping. Part 1: Investigation and Classification. The International Journal of Advanced Manufacturing Technology 21(4):291-301.

Cheah CM, Chua CK, Leong KF, Chua SW. 2003b. Development of a Tissue Engineering Scaffold Structure Library for Rapid Prototyping. Part 2: Parametric Library and Assembly Program. The International Journal of Advanced Manufacturing Technology 21(4):302-312.

Chen Z, Molloi S. 2002. Vascular tree object segmentation by deskeletonization of valley courses. Computerized Medical Imaging and Graphics 26(6):419-428.

Chen Z, Molloi S. 2003. Automatic 3D vascular tree construction in CT angiography. Computerized Medical Imaging and Graphics 27(6):469-479.

Chen Z, Ning R. 2005. Forest representation of vessels in cone-beam computed tomographic angiography. Computerized Medical Imaging and Graphics 29(1):1-14.

Chivate PN, Jablokow AG. 1993. Solid-model generation from measured point data. Computer-Aided Design 25(9):587-600.

Chivate PN, Jablokow AG. 1995. Review of surface representations and fitting for reverse engineering. Computer Integrated Manufacturing Systems 8(3):193-204.

Chivate PN, Puntambekar NV, Jablokow AG. 1999. Extending surfaces for reverse engineering solid model generation. Computers in Industry 38(3):285-294.

Chong CK, Rowe CS, Sivanesan S, Rattray A, Black RA, Shortland AP, How TV. 1999. Computer aided design and fabrication of models for in vitro studies of vascular fluid dynamics. Proceedings of the Institution of Mechanical Engineers Part H-Journal of Engineering in Medicine 213(H1):1-4.

Christiaens L, Coisne D, Allal J, Blouin P, Dubreuil F, Donal E, Barraine R. 1997. Three-dimensional power Doppler imaging: volume reconstruction of pulmonary artery flow with an in vitro pulsatile flow system. European Journal of Ultrasound 6(2):135-139.

Chua CK, Leong KF, Cheah CM, Chua SW. 2003. Development of a tissue engineering scaffold structure library for rapid prototyping. Part 2: Parametric library and assembly program. International Journal of Advanced Manufacturing Technology 21(4):302-312.

Chung HJ, Park TG. 2007. Surface engineered and drug releasing pre-fabricated scaffolds for tissue engineering. Advanced Drug Delivery Reviews 59(4-5):249-262.

Cleaver O, Quiat D, Xu K, Villasenor A. 2007. Morphogenesis of blood vessels during mouse vasculogenesis. Developmental Biology 306(1):445-213.

Cotta C, Troya JM. 2004. Reverse engineering of temporal Boolean networks from noisy data using evolutionary algorithms. Neurocomputing 62:111-129.

Couet F, Rajan N, Mantovani D. 2007. Macromolecular biomaterials for scaffold-based vascular tissue engineering. Macromol Biosci 7(5):701-18.

Courtney T, Sacks MS, Stankus J, Guan J, Wagner WR. 2006. Design and analysis of tissue engineering scaffolds that mimic soft tissue mechanical anisotropy. Biomaterials 27(19):3631-3638.

Croll TI, Gentz S, Mueller K, Davidson M, O'Connor AJ, Stevens GW, Cooper-White JJ. 2005. Modelling oxygen diffusion and cell growth in a porous, vascularising scaffold for soft tissue engineering applications. Chemical Engineering Science 60(17):4924-4934.

Cunningham LP, Veilleux MP, Campagnola PJ. 2006. Freeform multiphoton excited microfabrication for biological applications using a rapid prototyping CAD-based approach. Opt. Express 14(19):8613-8621.

Daly CD, Campbell GR, Walker PJ, Campbell JH. 2005. Vascular engineering for bypass surgery. Expert Rev Cardiovasc Ther 3(4):659-65.

Dankelman J, Cornelissen AJM, Lagro J, VanBavel E, Spaan JAE. 2007. Relation between branching patterns and perfusion in stochastic generated coronary arterial trees. Medical & Biological Engineering & Computing 45(1):25-34.

de Boer J, van Blitterswijk C, Lowik C. 2006. Bioluminescent imaging: Emerging technology for non-invasive imaging of bone tissue engineering. Biomaterials 27(9):1851-1858.

DeLong SA, Moon JJ, West JL. 2005. Covalently immobilized gradients of bFGF on hydrogel scaffolds for directed cell migration. Biomaterials 26(16):3227-3234.

Demir R, Kayisli UA, Cayli S, Huppertz B. 2006. Sequential Steps During Vasculogenesis and Angiogenesis in the Very Early Human Placenta. Placenta 27(6-7):535-539.

Demir R, Seval Y, Huppertz B. 2007. Vasculogenesis and angiogenesis in the early human placenta. Acta Histochemica 109(4):257-265.

Dong C-M, Wu X, Caves J, Rele SS, Thomas BS, Chaikof EL. 2005. Photomediated crosslinking of C6-cinnamate derivatized type I collagen. Biomaterials 26(18):4041-4049.

Doraiswamy A, Jin C, Narayan RJ, Mageswaran P, Mente P, Modi R, Auyeung R, Chrisey DB, Ovsianikov A, Chichkov B. 2006. Two photon induced polymerization of organic-inorganic hybrid biomaterials for microstructured medical devices. Acta Biomaterialia 2(3):267-275.

Dotsenko O, Barratt D, Ariff B, Thom S, Hughes A. 2004. Vascular geometry reconstruction with 3D ultrasound, applied to anthropomorphic phantoms models. Journal of Hypertension 22:S13-S13.

E. Niklason L, S. Langer R. 1997. Advances in tissue engineering of blood vessels and other tissues. Transplant Immunology 5(4):303-306.

Edelman ER. 1999. Vascular tissue engineering : designer arteries. Circ Res 85(12):1115-7.

Ehricke H-H, Donner K, Koller W, Straer W. 1994. Visualization of vasculature from volume data. Computers & Graphics 18(3):395-406.

Feng J, Chan-Park MB, Shen JY, Chan V. 2007. Quick layer-by-layer assembly of aligned multilayers of vascular smooth muscle cells in deep microchannels. Tissue Engineering 13(5):1003-1012.

Feng J, Han Cheng S, Chan PK, Ip HHS. 2005. Reconstruction and representation of caudal vasculature of zebrafish embryo from confocal scanning laser fluorescence microscopic images. Computers in Biology and Medicine 35(10):915-931.

Ferreira LS, Gerecht S, Fuller J, Shieh HF, Vunjak-Novakovic G, Langer R. 2007. Bioactive hydrogel scaffolds for controllable vascular differentiation of human embryonic stem cells. Biomaterials 28(17):2706-2717.

Formaggia L, Gerbeau JF, Nobile F, Quarteroni A. 2001. On the coupling of 3D and 1D Navier-Stokes equations for flow problems in compliant vessels. Computer Methods in Applied Mechanics and Engineering 191(6-7):561-582.

Françoise Peyrin MMRCRM. 2007. SEM and 3D synchrotron radiation micro-tomography in the study of bioceramic scaffolds for tissue-engineering applications. Biotechnology and Bioengineering 97(3):638-648.

Frerich B, Lindemann N, Kurtz-Hoffmann J, Oertel K. 2001. In vitro model of a vascular stroma for the engineering of vascularized tissues. Int J Oral Maxillofac Surg 30(5):414-20.

Galetto M, Vezzetti E. 2006. Reverse engineering of free-form surfaces: A methodology for threshold definition in selective sampling. International Journal of Machine Tools and Manufacture 46(10):1079-1086.

Gallego D, Ferrell N, Sun Y, Hansford DJ. Multilayer micromolding of degradable polymer tissue engineering scaffolds. Materials Science and Engineering: C In Press, Corrected Proof:531.

Gao J, Chen X, Zheng D, Yilmaz O, Gindy N. 2006. Adaptive restoration of complex geometry parts through reverse engineering application. Advances in Engineering Software 37(9):592-600.

Gaupp S, Wang Y, How TV, Fish PJ. 1999. Characterisation of vortex shedding in vascular anstomosis models using pulsed Doppler ultrasound. Journal of Biomechanics 32(7):639-645.

Gazell Mapili YLSCKR. 2005. Laser-layered microfabrication of spatially patterned functionalized tissue-engineering scaffolds. Journal of Biomedical Materials Research Part B: Applied Biomaterials 75B(2):414-424.

Ghosh S, Viana J, Reis R, Mano J. 2007. The double porogen approach as a new technique for the fabrication of interconnected poly(L-lactic acid) and starch based biodegradable scaffolds. Journal of Materials Science: Materials in Medicine 18(2):185-193.

Giri D, Jouaneh M, Stucker B. 2004. Error sources in a 3-D reverse engineering process. Precision Engineering 28(3):242-251.

Glenny R, Robertson HT. 1993. A 3-Dimensional Vascular Structure Models the Spatial Correlation of Regional Pulmonary Perfusion. American Review of Respiratory Disease 147(4):A921-A921.

Gong Z, Niklason LE. 2006. Blood Vessels Engineered from Human Cells. Trends in Cardiovascular Medicine 16(5):153-156.

Goyal A, Wang Y, Su H, Dobrucki LW, Brennan M, Fong P, Dardik A, Tellides G, Sinusas A, Pober JS and others. 2006. Development of a model system for

Guan J, Stankus JJ, Wagner WR. 2007. Biodegradable elastomeric scaffolds with basic fibroblast growth factor release. Journal of Controlled Release 120(1-2):70-78.

H. Y, Z. Y. 1999. Genetic algorithms for optimized re-triangulation in the context of reverse engineering. Computer-Aided Design 31(4):261-271.

Han BS, Fan CY, Liu SH. 2006. [Improvement of blood compatibility of small intestinal submucosa used as engineering vascular scaffolds by nano-bionic surface modification]. Zhonghua Yi Xue Za Zhi 86(29):2065-8.

He W, Yong T, Teo WE, Ma Z, Ramakrishna S. 2005. Fabrication and endothelialization of collagen-blended biodegradable polymer nanofibers: potential vascular graft for blood vessel tissue engineering. Tissue Eng 11(9-10):1574-88.

Heyligers JMM, Arts CHP, Verhagen HJM, de Groot PG, Moll FL. 2005. Improving Small-Diameter Vascular Grafts: From the Application of an Endothelial Cell Lining to the Construction of a Tissue-Engineered Blood Vessel. Annals of Vascular Surgery 19(3):448-456.

Hill RT, Shear JB. 2006. Enzyme-nanoparticle functionalization of three-dimensional protein scaffolds. Analytical Chemistry 78(19):7022-7026.

Ho J, Kleiven S. 2007. Dynamic response of the brain with vasculature: A three-dimensional computational study. Journal of Biomechanics 40(13):3006-3012.

Hollister SJ, Maddox RD, Taboas JM. 2002. Optimal design and fabrication of scaffolds to mimic tissue properties and satisfy biological constraints. Biomaterials 23(20):4095-4103.

Hou S, Xu Q, Tian W, Cui F, Cai Q, Ma J, Lee I-S. 2005. The repair of brain lesion by implantation of hyaluronic acid hydrogels modified with laminin. Journal of Neuroscience Methods 148(1):60-70.

Houbertz R. 2005. Laser interaction in sol-gel based materials--3-D lithography for photonic applications. Applied Surface Science 247(1-4):504-512.

Hutmacher DW. 2006. Regenerative medicine will impact, but not replace, the medical device industry. Expert Review of Medical Devices 3(4):409-412.

Hutmacher DW, Sittinger M, Risbud MV. 2004. Scaffold-based tissue engineering: rationale for computer-aided design and solid free-form fabrication systems. Trends in Biotechnology 22(7):354-362.

In Jeong S, Kim SY, Cho SK, Chong MS, Kim KS, Kim H, Lee SB, Lee YM. 2007. Tissue-engineered vascular grafts composed of marine collagen and PLGA fibers using pulsatile perfusion bioreactors. Biomaterials 28(6):1115-1122.

Ionita C, Chityala R, Rudin S, Hoffmann K, Kyprianou I, Bednarek D. 2003. Cone-beam CT of vessel phantoms: Comparison of image intensifier and high-resolution micro-angiographic systems. Medical Physics 30(6):1423-1423.

Iosin M, Stephan O, Astilean S, Dupperay A, Baldeck PL. 2007. Microstructuration of protein matrices by laser-induced photochemistry. Journal of Optoelectronics and Advanced Materials 9(3):716-720.

Jakobsson L, Kreuger J, Claesson-Welsh L. 2007. Building blood vessels - stem cell models in vascular biology. Journal of Cell Biology 177(5):751-755.

Jang D, Kim K, Jung J. 2000. Voxel-Based Virtual Multi-Axis Machining. The International Journal of Advanced Manufacturing Technology 16(10):709-713.

Jayagopal A, Russ PK, Haselton FR. 2007. Surface Engineering of Quantum Dots for In Vivo Vascular Imaging. Bioconjug Chem.preliminary evaluation of tissue-engineered vascular conduits. Journal of Pediatric Surgery 41(4):787-791.

Jian C, Amini AA. 2004. Quantifying 3-D vascular structures in MRA images using hybrid PDE and geometric deformable models. Ieee Transactions on Medical Imaging 23(10):1251-1262.

Jiang Z-W, Zhou Y-J, Yuan D-J, Huang W-H, Xia A-D. 2003. A Two-Photon Femtosecond Laser System for Three-Dimensional Microfabrication and Data Storage. Chinese Physics Letters(12):2126.

Jin D, Cordy JR. 2005. Factbase Filtering Issues in an Ontology-Based Reverse Engineering Tool Integration System. Electronic Notes in Theoretical Computer Science 137(3):65-75.

Johnson TL, Barabino GA, Nerem RM. 2006. Engineering more physiologic in vitro models for the study of vascular biology. Progress in Pediatric Cardiology 21(2):201-210.

Jun Y. 2005. A piecewise hole filling algorithm in reverse engineering. Computer-Aided Design 37(2):263-270.

Jung I, Lee MH, Bae S. 2006. Neural based CAD and CAP agent system framework for high risk patients in ubiquitous environment. Fuzzy Systems and Knowledge Discovery, Proceedings 4223:1054-1057.

Joung IS, Iwamoto MN, Shiu Y-T, Quam CT. 2006. Cyclic strain modulates tubulogenesis of endothelial cells in a 3D tissue culture model. Microvascular Research 71(1):1-11.

Kaehr B, Ertas N, Nielson R, Allen R, Hill RT, Plenert M, Shear JB. 2006. Direct-write fabrication of functional protein matrixes using a low-cost Q-switched laser. Analytical Chemistry 78(9):3198-3202.

Kaimovitz B, Lanir Y, Kassab GS. 2005. Large-scale 3-D geometric reconstruction of the porcine coronary arterial vasculature based on detailed anatomical data. Annals of Biomedical Engineering 33(11):1517-1535.

Kakisis JD, Liapis CD, Breuer C, Sumpio BE. 2005. Artificial blood vessel: The Holy Grail of peripheral vascular surgery. Journal of Vascular Surgery 41(2):349-354.

Kakou A, Louis H, Cattan V, Lacolley P, Thornton SN. 2007. Correlation between arterial mechanical properties, vascular biomaterial and tissue engineering. Clin Hemorheol Microcirc 37(1-2):71-5.

Kamiya A, Togawa T, Yamamoto A. 1974. Theoretical Relationship between Optimal Models of Vascular Tree. Bulletin of Mathematical Biology 36(3):311-323.

Kao JH, Chen YH, Chuang JH. 2005. Identity verification by relative 3-D structure using multiple facial images. Pattern Recognition Letters 26(9):1292-1303.

Karau KL, Krenz GS, Dawson CA. 2001. Branching exponent heterogeneity and wall shear stress distribution in vascular trees. Am J Physiol Heart Circ Physiol 280(3):H1256-1263.

Ke Y, Fan S, Zhu W, Li A, Liu F, Shi X. 2006a. Feature-based reverse modeling strategies. Computer-Aided Design 38(5):485-506.

Kennedy S, Oon TT. 1987. Exploration of Pulsed Laser Vascular Specific Injury Mechanisms in Invitro Blood-Vessel Models. Lasers in Surgery and Medicine 7(1):73-73.

Khalil S, Sun W. 2007. Biopolymer deposition for freeform fabrication of hydrogel tissue constructs. Materials Science and Engineering: C 27(3):469-478.

Kielty CM, Stephan S, Sherratt MJ, Williamson M, Shuttleworth CA. 2007. Applying elastic fibre biology in vascular tissue engineering. Philos Trans R Soc Lond B Biol Sci 362(1484):1293-312.

Kim SH, Kwon JH, Chung MS, Chung E, Jung Y, Kim SH, Kim YH. 2006. Fabrication of a new tubular fibrous PLCL scaffold for vascular tissue engineering. J Biomater Sci Polym Ed 17(12):1359-74.

Kirbas C, Quek FKH. 3d wave propagation and traceback in vascular extraction; 2002. p 1078-1079 vol.2.

Kirbas C, Quek FKH. Vessel extraction in medical images by 3D wave propagation and traceback; 2003. p 174-181.

Kostopoulos S, Glotsos D, Kagadis GC, Daskalakis A, Spyridonos P, Kalatzis I, Karamessini M, Petsas T, Cavouras D, Nikiforidis G. 2007. A hybrid pixel-based classification method for blood vessel segmentation and aneurysm detection on CTA. Computers & Graphics 31(3):493-500.

Kruth JP, Kerstens A. 1998. Reverse engineering modelling of free-form surfaces from point clouds subject to boundary conditions. Journal of Materials Processing Technology 76(1-3):120-127.

Kurane A, Simionescu DT, Vyavahare NR. 2007. In vivo cellular repopulation of tubular elastin scaffolds mediated by basic fibroblast growth factor. Biomaterials 28(18):2830-2838.

Lacroix D, Chateau A, Ginebra M-P, Planell JA. 2006. Micro-finite element models of bone tissue-engineering scaffolds. Biomaterials 27(30):5326-5334.

LaDisa JJF, Olson LE, Ropella KM, Molthen RC, Haworth ST, Kersten JR, Warltier DC, Pagel PS. 2005. Microfocal X-ray computed tomography post-processing operations for optimizing reconstruction volumes of stented arteries during 3D computational fluid dynamics modeling. Computer Methods and Programs in Biomedicine 79(2):121-134.

Lai J-Y, Lai H-C. 2006. Repairing triangular meshes for reverse engineering applications. Advances in Engineering Software 37(10):667-683.

Lanzarone E, Liani P, Baselli G, Costantino ML. 2007. Model of arterial tree and peripheral control for the study of physiological and assisted circulation. Medical Engineering & Physics 29(5):542-555.

Leach JB, Wolinsky JB, Stone PJ, Wong JY. 2005. Crosslinked [alpha]-elastin biomaterials: towards a processable elastin mimetic scaffold. Acta Biomaterialia 1(2):155-164.

Leclerc E, Furukawa KS, Miyata F, Sakai Y, Ushida T, Fujii T. 2004. Fabrication of microstructures in photosensitive biodegradable polymers for tissue engineering applications. Biomaterials 25(19):4683-4690.

Lee J, Beighley P, Ritman E, Smith N. Automatic segmentation of 3D micro-CT coronary vascular images. Medical Image Analysis In Press, Corrected Proof:2300.

Lee KH, Woo H. 1998. Use of reverse engineering method for rapid product development. Computers & Industrial Engineering 35(1-2):21-24.

Lee RS, Tsai JP, Kao YC, Lin GCI, Fan KC. 2003. STEP-based product modeling system for remote collaborative reverse engineering. Robotics and Computer-Integrated Manufacturing 19(6):543-553.

Lee S-C, Bajcsy P. Trajectory fusion for three-dimensional volume reconstruction. Computer Vision and Image Understanding In Press, Corrected Proof:156.

Leong KF, Cheah CM, Chua CK. 2003. Solid freeform fabrication of three-dimensional scaffolds for engineering replacement tissues and organs. Biomaterials 24(13):2363-2378.

Lepidi S, Grego F, Vindigni V, Zavan B, Tonello C, Deriu GP, Abatangelo G, Cortivo R. 2006. Hyaluronan Biodegradable Scaffold for Small-caliber Artery Grafting: Preliminary Results in an Animal Model. European Journal of Vascular and Endovascular Surgery 32(4):411-417.

Levenberg S. 2005. Engineering blood vessels from stem cells: recent advances and applications. Current Opinion in Biotechnology 16(5):516-523.

Li B, Christensen GE, Hoffman EA, McLennan G, Reinhardt JM. 2003. Establishing a Normative Atlas of the Human Lung: Intersubject Warping and Registration of Volumetric CT Images. Academic Radiology 10(3):255-265.

Li L, Schemenauer N, Peng X, Zeng Y, Gu P. 2002b. A reverse engineering system for rapid manufacturing of complex objects. Robotics and Computer-Integrated Manufacturing 18(1):53-67.

Li LJ, Fourkas JT. 2007. Multiphoton polymerization. Materials Today 10(6):30-37.

Li X, Yang J, Xie K, Zhu YM. 2006. High-quality rendering with depth cueing of volumetric data using Monte Carlo integration. Computers in Biology and Medicine 36(9):1014-1025.

Liang H, Arangarasan R, Theller L. 2007. Dynamic visualization of high resolution GIS dataset on multi-panel display using ArcGIS engine. Computers and Electronics in Agriculture 58(2):174-188.

Lillie MA, Gosline JM. 2007. Limits to the durability of arterial elastic tissue. Biomaterials 28(11):2021-2031.

Lin AC, Lin S-Y, Fang T-H. 1998. Automated sequence arrangement of 3D point data for surface fitting in reverse engineering. Computers in Industry 35(2):149-173.

Lin ASP, Barrows TH, Cartmell SH, Guldberg RE. 2003. Microarchitectural and mechanical characterization of oriented porous polymer scaffolds. Biomaterials 24(3):481-489.

Lin Y-P, Wang C-T, Dai K-R. 2005. Reverse engineering in CAD model reconstruction of customized artificial joint. Medical Engineering & Physics 27(2):189-193.

Linnes MP, Ratner BD, Giachelli CM. A fibrinogen-based precision microporous scaffold for tissue engineering. Biomaterials In Press, Corrected Proof:892.

Liu JY, Swartz DD, Peng HF, Gugino SF, Russell JA, Andreadis ST. 2007. Functional tissue-engineered blood vessels from bone marrow progenitor cells. Cardiovascular Research 75(3):618-628.

Liu SQ. 1999. Biomechanical basis of vascular tissue engineering. Crit Rev Biomed Eng 27(1-2):75-148.

Liu W, Cao Y. Application of scaffold materials in tissue reconstruction in immunocompetent mammals: Our experience and future requirements. Biomaterials In Press, Corrected Proof:3348.

Liu X, Won Y, Ma PX. 2006a. Porogen-induced surface modification of nano-fibrous poly(l-lactic acid) scaffolds for tissue engineering. Biomaterials 27(21):3980-3987.

Liu Y-S, Paul J-C, Yong J-H, Yu P-Q, Zhang H, Sun J-G, Ramani K. 2006b. Automatic least-squares projection of points onto point clouds with applications in reverse engineering. Computer-Aided Design 38(12):1251-1263.

Liu Z, Wang L, Lu B. 2006c. Integrating cross-sectional imaging based reverse engineering with rapid prototyping. Computers in Industry 57(2):131-140.

Lorigo LM, Faugeras OD, Grimson WEL, Keriven R, Kikinis R, Nabavi A, Westin CF. 2001. CURVES: Curve evolution for vessel segmentation. Medical Image Analysis 5(3):195-206.

Lovett M, Cannizzaro C, Daheron L, Messmer B, Vunjak-Novakovic G, Kaplan DL. Silk fibroin microtubes for blood vessel engineering. Biomaterials In Press, Corrected Proof.

Maina JN. 2004. Systematic analysis of hematopoietic, vasculogenetic, and angiogenetic phases in the developing embryonic avian lung, Gallus gallus variant domesticus. Tissue and Cell 36(5):307-322.

Makowski P, Sorensen TS, Therkildsen SV, Materka A, Stodkilde-Jorgensen H, Pedersen EM. 2002. Two-phase active contour method for semiautomatic segmentation of the heart and blood vessels from MRI images for 3D visualization. Computerized Medical Imaging and Graphics 26(1):9-17.

Mao F-l, Xing Q-r, Wang K, Lang L-y, Wang Z, Chai L, Wang Q-y. 2005. Optical trapping of red blood cells and two-photon excitation-based photodynamic study using a femtosecond laser. Optics Communications 256(4-6):358-363.

Marquez J, Schmitt F. 2000. Radiometric homogenization of the color cryosection images from the VHP Lungs for 3D segmentation of blood vessels. Computerized Medical Imaging and Graphics 24(3):181-191.

Martin ND, Schaner PJ, Tulenko T, Shapiro I, Dimatteo C, Dimuzio PJ. 2004. Endothelial cell-seeding decellularized vein transplants: A novel arterial bypass conduit. Journal of Surgical Research 121(2):303-2098.

Mason C. 2006. The time has come to engineer tissues and not just tissue engineer. Regenerative Medicine 1(3):303-306.

Mason C. 2007. Regenerative medicine 2.0. Regenerative Medicine 2(1):11-18.

McEvily AJ. 2005. Reverse engineering gone wrong: A case study. Engineering Failure Analysis 12(5):834-838.

McFetridge PS, Bodamyali T, Horrocks M, Chaudhuri JB. 2004a. Endothelial and smooth muscle cell seeding onto processed ex vivo arterial scaffolds using 3D vascular bioreactors. Asaio Journal 50(6):591-600.

Meddahi-Pelle A, Bataille I, Subra P, Letourneur D. 2004. Vascular biomaterials: from biomedical engineering to tissue engineering. Med Sci (Paris) 20(6-7):679-84.

Mertsching H, Walles T, Hofmann M, Schanz J, Knapp WH. 2005. Engineering of a vascularized scaffold for artificial tissue and organ generation. Biomaterials 26(33):6610-6617.

Methe H, Edelman ER. 2006. Tissue Engineering of Endothelial Cells and the Immune Response. Transplantation Proceedings 38(10):3293-3299.

Method. International Journal of Information Technology Vol. No. 9 2005 11(9):119 - 127.

Milroy MJ, Bradley C, Vickers GW, Weir DJ. 1995. G1 continuity of B-spline surface patches in reverse engineering. Computer-Aided Design 27(6):471-478.

Mironov V, Boland T, Trusk T, Forgacs G, Markwald RR. 2003a. Organ printing: computer-aided jet-based 3D tissue engineering. Trends in Biotechnology 21(4):157-161.

Mironov V, Kasyanov V, McAllister K, Oliver S, Sistino J, Markwald R. 2003b. Perfusion bioreactor for vascular tissue engineering with capacities for longitudinal stretch. J Craniofac Surg 14(3):340-7.

Mondrinos MJ, Dembzynski R, Lu L, Byrapogu VKC, Wootton DM, Lelkes PI, Zhou J. 2006. Porogen-based solid freeform fabrication of polycaprolactone-calcium phosphate scaffolds for tissue engineering. Biomaterials 27(25):4399-4408.

2005 11(9):119 - 127.

Mondy, W. L., D. Cameron, Jean-Pierre Timmermans, and A. S. N. De Clerck, C. Casteleyn, L. A. Piegl (2009, submitted). "Computer Aided Design of Microvasculature Systems Biofabrication

Naegel B. 2007. Using mathematical morphology for the anatomical labeling of vertebrae from 3D CT-scan images. Computerized Medical Imaging and Graphics 31(3):141-156.

Neal CR, Crook H, Bell E, Harper SJ, Bates DO. 2005. Three-Dimensional Reconstruction of Glomeruli by Electron Microscopy Reveals a Distinct Restrictive Urinary Subpodocyte Space. J Am Soc Nephrol 16(5):1223-1235.

Neofytou P, Tsangaris S. 2006. Flow effects of blood constitutive equations in 3D models of vascular anomalies. International Journal for Numerical Methods in Fluids 51(5):489-510.

Nerem RM. 2003. Role of mechanics in vascular tissue engineering. Biorheology 40(1-3):281-7.

Nerem RM. 2004a. Critical issues in vascular tissue engineering. International Congress Series 1262:122-125.

Nerem RM. 2004b. Tissue engineering of the vascular system. Vox Sang 87 Suppl 2:158-60.

Nerem RM, Seliktar D. 2001. Vascular tissue engineering. Annu Rev Biomed Eng 3:225-43.

Ngan EM, Rebeyka IM, Ross DB, Hirji M, Wolfaardt JF, Seelaus R, Grosvenor A, Noga ML. 2006. The rapid prototyping of anatomic models in pulmonary atresia. The Journal of Thoracic and Cardiovascular Surgery 132(2):264-269.

Nikolajewa S, Friedel M, Wilhelm T. 2007. Boolean networks with biologically relevant rules show ordered behavior. Biosystems 90(1):40-47.

Nillesen STM, Geutjes PJ, Wismans R, Schalkwijk J, Daamen WF, van Kuppevelt TH. 2007. Increased angiogenesis and blood vessel maturation in acellular collagen-heparin scaffolds containing both FGF2 and VEGF. Biomaterials 28(6):1123-1131.

Ning R, Kruger RA. 1996. Image intensifier-based computed tomography volume scanner for angiography. Academic Radiology 3(4):344-350.

Noel P, Hoffmann KR, Walczak AM, Dmochowski J. 2004. Registration of vascular 3D data sets obtained from multiple-view reconstructions. International Congress Series 1268:329-334.

Noser PDDH, Stern DC, Stucki PP. 2004. Automatic path searching for interactive navigation support within virtual medical 3-dimensional objects. Academic Radiology 11(8):919-930.

Nyflot M, Grudzinski J, Jeraj R. 2007. Novel MicroCT imaging techniques for in vivo quantification of vascular volume in murine tumor models. Medical Physics 34(6):2365-2365.

Oh SH, Kang SG, Kim ES, Cho SH, Lee JH. 2003. Fabrication and characterization of hydrophilic poly(lactic-co-glycolic acid)/poly(vinyl alcohol) blend cell scaffolds by melt-molding particulate-leaching method. Biomaterials 24(22):4011-4021.

Ovsianikov A, Ostendorf A, Chichkov BN. 2007. Three-dimensional photofabrication with femtosecond lasers for applications in photonics and biomedicine. Applied Surface Science 253(15):6599-6602.

Palagyi K, Tschirren J, Hoffman EA, Sonka M. 2006. Quantitative analysis of pulmonary airway tree structures. Computers in Biology and Medicine 36(9):974-996.

Parker HG, Hippenst.Jr, Dobson EL. 1972. Mathematical Models for Exchange of Substances in Regional Vascular Beds - Measurement of Rates with in-Vivo Counters. Bulletin of Mathematical Biophysics 34(4):503-520.

Patel A, Fine B, Sandig M, Mequanint K. 2006. Elastin biosynthesis: The missing link in tissue-engineered blood vessels. Cardiovascular Research 71(1):40-49.

Pellot C, Bloch I, Herment A, Sureda F. 1996. An attempt to 3D reconstruct vessel morphology from X-ray projections and intravascular ultrasounds modeling and fusion. Computerized Medical Imaging and Graphics 20(3):141-151.

Peng Q, Loftus M. 1998. A new approach to reverse engineering based on vision information. International Journal of Machine Tools and Manufacture 38(8):881-899.

Perea H, Aigner J, Hopfner U, Wintermantel E. 2006. Direct magnetic tubular cell seeding: a novel approach for vascular tissue engineering. Cells Tissues Organs 183(3):156-65.

Perez-Pomares JM, Mironov V, Guadix JA, Macias D, Markwald RR, Munoz-Chapuli R. 2006. In vitro self-assembly of proepicardial cell aggregates: an embryonic vasculogenic model for vascular tissue engineering. Anat Rec A Discov Mol Cell Evol Biol 288(7):700-13.

Peters MC, Polverini PJ, Mooney DJ. 2002. Engineering vascular networks in porous polymer matrices. J Biomed Mater Res 60(4):668-78.

Pins GD, Bush KA, Cunningham LP, Carnpagnola PJ. 2006. Multiphoton excited fabricated nano and micro patterned extracellular matrix proteins direct cellular morphology. Journal of Biomedical Materials Research Part A 78A(1):194-204.

Poh M, Boyer M, Solan A, Dahl SLM, Pedrotty D, Banik SSR, McKee JA, Klinger RY, Counter CM, Niklason LE. Blood vessels engineered from human cells. The Lancet 365(9477):2122-2124.

Quek FKH, Kirbas C. 2001. Vessel extraction in medical images by wave-propagation and traceback. Medical Imaging, IEEE Transactions on 20(2):117-131.

Rabbani T, Dijkman S, van den Heuvel F, Vosselman G. 2007. An integrated approach for modelling and global registration of point clouds. ISPRS Journal of Photogrammetry and Remote Sensing 61(6):355-370.

Rajagopalan S, Robb RA. 2006. Schwarz meets Schwann: Design and fabrication of biomorphic and durataxic tissue engineering scaffolds. Medical Image Analysis 10(5):693-712.

Rennie MY, Whiteley KJ, Kulandavelu S, Adamson SL, Sled JG. 2007. 3D Quantification by Microcomputed Tomography of Late Gestational Changes in the Arterial and Venous Feto-Placental Vasculature of the Mouse. Placenta 28(8-9):833-840.

Rhim C, Niklason LE. 2006. Tissue engineered vessels: Cells to telomeres. Progress in Pediatric Cardiology 21(2):185-191.

Ribatti D. 2007. The discovery of endothelial progenitor cells: An historical review. Leukemia Research 31(4):439-444.

Riha GM, Lin PH, Lumsden AB, Yao Q, Chen C. 2005. Review: application of stem cells for vascular tissue engineering. Tissue Eng 11(9-10):1535-52.

Roberto Toni CDC, Giulia Spaletta, Giacomo Marchetti, Perseo Mazzoni,, Monica Bodria SR, Davide Dallatana, Sergio Castorina, Vincenzo Riccioli,, Emilio Giovanni Castorina SA, Enrico Campanile, Gabriella Scalise, Raffaella, Rossi GU, Andrew Martorella, Elio Roti, Fiorella Sgallari, Aldo Pinchera. 2007. The bioartificial thyroid: a biotechnological perspective in endocrine organ engineering for transplantation replacement. Acta Bio Medica Atenei Parmensis 78 (Suppl 1):129-55.

Rucker M, Laschke MW, Junker D, Carvalho C, Schramm A, Mulhaupt R, Gellrich N-C, Menger MD. 2006. Angiogenic and inflammatory response to biodegradable scaffolds in dorsal skinfold chambers of mice. Biomaterials 27(29):5027-5038.

Ryu W, Min SW, Hammerick KE, Vyakarnam M, Greco RS, Prinz FB, Fasching RJ. 2007. The construction of three-dimensional micro-fluidic scaffolds of biodegradable polymers by solvent vapor based bonding of micro-molded layers. Biomaterials 28(6):1174-1184.

Sachlos E, Reis N, Ainsley C, Derby B, Czernuszka JT. 2003. Novel collagen scaffolds with predefined internal morphology made by solid freeform fabrication. Biomaterials 24(8):1487-1497.

Sakuma J, Matsumoto M, Muramatsu H, Oinuma M, Suzuki K, Sasaki T, Kodama N, Suzuki K, Katakura T, Shishido F. 2004. Evaluation of cervical arteries with 3D-CTA using multi-detector row CT--one-session scanning of the head and neck using single or double injection of contrast medium. International Congress Series 1259:427-433.

Sales KM, Salacinski HJ, Alobaid N, Mikhail M, Balakrishnan V, Seifalian AM. 2005. Advancing vascular tissue engineering: the role of stem cell technology. Trends Biotechnol 23(9):461-7.

Schenke-Layland K, Riemann I, Damour O, Stock UA, Konig K. 2006. Two-photon microscopes and in vivo multiphoton tomographs -- Powerful diagnostic tools for tissue engineering and drug delivery. Advanced Drug Delivery Reviews 58(7):878-896.

Schmidt CE, Baier JM. 2000. Acellular vascular tissues: natural biomaterials for tissue repair and tissue engineering. Biomaterials 21(22):2215-31.

Schmidt D, Asmis LM, Odermatt B, Kelm J, Breymann C, Gossi M, Genoni M, Zund G, Hoerstrup SP. 2006. Engineered Living Blood Vessels: Functional Endothelia Generated From Human Umbilical Cord-Derived Progenitors. The Annals of Thoracic Surgery 82(4):1465-1471.

Schmitt H, Grass M, Kohler T, Suurmond R, Rasche V, Hahnel S, Heiland S. 2004. A linear programming framework for blood flow reconstruction in cerebral vessel trees. International Congress Series 1268:1061-1066.

Schmitt H, Grass M, Suurmond R, Kohler T, Rasche V, Hahnel S, Heiland S. 2005. Reconstruction of blood propagation in three-dimensional rotational X-ray

angiography (3D-RA). Computerized Medical Imaging and Graphics 29(7):507-520.

Shima DT, Mailhos C. 2000. Vascular developmental biology: getting nervous. Current Opinion in Genetics & Development 10(5):536-542.

24(24):4353-4364.

Sijbers J, Postnovz A. 2004. Reduction of ring artefacts in high resolution micro-CT reconstructions. Physics in Medicine and Biology 49(14):N247-N253.

Silva MMCG, Cyster LA, Barry JJA, Yang XB, Oreffo ROC, Grant DM, Scotchford CA, Howdle SM, Shakesheff KM, Rose FRAJ. 2006. The effect of anisotropic architecture on cell and tissue infiltration into tissue engineering scaffolds. Biomaterials 27(35):5909-5917.

Simionescu DT, Lu Q, Song Y, Lee J, Rosenbalm TN, Kelley C, Vyavahare NR. 2006. Biocompatibility and remodeling potential of pure arterial elastin and collagen scaffolds. Biomaterials 27(5):702-713.

Sodian R, Fu P, Lueders C, Szymanski D, Fritsche C, Gutberlet M, Hoerstrup SP, Hausmann H, Lueth T, Hetzer R. 2005. Tissue engineering of vascular conduits: fabrication of custom-made scaffolds using rapid prototyping techniques. Thorac Cardiovasc Surg 53(3):144-9.

Srinivasan VJ, Wojtkowski M, Witkin AJ, Duker JS, Ko TH, Carvalho M, Schuman JS, Kowalczyk A, Fujimoto JG. 2006. High-Definition and 3-dimensional Imaging of Macular Pathologies with High-speed Ultrahigh-Resolution Optical Coherence Tomography. Ophthalmology 113(11):2054-2065.e3.

Stankus JJ, Guan J, Fujimoto K, Wagner WR. 2006. Microintegrating smooth muscle cells into a biodegradable, elastomeric fiber matrix. Biomaterials 27(5):735-744.

Stankus JJ, Soletti L, Fujimoto K, Hong Y, Vorp DA, Wagner WR. 2007. Fabrication of cell microintegrated blood vessel constructs through electrohydrodynamic atomization. Biomaterials 28(17):2738-2746.

Starly B, Lau W, Bradbury T, Sun W. 2006. Internal architecture design and freeform fabrication of tissue replacement structures. Computer-Aided Design 38(2):115-124.

Stephan S, Ball SG, Williamson M, Bax DV, Lomas A, Shuttleworth CA, Kielty CM. 2006. Cell-matrix biology in vascular tissue engineering. J Anat 209(4):495-502.

Stoltz JF, Blondel W, Bensoussan D, Lehalle B, Wang X, Labrador V. 2001a. Plenary lecture. New trends in vascular engineering. Clin Hemorheol Microcirc 24(4):263-72.

Stoltz JF, Lehalle B, Blondel WC, Bensoussan D, Paulus F. 2001b. [Introduction to vascular engineering]. J Mal Vasc 26(3):183-90.

Suetens P, Jansen P, Haegemans A, Oosterlinck A, Gybels J. 1983. 3D reconstruction of the blood vessels of the brain from a stereoscopic pair of subtraction angiograms. Image and Vision Computing 1(1):43-51.

Sumaru K, Kanamori T. 2004. Optimal design of bio-hybrid systems with a hollow fiber scaffold: model analysis of oxygen diffusion/consumption. Biochemical Engineering Journal 20(2-3):127-136.i

Sun KS, Nong Zhao, Erdun. 2005a. Extraction of Vascular Tree on Angiogram with Fuzzy Morphological Method. International Journal of Information Technology Vol. No. 9

Sun W. 2003. Special issue of computer-aided design: Bio-CAD. Computer-Aided Design 35(13):III-1114.

Sun W. 2004. Call for papers: Bio-CAD. Computer-Aided Design 36(2):III-1114.

Sun W, Lal P. 2002. Recent development on computer aided tissue engineering -- a review. Computer Methods and Programs in Biomedicine 67(2):85-103.

Suuronen EJ, Sheardown H, Newman KD, McLaughlin CR, Griffith M, Kwang WJ. 2005. Building In Vitro Models of Organs. International Review of Cytology: Academic Press. p 137-173.

Tam KW, Chan KW. 2007. Thermoforming mould design using a reverse engineering approach. Robotics and Computer-Integrated Manufacturing 23(3):305-314.

Tan Q, Steiner R, Yang L, Welti M, Neuenschwander P, Hillinger S, Weder W. 2007. Accelerated angiogenesis by continuous medium flow with vascular endothelial growth factor inside tissue-engineered trachea. European Journal of Cardio-Thoracic Surgery 31(5):806-811.

Tao J, Jiyong K. 2007. A 3D point sets registration method in reverse engineering. Computers & Industrial Engineering 53(2):270-276.

Tessmar JK, Gopferich AM. 2007. Matrices and scaffolds for protein delivery in tissue engineering. Advanced Drug Delivery Reviews 59(4-5):274-291.

Thebaud NB, Pierron D, Bareille R, Le Visage C, Letourneur D, Bordenave L. 2007. Human endothelial progenitor cell attachment to polysaccharide-based hydrogels: a pre-requisite for vascular tissue engineering. J Mater Sci Mater Med 18(2):339-45.

Thomas AC, Campbell GR, Campbell JH. 2003. Advances in vascular tissue engineering. Cardiovasc Pathol 12(5):271-6.

Timm W, Barkmann R, Scheffczyk R, Lochmueller EM, Glaser C, Heller M, Glueer CC. 2000. High-resolution imaging by a new micro-CT for the assessment of novel shape-based structural and geometrical parameters at peripheral sites. Osteoporosis International 11:9-10.

Todros T, Sciarrone A, Guiot C, Pianta PG, Kosankoe G, Konen G, Kaufmann P. 1993. The vascular tree of the human term placenta: Morphometric evaluation and mathematical modelling. Placenta 14(4):A77-236.

Tsai T-H, Fan K-C. 2007. An image matching algorithm for variable mesh surfaces. Measurement 40(3):329-337.

Tuan HS, Hutmacher DW. 2005. Application of micro CT and computation modeling in bone tissue engineering. Computer-Aided Design 37(11):1151-1161.

Uchida T, Ikeda S, Oura H, Tada M, Nakano T, Fukuda T, Matsuda T, Negoro M, Arai F. Development of biodegradable scaffolds based on patient-specific arterial configuration. Journal of Biotechnology In Press, Corrected Proof.

van Tuyl M, Groenman F, Wang J, Kuliszewski M, Liu J, Tibboel D, Post M. 2007. Angiogenic factors stimulate tubular branching morphogenesis of sonic hedgehog-deficient lungs. Developmental Biology 303(2):514-526.

van Velthoven MEJ, Faber DJ, Verbraak FD, van Leeuwen TG, de Smet MD. 2007. Recent developments in optical coherence tomography for imaging the retina. Progress in Retinal and Eye Research 26(1):57-77.

Varady T, Martin RR, Cox J. 1997. Reverse engineering of geometric models--an introduction. Computer-Aided Design 29(4):255-268.

Vaz CM, van Tuijl S, Bouten CVC, Baaijens FPT. 2005. Design of scaffolds for blood vessel tissue engineering using a multi-layering electrospinning technique. Acta Biomaterialia 1(5):575-582.

Velazquez OC. 2007. Angiogenesis and vasculogenesis: Inducing the growth of new blood vessels and wound healing by stimulation of bone marrow-derived progenitor cell mobilization and homing. Journal of Vascular Surgery 45(6, Supplement 1):A39-A47.

Vicini P, Ewart C, Claudio C. 2001. Blood-Tissue Exchange Modelling. Modeling Methodology for Physiology and Medicine. San Diego: Academic Press. p 373-401.

Vorp DA, Maul T, Nieponice A. 2005. Molecular aspects of vascular tissue engineering. Front Biosci 10:768-89.

Vu TH, Alemayehu Y, Werb Z. 2003. New insights into saccular development and vascular formation in lung allografts under the renal capsule. Mechanisms of Development 120(3):305-313.

Wang H, Dai W, Bejan A. 2007a. Optimal temperature distribution in a 3D triple-layered skin structure embedded with artery and vein vasculature and induced by electromagnetic radiation. International Journal of Heat and Mass Transfer 50(9-10):1843-1854.

Wang L, Wu Y, Chen L, Gu Y, Xi T, Zhang A, Feng Z-g. 2005a. Fabrication and evaluation of tissue engineering vascular scaffolds based on biodegradable aliphatic-aromatic copolyesters. Current Applied Physics 5(5):557-560.

Wang Z, Zeng F, Li H, Ye Z, Bai Y, Xia W, Liang B. 2007c. Three-dimensional reconstruction on PC-Windows platform for evaluation of living donor nephrectomy. Computer Methods and Programs in Biomedicine 86(1):39-44.

Wehmoeller M. 1996. Verification of reconstructed computed tomography data by reverse engineering methods. Journal of Cranio-Maxillofacial Surgery 24(Supplement 1):124-254.

Weigel T, Schinkel G, Lendlein A. 2006. Design and preparation of polymeric scaffolds for tissue engineering. Expert Review of Medical Devices 3:835-851.

Weiss LE, Amon CH, Finger S, Miller ED, Romero D, Verdinelli I, Walker LM, Campbell PG. 2005. Bayesian computer-aided experimental design of heterogeneous scaffolds for tissue engineering. Computer-Aided Design 37(11):1127-1139.

Wen SJ, Zhao LM, Li P, Li JX, Liu Y, Liu JL, Chen YC. 2005. [Blood vessel tissue engineering: seeding vascular smooth muscle cells and endothelial cells sequentially on biodegradable scaffold in vitro]. Zhonghua Yi Xue Za Zhi 85(12):816-8.

Wentzel JJ, Gijsen FJH, Stergiopulos N, Serruys PW, Slager CJ, Krams R. 2003. Shear stress, vascular remodeling and neointimal formation. Journal of Biomechanics 36(5):681-688.

Williams J, Wolff L. 1997. Analysis of the Pulmonary Vascular Tree Using Differential Geometry Based Vector Fields. Computer Vision and Image Understanding 65(2):226-236.

Williamson MR, Shuttleworth A, Canfield AE, Black RA, Kielty CM. The role of endothelial cell attachment to elastic fibre molecules in the enhancement of monolayer formation and retention, and the inhibition of smooth muscle cell recruitment. Biomaterials In Press, Corrected Proof.

Williamson MR, Woollard KJ, Griffiths HR, Coombes AG. 2006b. Gravity spun polycaprolactone fibers for applications in vascular tissue engineering: proliferation and function of human vascular endothelial cells. Tissue Eng 12(1):45-51.

Windyga P, Garreau M, Coatrieux JL. 1998. Estimation of search-space in 3D coronary artery reconstruction using angiographic biplane images. Pattern Recognition Letters 19(14):1325-1330.

Wu H-C, Wang T-W, Kang P-L, Tsuang Y-H, Sun J-S, Lin F-H. 2007. Coculture of endothelial and smooth muscle cells on a collagen membrane in the development of a small-diameter vascular graft. Biomaterials 28(7):1385-1392.

Wu L, Jing D, Ding J. 2006a. A "room-temperature" injection molding/particulate leaching approach for fabrication of biodegradable three-dimensional porous scaffolds. Biomaterials 27(2):185-191.

Wu L, Zhang H, Zhang J, Ding J. 2005. Fabrication of Three-Dimensional Porous Scaffolds of Complicated Shape for Tissue Engineering. I. Compression Molding Based on Flexible–Rigid Combined Mold. Tissue Engineering 11(7-8):1105-1114.

Wu S, Serbin J, Gu M. 2006b. Two-photon polymerisation for three-dimensional micro-fabrication. Journal of Photochemistry and Photobiology A: Chemistry 181(1):1-11.

Wu X, Kathuria N, Patrick CW, Reece GP. Quantitative analysis of the microvasculature growing in the fibrin interface between a skin graft and the recipient site. Microvascular Research In Press, Corrected Proof:990.

Xie K, Yang J, Zhu YM. 2005. Real-time rendering of 3D medical data sets. Future Generation Computer Systems 21(4):573-581.

Xu C, Inai R, Kotaki M, Ramakrishna S. 2004a. Electrospun nanofiber fabrication as synthetic extracellular matrix and its potential for vascular tissue engineering. Tissue Eng 10(7-8):1160-8.

Xu CY, Inai R, Kotaki M, Ramakrishna S. 2004b. Aligned biodegradable nanofibrous structure: a potential scaffold for blood vessel engineering. Biomaterials 25(5):877-886.

Xu J, Ge H, Zhou X, Yan J, Chi Q, Zhang Z. 2005a. Prediction of vascular tissue engineering results with artificial neural networks. J Biomed Inform 38(6):417-21.

Xu T, Jin J, Gregory C, Hickman JJ, Boland T. 2005b. Inkjet printing of viable mammalian cells. Biomaterials 26(1):93-99.

Yan Y, Xiong Z, Hu Y, Wang S, Zhang R, Zhang C. 2003. Layered manufacturing of tissue engineering scaffolds via multi-nozzle deposition. Materials Letters 57(18):2623-2628.

Yang Z, Chen Y. 2005. A reverse engineering method based on haptic volume removing. Computer-Aided Design 37(1):45-54.

Young PP, Vaughan DE, Hatzopoulos AK. 2007. Biologic Properties of Endothelial Progenitor Cells and Their Potential for Cell Therapy. Progress in Cardiovascular Diseases 49(6):421-429.

Yu C, Peng Q. 2007. A unified-calibration method in FTP-based 3D data acquisition for reverse engineering. Optics and Lasers in Engineering 45(3):396-404.

Zammaretti P, Zisch AH. 2005. Adult `endothelial progenitor cells': Renewing vasculature. The International Journal of Biochemistry & Cell Biology 37(3):493-503.

Zhai XY, Thomsen JS, Birn H, Kristoffersen IB, Andreasen A, Christensen EI. 2006. Three-dimensional reconstruction of the mouse nephron. Journal of the American Society of Nephrology 17(1):77-88.

Zhang G, Suggs LJ. 2007. Matrices and scaffolds for drug delivery in vascular tissue engineering. Adv Drug Deliv Rev 59(4-5):360-73.

Zhang L, Zheng Z, Xi J, Gao Y, Ao Q, Gong Y, Zhao N, Zhang X. 2007a. Improved mechanical property and biocompatibility of poly(3-hydroxybutyrate-co-3-hydroxyhexanoate) for blood vessel tissue engineering by blending with poly(propylene carbonate). European Polymer Journal 43(7):2975-2986.

Zhang Y, Pajarola R. 2007. Deferred blending: Image composition for single-pass point rendering. Computers & Graphics 31(2):175-189.

Zheng L, Wang Q. 2005. Study of antithrombotic function of endothelium in vascular tissue engineering. Zhongguo Xiu Fu Chong Jian Wai Ke Za Zhi 19(1):74-7.

Zhou W, Kuebler SM, Braun KL, Yu T, Cammack JK, Ober CK, Perry JW, Marder SR. 2002. An Efficient Two-Photon-Generated Photoacid Applied to Positive-Tone 3D Microfabrication. Science 296(5570):1106-1109.

Ziegler T, Nerem RM. 1994. Tissue engineering a blood vessel: regulation of vascular biology by mechanical stresses. J Cell Biochem 56(2):204-9.

About the Author

William Lafayette Mondy William graduated from Theodore Roosevelt Senior high school in 1976 earning a Frederick Douglass scholarship to attend the University of Maryland College Park. In 1998 William returned to the University of Maryland and completed a Master's degree in biology where he served as the Biology Graduate School's representative to the faculty Senate, received the Distinguished Teaching Award, the Hitachi Scientific Instrumentation Award for Excellence in Microscopy, and was awarded William the John H.L. Watson Memorial Scholarship from the Microscopy Society of America. William received the Richard Pride Ph.D. Fellowship from the University of South Florida, was awarded for academic excellence and elected to the Phi Kappa Phi Honor Society. In 2006 he received the NSF IGERT Fellowship and the Alfred P. Sloan Minority Ph.D. Fellowship. In 2008 William studied in Belgium at University of Antwerp and the Universe Gent obtaining data reported in this dissertation.